https://www.mdc-berlin.de/de/veroeffentlichungstypen/clinical-journal-club

Als gemeinsame Einrichtung von MDC und Charité fördert das Experimental and Clinical Research Center die Zusammenarbeit zwischen Grundlagenwissenschaftlern und klinischen Forschern. Hier werden neue Ansätze für Diagnose, Prävention und Therapie von Herz-Kreislauf- und Stoffwechselerkrankungen, Krebs sowie neurologischen Erkrankungen entwickelt und zeitnah am Patienten eingesetzt. Sie sind eingeladen, uns beizutreten. Bewerben Sie sich!

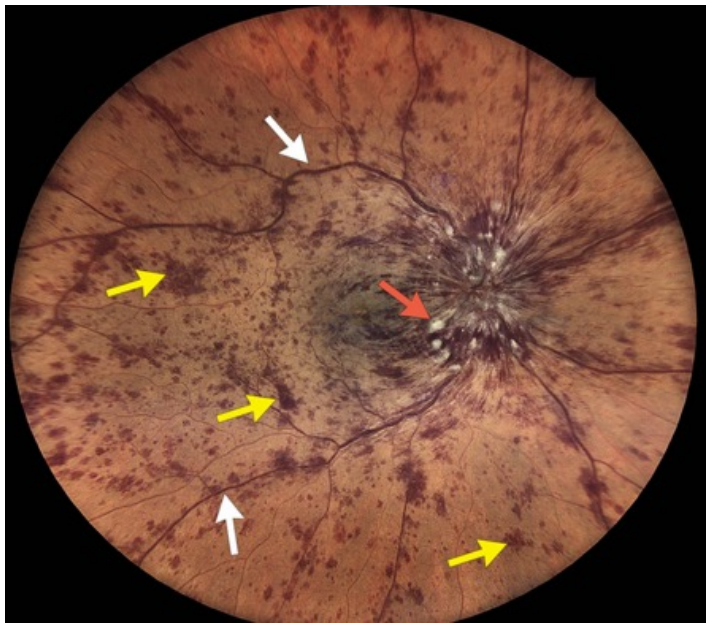

A diagnosis of central retinal-vein occlusion was made. Fundoscopy of the right eye showed retinal hemorrhages and marked venous dilatation in all four quadrants — findings known as “blood and thunder” appearance. Cotton-wool spots and optic-disk edema were also seen. Central retinal-vein occlusion occurs when an acute thrombus obstructs venous outflow from a proximal retinal vein, resulting in sudden-onset, painless vision loss. Improved control of cardiovascular disease risk factors was initiated.

A 65-year-old woman with diabetes, hypertension, and dyslipidemia presented to the ophthalmology clinic with a 14-hour history of painless, progressively worsening, blurry vision in the right eye. Physical examination was notable for a visual acuity of 20/400 in the right eye, with the patient unable to see fingers in the peripheral visual fields. There was a relative afferent pupillary defect in the right eye. What is the primary cause of this condition?

Acute ischemia of the optic nerve head

Compression of a distal retinal vein by an overlying arteriole

Degeneration of photoreceptors and retinal pigment epithelium

Obstruction of venous outflow from a proximal retinal vein

Occlusion of a central retinal artery from an embolism

Ein Zentralvenenverschluss (ZVV) ist eine ernste Gefäßerkrankung des Auges, bei der die Hauptvene der Netzhaut blockiert ist, was zu plötzlichem, schmerzlosem Sehverlust oder verschwommenem Sehen auf einem Auge führt. Er tritt meist bei über 55-Jährigen auf, oft begünstigt durch Bluthochdruck, Diabetes oder Gefäßerkrankungen. Die Diagnose erfolgt durch Funduskopie, die Behandlung zielt mit Anti-VEGF-Spritzen auf den Erhalt der Sehkraft ab.

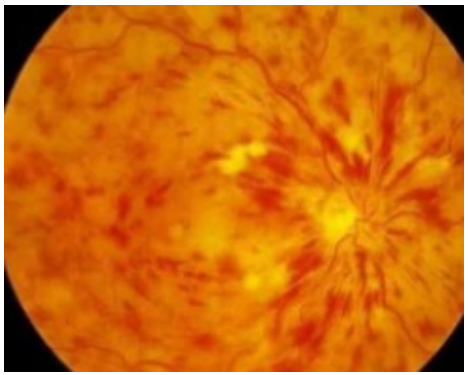

Wichtige Fakten zum Zentralvenenverschluss (CRVO):

•**Symptome:** Plötzliche, schmerzlose Sehverschlechterung, verschwommenes Sehen, Verzerrtsehen oder ein "dunkler Vorhang".

•**Ursachen:** Häufig ein Blutgerinnsel (Thrombose), oft assoziiert mit Bluthochdruck, Diabetes, hohen Blutfettwerten oder grünem Star (Glaukom).

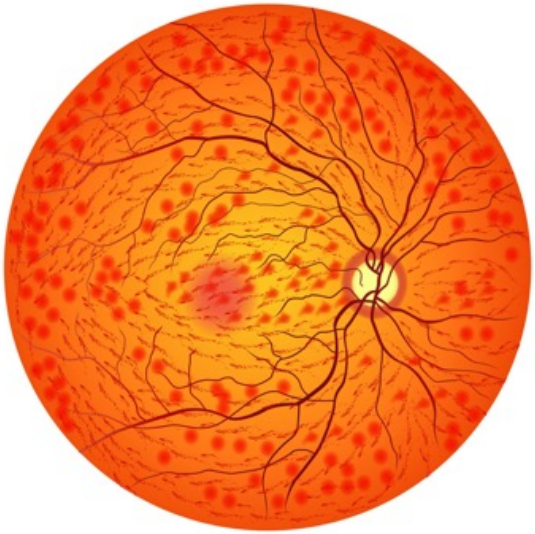

•**Formen:** Man unterscheidet zwischen der nicht-ischämischen Form (oft besserer Verlauf) und der schwereren ischämischen Form (schlechte Durchblutung).

•**Diagnose:** Augenärztliche Untersuchung des Augenhintergrunds (Funduskopie), Optische Kohärenztomographie (OCT) zur Darstellung von Schwellungen (Makulaödem), Fluoreszenzangiographie.

•**Behandlung:** Intravitreale operative Medikamenteneingabe (Anti-VEGF-Injektionen oder Steroide), um Schwellungen zu reduzieren. Manchmal Laserbehandlung.

•**Prognose:** Ohne Behandlung kann es zu dauerhaftem Sehverlust kommen; Früherkennung ist entscheidend.

Mikroaxiale Flowpumpen sind winzige mechanische Herzunterstützungssysteme, die Blut direkt aus dem Herzen in den Kreislauf befördern. Sie werden meist minimalinvasiv über einen Katheter (perkutan) eingesetzt, um ein geschwächtes Herz vorübergehend zu entlasten.

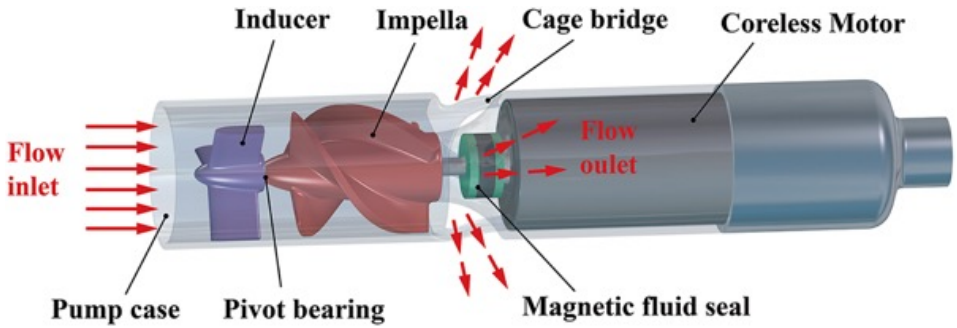

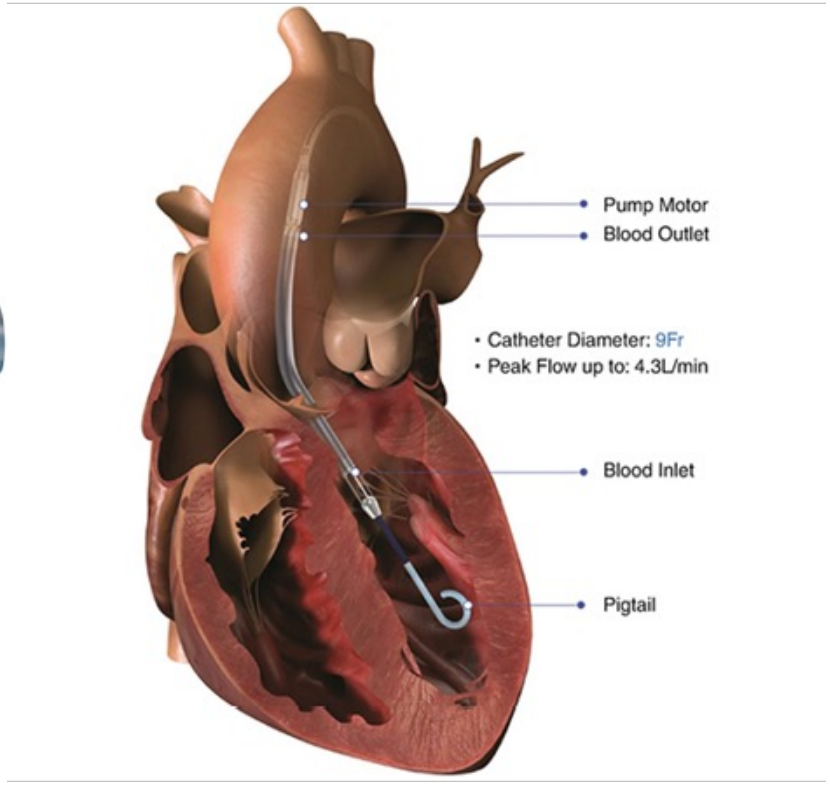

Left Ventricular Unloading in High-Risk Percutaneous Coronary Intervention

Complex percutaneous coronary intervention (PCI) in patients with severely impaired left ventricular function carries a high risk of death and complications. Whether percutaneous left ventricular unloading improves outcomes remains unclear.

We randomly assigned 300 patients with severe left ventricular dysfunction and extensive coronary artery disease in a 1:1 ratio to a strategy of elective unloading with a microaxial flow pump or to standard care during planned complex PCI. The primary outcome was a hierarchical composite that included death from any cause, disabling stroke, spontaneous myocardial infarction, hospitalization for cardiovascular causes, or periprocedural myocardial injury at a minimum of 12 months, as analyzed according to a win ratio.

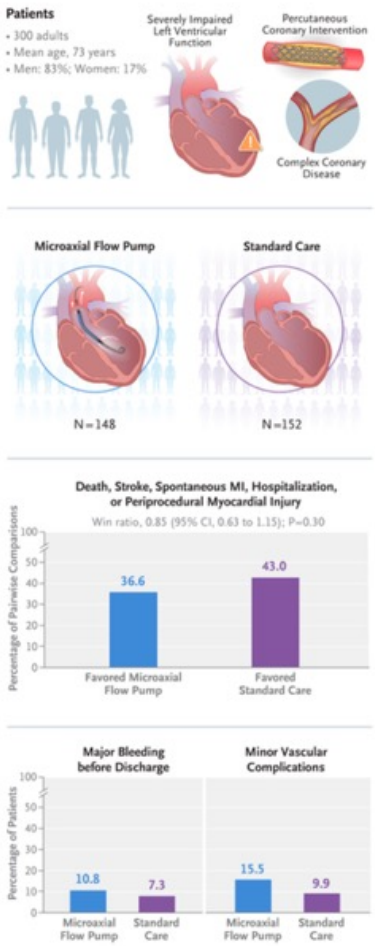

Microaxial flow pumps are percutaneous left ventricular assist devices that are advanced across the aortic valve to provide continuous nonpulsatile unloading of the left ventricle. In 2015, the Food and Drug Administration approved the use of these devices in patients with severe left ventricular dysfunction who were undergoing PCI. The indication was expanded in 2018 to include patients who were at lower risk with only a mildly reduced ejection fraction. Since then, the use of microaxial flow pumps to support high-risk PCI, a strategy that has been termed Protected PCI, has rapidly increased.

The randomized PROTECT II trial evaluated balloon counterpulsation as compared with a microaxial flow pump (Impella 2.5) in patients who were undergoing high-risk PCI. The trial was stopped prematurely because of likely futility. The safety and efficacy of these devices have not been compared with those of PCI without planned mechanical circulatory support in a randomized trial, even though the strategy has been shown to have fiscal implications and potential clinical disadvantages, including the risk of bleeding and vascular complications related to the need for large-bore vascular access. We designed the Controlled Trial of High-Risk Coronary Intervention with Percutaneous Left Ventricular Unloading (CHIP-BCIS3) to address the hypothesis that percutaneous left ventricular unloading with a microaxial flow pump would reduce the incidence of death and major adverse events, as compared with a strategy of PCI without planned circulatory support.

Methods

Trial Design and Oversight

The trial design has been described previously. CHIP-BCIS3 was a prospective, multicenter, open-label, randomized trial funded by the National Institute for Health and Care Research in the United Kingdom. Ethical approval was provided by the U.K. Health Research Authority; all the patients provided written informed consent.

Patients

Patients who were scheduled to undergo complex PCI were eligible for enrollment if they had a left ventricular ejection fraction of 35% or less (or ≤45% in the presence of severe mitral regurgitation) and had extensive coronary artery disease, as indicated by a British Cardiovascular Intervention Society Jeopardy Score (BCIS-JS) of 8 or more (on a scale ranging from 0 to 12, with higher scores indicating more extensive coronary artery disease).

Outcomes and Follow-up

The primary outcome was a hierarchical composite of death from any cause, disabling stroke, spontaneous myocardial infarction, hospitalization for cardiovascular causes, and periprocedural myocardial injury, as analyzed by means of a win ratio calculated with all available follow-up data.

Demogrraphics

	Microaxial Flow Pump (N=148)	Standard Care (N=152)
Age — yr	72.2±10.1	73.3±9.3
Male sex — no. (%)	125 (84.5)	123 (80.9)
Race or ethnic group — no. (%)†		
White	124 (83.8)	131 (86.2)
Black	3 (2.0)	2 (1.3)
Asian	21 (14.2)	16 (10.5)
Other ethnic group or missing data	0	3/152 (2.0)
Body-mass index‡	26.9±4.6	27.2±5.3
Medical history — no. (%)		
Hypertension	105 (70.9)	106 (69.7)
Diabetes	83 (56.1)	73 (48.0)
Current or previous smoker	88 (59.5)	92 (60.5)
Previous PCI	33 (22.3)	34 (22.4)
Previous CABG	11 (7.4)	5 (3.3)
Peripheral vascular disease	21 (14.2)	28 (18.4)
Median left ventricular ejection fraction (IQR) — %	26 (20–31)	28 (20–32)
Median pre-PCI high-sensitivity cardiac troponin level (IQR) — × ULN§	5 (1–26)	13 (3–55)
CCS angina severity class — no./total no. (%)¶		
0	32/137 (23.4)	30/136 (22.1)
1	15/137 (10.9)	20/136 (14.7)
2	32/137 (23.4)	30/136 (22.1)
3	39/137 (28.5)	35/136 (25.7)
4	19/137 (13.9)	21/136 (15.4)
NYHA functional class — no./total no. (%)‖		
I	21/141 (14.9)	17/135 (12.6)
II	56/141 (39.7)	55/135 (40.7)
III	51/141 (36.2)	52/135 (38.5)
IV	13/141 (9.2)	11/135 (8.1)
Median BCIS-JS (IQR)**	12 (10–12)	12 (10–12)
Median SYNTAX score (IQR)††	38 (28–47)	38 (31–49)
Urgent indication for PCI — no. (%)	107 (72.3)	121 (79.6)
Predicted PCI complexity — no. (%)		
Intended calcium modification	118 (79.7)	126 (82.9)
Intended left mainstem procedure	105 (70.9)	111 (73.0)
Intended retrograde procedure for chronic total occlusion	43 (29.1)	39 (25.7)

Secondary Outcomes.

Outcome	Microaxial Flow Pump (N=148)	Standard Care (N=152)	Hazard or Risk Ratio (95% CI)†
	number of patients (total number)		
Major secondary outcomes			
Death			
From any cause	47/148 (32.6)	33/152 (23.4)	1.54 (0.99–2.41)
From cardiovascular cause‡	36/148 (26.7)	20/152 (14.5)	1.91 (1.11–3.30)
Disabling stroke‡	3/148 (3.5)	6/152 (4.5)	0.53 (0.13–2.11)
Spontaneous myocardial infarction‡	9/148 (6.8)	15/152 (12.4)	0.64 (0.28–1.47)
Hospitalization for cardiovascular cause‡	32/148 (24.5)	29/152 (21.0)	1.20 (0.72–1.98)
Periprocedural myocardial injury§	82/133 (61.7)	62/124 (50.0)	1.23 (0.99–1.54)
Sensitivity analyses			
Nonhierarchical composite outcome			
Including periprocedural myocardial injury ¶	111/140 (79.3)	100/139 (73.6)	1.24 (0.94–1.62)
Excluding periprocedural myocardial injury	64/148 (45.3)	65/152 (45.4)	1.06 (0.75–1.49)

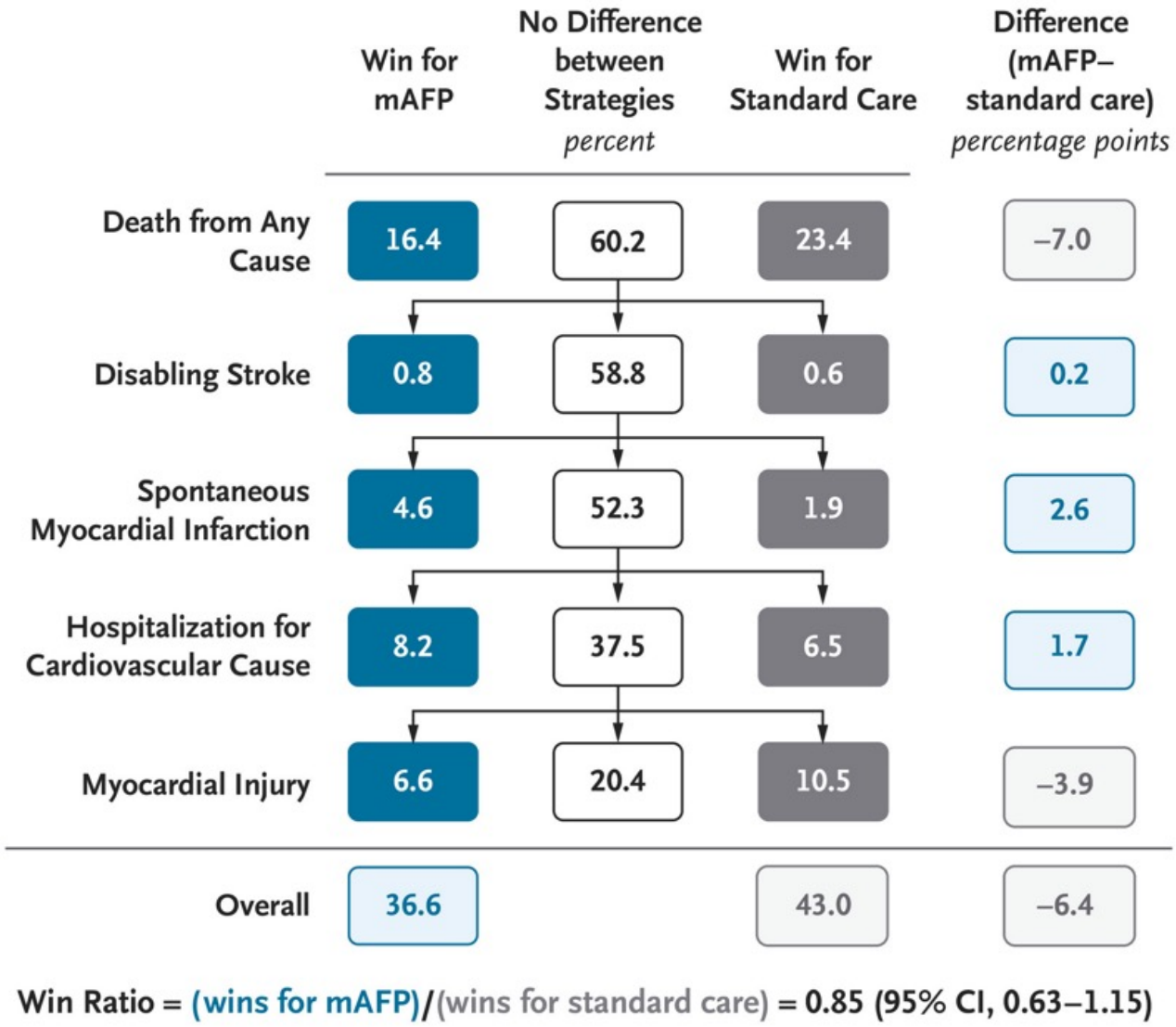

Win Ratio for the Hierarchical Composite Primary Outcome.

Shown are the results of pairwise comparisons, expressed as a percentage of all 22,496 comparisons, in the calculation of the win ratio for the primary outcome. Ties at each tier of the hierarchy were resolved by each successive tier (depicted by arrows). Overall, 36.6% favored the microaxial flow pump (mAFP), 43.0% favored standard care, and 20.4% resulted in a tie that could not be resolved. The between-group difference in the win ratio was –6.4 percentage points (95% CI, –18.4 to 5.7). The overall values may reflect rounding in individual categories.

Subgroup	No. of Patients	Win for mAFP	Win for Standard Care	Ties	Win Ratio (95% CI)
			percent		
Overall		36.6	43.0	20.4	0.85 (0.63–1.15)
Age					
<74.6 yr	150	35.9	39.5	24.6	0.91 (0.58–1.42)
≥74.6 yr	150	37.2	46.5	16.3	0.80 (0.53–1.21)
Sex					
Female	52	38.7	52.5	8.8	0.74 (0.37–1.46)
Male	248	35.3	41.0	23.7	0.86 (0.61–1.22)
Body-surface area					
<1.91 m^2	150	40.6	45.1	14.3	0.90 (0.60–1.35)
≥1.91 m^2	150	32.0	40.6	27.4	0.79 (0.50–1.24)
BCIS-JS					
<12	98	36.8	34.2	29.0	1.07 (0.61–1.90)
12	198	35.2	48.0	16.8	0.73 (0.51–1.06)
Left ventricular ejection fraction					
<27%	144	39.0	41.6	19.4	0.94 (0.61–1.45)
≥27%	156	34.8	44.6	20.6	0.78 (0.51–1.19)
NT-pro-BNP					
<3545 pg/ml	117	37.2	33.4	29.3	1.11 (0.66–1.89)
≥3545 pg/ml	117	32.2	56.6	11.2	0.57 (0.36–0.91)
Intended left main stem PCI					
Yes	216	39.7	42.7	17.6	0.93 (0.65–1.32)
No	84	27.6	44.5	28.0	0.62 (0.33–1.15)
Indication for PCI					
Stable	112	37.3	37.2	25.5	1.00 (0.60–1.68)
Acute coronary syndrome	188	36.0	45.9	18.1	0.78 (0.54–1.15)

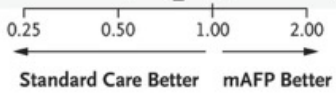

Subgroup Analysis of the Primary Outcome.

Shown is the between-group difference in the win ratio for the composite primary outcome according to prespecified subgroups among the patients who had received a microaxial flow pump and those who had received standard care. The British Cardiovascular Intervention Society Jeopardy Score (BCIS-JS) ranges from 0 to 12, with higher scores indicating more extensive coronary artery disease. CI denotes confidence interval, NT-pro-BNP N-terminal pro–B-type natriuretic peptide, and PCI percutaneous coronary intervention. The widths of the confidence intervals have not been adjusted for multiplicity and should not be used to infer treatment effect.

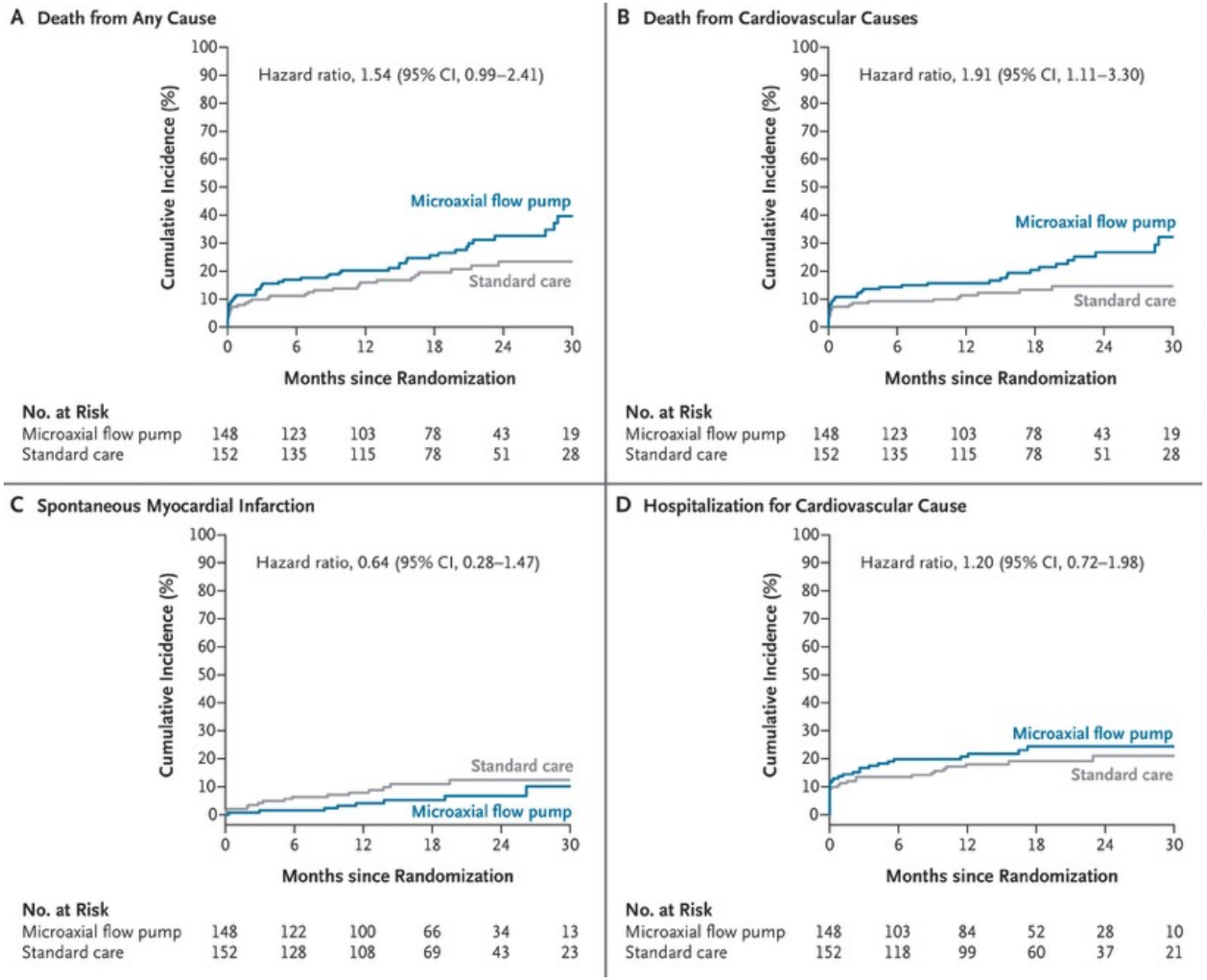

Secondary Outcomes.

Shown are Kaplan–Meier plots for death from any cause (Panel A), death from cardiovascular causes (Panel B), spontaneous myocardial infarction (Panel C), and hospitalization for cardiovascular cause (Panel D). The widths of the confidence intervals have not been adjusted for multiplicity and should not be used to infer treatment effect.

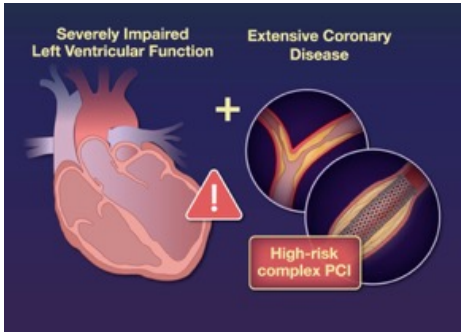
Severely Impaired Left Ventricular Function
Extensive Coronary Disease
High-risk complex PCI

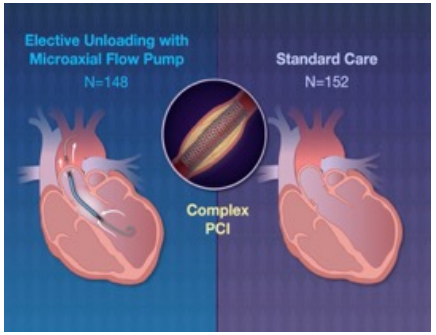
Elective Unloading with Microaxial Flow Pump
N=148
Standard Care
N=152
Complex PCI

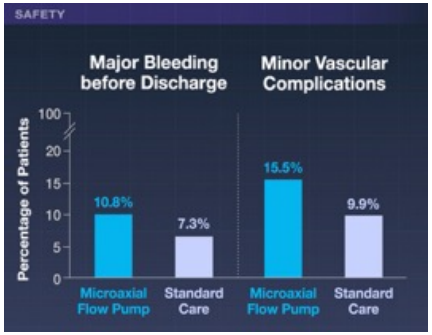
SAFETY
Major Bleeding before Discharge
Minor Vascular Complications
Percentage of Patients
100
20
15
10
5
0
10.8%
7.3%
15.5%
9.9%
Microaxial Flow Pump
Standard Care
Microaxial Flow Pump
Standard Care

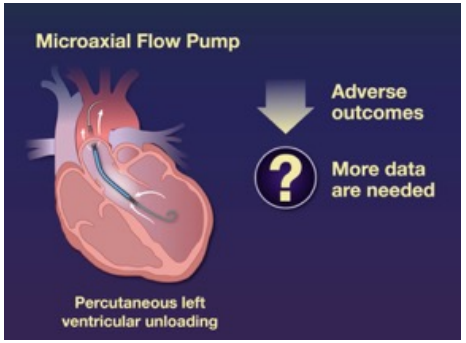
Microaxial Flow Pump
Adverse outcomes
More data are needed
Percutaneous left ventricular unloading

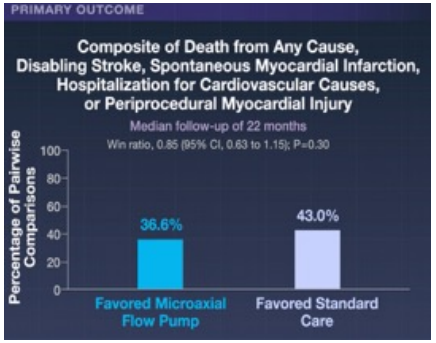
PRIMARY OUTCOME
Composite of Death from Any Cause, Disabling Stroke, Spontaneous Myocardial Infarction, Hospitalization for Cardiovascular Causes, or Periprocedural Myocardial Injury
Median follow-up of 22 months
Win ratio, 0.85 (95% CI, 0.63 to 1.15); P=0.30
Percentage of Pairwise Comparisons
100
80
60
40
20
0
36.6%
43.0%
Favored Microaxial Flow Pump
Favored Standard Care

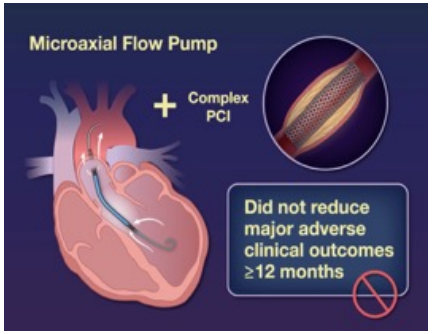
Microaxial Flow Pump
Complex PCI
Did not reduce major adverse clinical outcomes ≥12 months

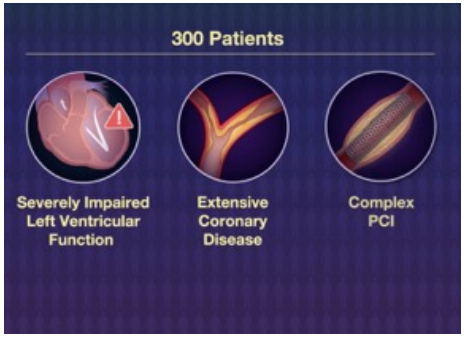
300 Patients
Severely Impaired Left Ventricular Function
Extensive Coronary Disease
Complex PCI

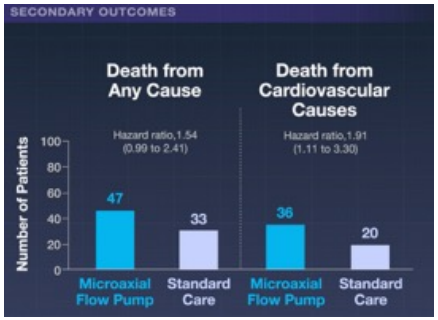
SECONDARY OUTCOMES
Death from Any Cause
Death from Cardiovascular Causes
Hazard ratio,1.54 (0.99 to 2.41)
Hazard ratio,1.91 (1.11 to 3.30)
Number of Patients
100
80
60
40
20
0
47
33
36
20
Microaxial Flow Pump
Standard Care
Microaxial Flow Pump
Standard Care

Das duktale Adenokarzinom des Pankreas (PDAC) ist die häufigste Form von Bauchspeicheldrüsenkrebs und macht über **90 % aller Fälle** aus. Es entsteht in den Zellen, die die Gänge der Bauchspeicheldrüse auskleiden.

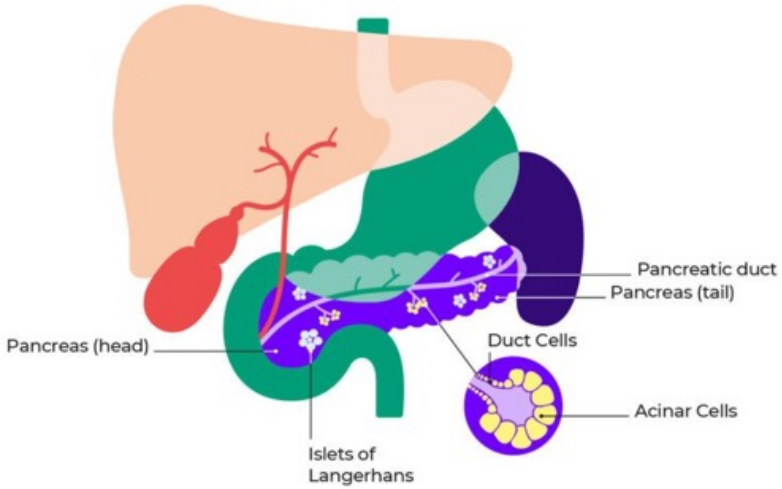

Wichtige Fakten auf einen Blick

•**Häufigkeit:** Es ist weltweit die vierthäufigste Krebstodesursache.

•**Prognose:** Die 5-Jahres-Überlebensrate liegt oft bei unter **10 %**.

•**Diagnose:** Meist erst in fortgeschrittenem Stadium entdeckt, da frühe Symptome fehlen.

•**Lage:** Etwa zwei Drittel der Tumoren treten im Pankreaskopf auf

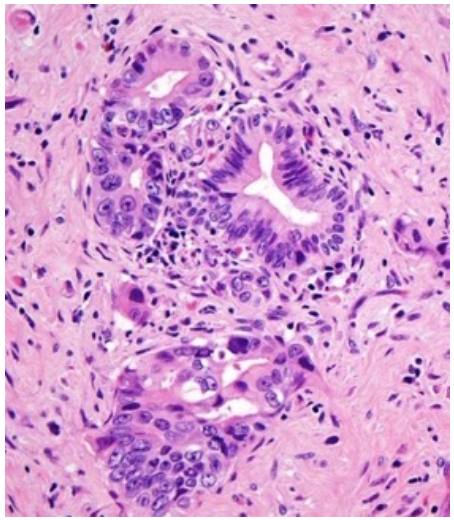

Daraxonrasib (Entwicklungscode: **RMC-6236**) ist ein neuartiges Krebsmedikament, das als Durchbruch in der Behandlung von Tumoren mit Mutationen im **RAS-Gen** (insbesondere **KRAS-Mutationen**) gilt. Es wird vom US-Biotech-Unternehmen **Revolution Medicines** entwickelt.

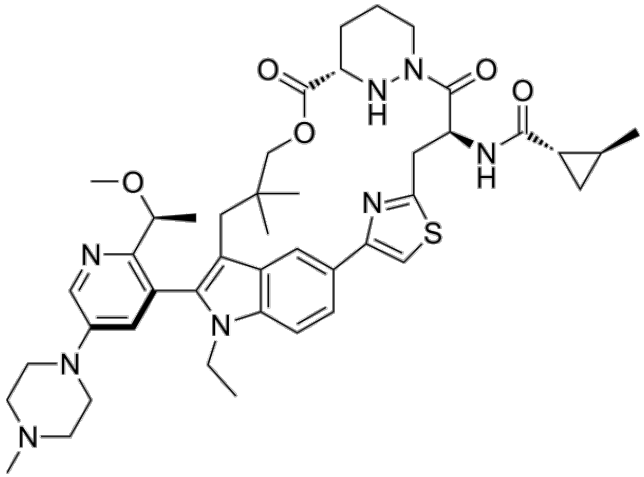

- **Wirkmechanismus**: Als sogenannter **multi-selektiver RAS(ON)-Inhibitor** blockiert Daraxonrasib die aktive Form verschiedener RAS-Proteine, die das Zellwachstum bei Krebs antreiben.
- **Haupteinsatzgebiete**: Das Medikament wird primär zur Behandlung von **metastasiertem Bauchspeicheldrüsenkrebs** (PDAC) und **nicht-kleinzelligem Lungenkrebs** (NSCLC) erforscht.
- **Studienergebnisse**: In der klinischen Phase-3-Studie **RASolute 302** konnte bei Patienten mit Bauchspeicheldrüsenkrebs eine signifikante Verlängerung des Gesamtüberlebens nachgewiesen werden – in einigen Berichten ist von einer Verdopplung der Überlebenszeit die Rede.

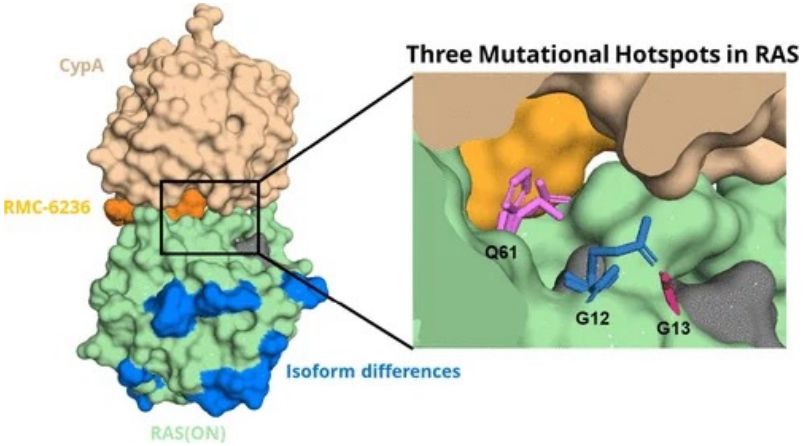

Daraxonrasib in Previously Treated Advanced *RAS*-Mutated Pancreatic Cancer

Current therapies for patients with pancreatic ductal adenocarcinoma (PDAC) provide modest benefit. Activating *RAS* mutations occur in more than 90% of PDAC tumors. Daraxonrasib (RMC-6236) is an oral RAS(ON) multiselective inhibitor that targets guanosine triphosphate–bound mutant and wild-type RAS.

In this phase 1–2 study, we evaluated daraxonrasib in patients with advanced solid tumors with activating *RAS* mutations. Patients received 10 to 400 mg of daraxonrasib orally once daily; 300 mg was selected as the phase 3 dose. The primary end point was safety. Pharmacokinetics and antitumor activity were secondary end points. This report focuses on the 168 study patients with previously treated *RAS*-mutated PDAC.

Conclusions

Daraxonrasib was associated with treatment-related adverse events of grade 3 or higher in one third of patients with previously treated *RAS*-mutated PDAC; antitumor activity was also reported. (Funded by Revolution Medicines; RMC-6236-001 ClinicalTrials.gov number, NCT05379985.)

KRAS G12C mutations are rare in PDAC (with a frequency of 1 to 2%), which limits the clinical utility of these agents in this disease. Moreover, because most *RAS* mutations in PDAC drive constitutive signaling through the GTP-bound(ON) state, the inhibition of activated RAS by RAS(OFF) inhibitors is often incomplete. The efficacy of these inhibitors is further limited by resistance, including the development of secondary *RAS* mutations. Thus, therapies that target active, GTP-bound RAS and address diverse *RAS* variants are needed.

Daraxonrasib (RMC-6236) is an orally bioavailable, RAS(ON) multiselective, noncovalent inhibitor with activity against the active state of mutant and wild-type KRAS, HRAS, and NRAS. By forming a tri-complex with cyclophilin A and GTP-bound RAS within cells, daraxonrasib sterically blocks RAS effector binding and potently suppresses downstream signaling. Preclinical studies have shown deep and durable responses to daraxonrasib across *RAS*-mutated cancers, which have been most pronounced in tumors with mutations at codon 12. These findings have included marked regressions in pancreatic cancer models. In an earlier analysis of this multicenter, open-label, phase 1–2 study involving patients with advanced solid tumors harboring *RAS* mutations, treatment-related adverse events of grade 3 or more occurred in 16 of 111 (14.4%) patients, and preliminary antitumor activity was observed. Here, we report the results of the RMC-6236-001 study, in which we evaluated the safety, dose-optimization level, and antitumor activity of daraxonrasib in patients with previously treated advanced *RAS*-mutated PDAC.

Characteristic	All Pati… (N=1…)
Median age (range) — yr	65 (30–86)
Sex — no. (%)	
Female	75 (45)
Male	93 (55)
Race — no. (%)†	
White	129 (77)
Black	3 (2)
Other	22 (13)
Missing data	14 (8)
ECOG performance-status score — no. (%)‡	
0	53 (32)
1	115 (68)
Cancer stage at diagnosis — no. (%)	
I	15 (9)
II	30 (18)
III	32 (19)
IV	88 (52)
Missing data	3 (2)
Previous systemic therapy	
Median number (range)	2 (1–6)
Anticancer treatment for metastatic disease — no. (%)	
1	70 (42)
≥2	98 (58)
Specific chemotherapy regimen for metastatic disease — no. (%)	
Gemcitabine and nab-paclitaxel	101 (60)
FOLFIRINOX§	73 (43)
FOLFIRI¶	19 (11)
FOLFOX‖	13 (8)
Nanoliposomal irinotecan, 5-fluorouracil, and leucovorin	5 (3)
History of pancreatic resection — no. (%)	66 (39)
Whipple procedure	60 (36)
Other	6 (4)
Sites of metastases — no. (%)	
Liver	112 (67)
Lung	78 (46)
RAS mutation — no. (%)	
KRAS G12D	65 (39)
KRAS G12V	52 (31)
KRAS G12R	28 (17)
Other *RAS* G12**	4 (2)
Non-*RAS* G12††	19 (11)
Co-occurring genomic alterations — no./total no. (%)	
TP53	120/162 (74)
SMAD4	40/162 (25)
CDKN2A	56/162 (35)
CDKN2B	13/162 (8)
Missing data	6/168 (4)

Safety Summary in Patients with *RAS*-Mutated PDAC.

Adverse Event	Dose of Daraxonrasib							
	All Doses (N=168)		≤120 mg (N=34)		160–220 mg (N=51)		300 mg (N=83)	
	Any Grade	Grade ≥3	Any Grade	Grade ≥3	Any Grade	Grade ≥3	Any Grade	Grade ≥3
	number of patients (percent)							
Treatment-related adverse event								
Any	161 (96)	50 (30)	30 (88)	9 (26)	51 (100)	13 (25)	80 (96)	28 (34)
Leading to dose modification	67 (40)	34 (20)	8 (24)	5 (15)	19 (37)	11 (22)	40 (48)	18 (22)
Dose interruption	62 (37)	33 (20)	8 (24)	5 (15)	18 (35)	11 (22)	36 (43)	17 (20)
Dose reduction	36 (21)	19 (11)	4 (12)	3 (9)	7 (14)	5 (10)	25 (30)	11 (13)
Leading to discontinuation	1 (1)	1 (1)	1 (3)	1 (3)	0	0	0	0
Treatment-related serious adverse event	10 (6)	7 (4)	2 (6)	1 (3)	3 (6)	2 (4)	5 (6)	4 (5)
Treatment-related adverse event reported in >10% of patients								
Rash†	147 (88)	11 (7)	26 (76)	0	46 (90)	5 (10)	75 (90)	6 (7)
Diarrhea	77 (46)	5 (3)	13 (38)	2 (6)	21 (41)	0	43 (52)	3 (4)
Nausea	70 (42)	0	11 (32)	0	27 (53)	0	32 (39)	0
Stomatitis or mucositis‡	67 (40)	6 (4)	4 (12)	1 (3)	18 (35)	2 (4)	45 (54)	3 (4)
Vomiting	52 (31)	0	10 (29)	0	12 (24)	0	30 (36)	0
Fatigue	33 (20)	3 (2)	5 (15)	0	14 (27)	2 (4)	14 (17)	1 (1)
Paronychia	25 (15)	0	2 (6)	0	8 (16)	0	15 (18)	0
Decreased appetite	18 (11)	2 (1)	4 (12)	1 (3)	4 (8)	1 (2)	10 (12)	0
Dry skin	17 (10)	0	1 (3)	0	4 (8)	0	12 (14)	0

Confirmed Best Overall Response, According to Line of Therapy.

Response	Second-Line Therapy†		Third- or Later-Line Therapy	
	RAS G12–Mutated (N=26)	All *RAS*-Mutated (N=38)	*RAS* G12–Mutated (N=38)	All *RAS*-Mutated (N=45)
Any objective response‡				
No. of patients	9	11	8	9
% (95% CI)	35 (17–56)	29 (15–46)	21 (10–37)	20 (10–35)
Type of response — no. (%)				
Complete	1 (4)	1 (3)	0	0
Partial	8 (31)	10 (26)	8 (21)	9 (20)
Stable disease	15 (58)	25 (66)	25 (66)	29 (64)
Progressive disease	1 (4)	1 (3)	4 (11)	5 (11)
Not evaluable§	1 (4)	1 (3)	1 (3)	2 (4)
Disease control¶				
No. of patients	24	36	33	38
% (95% CI)	92 (75–99)	95 (82–99)	87 (72–96)	84 (71–94)
Median duration of response (95% CI) — months	8.2 (3.8–NE)	8.2 (3.8–8.8)	3.5 (2.9–NE)	3.3 (2.8–NE)

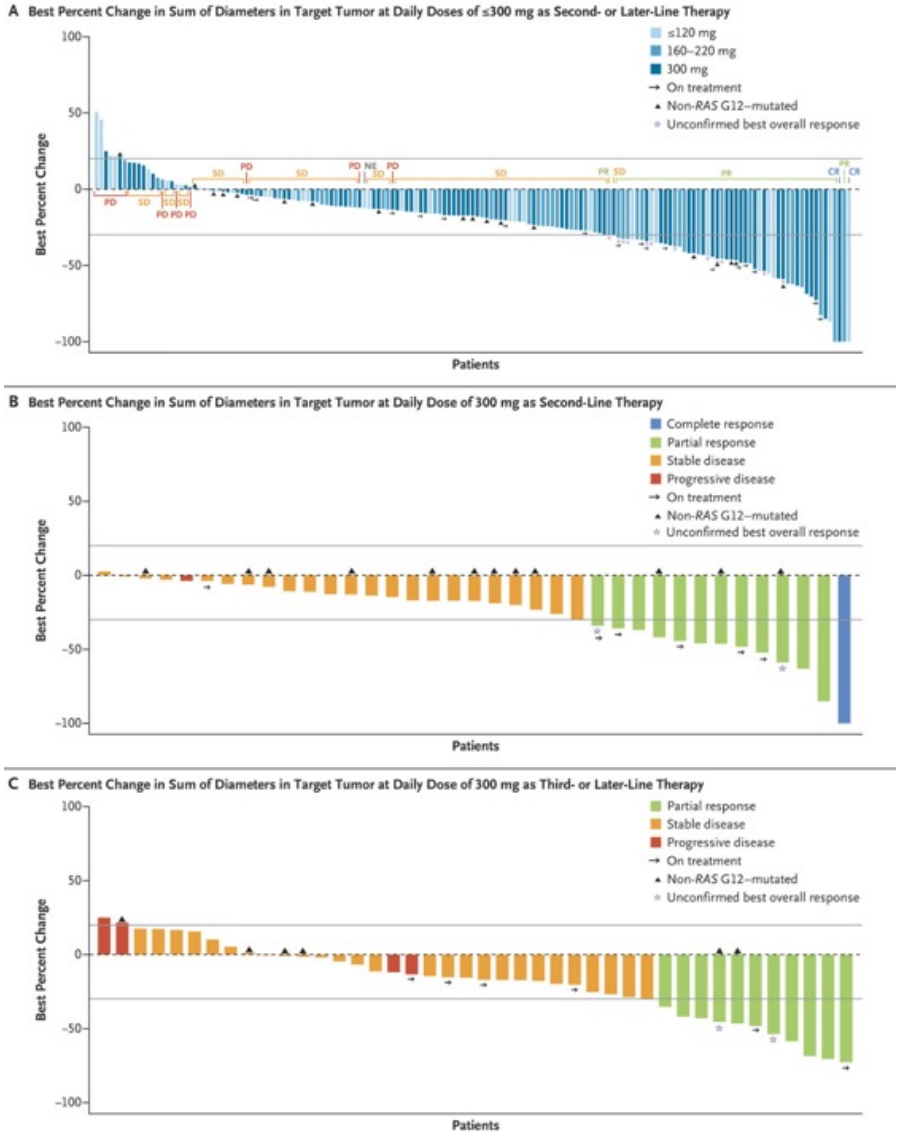

Antitumor Activity of Daraxonrasib in *RAS*-Mutated PDAC.

Shown is the best percent change from baseline in tumor burden among patients with pancreatic ductal adenocarcinoma (PDAC) who received daraxonrasib at daily doses of 300 mg or less as second- or later-line therapy (Panel A), among those who received 300 mg as second-line therapy (Panel B), and among those who received 300 mg as third- or later-line therapy (Panel C). In each panel, the asterisk indicates that the value was the unconfirmed best overall response according to the Response Evaluation Criteria in Solid Tumors (RECIST), version 1.1. CR denotes complete response, G12 glycine 12, NE not evaluable, PD progressive disease, PR partial response, and SD stable disease.

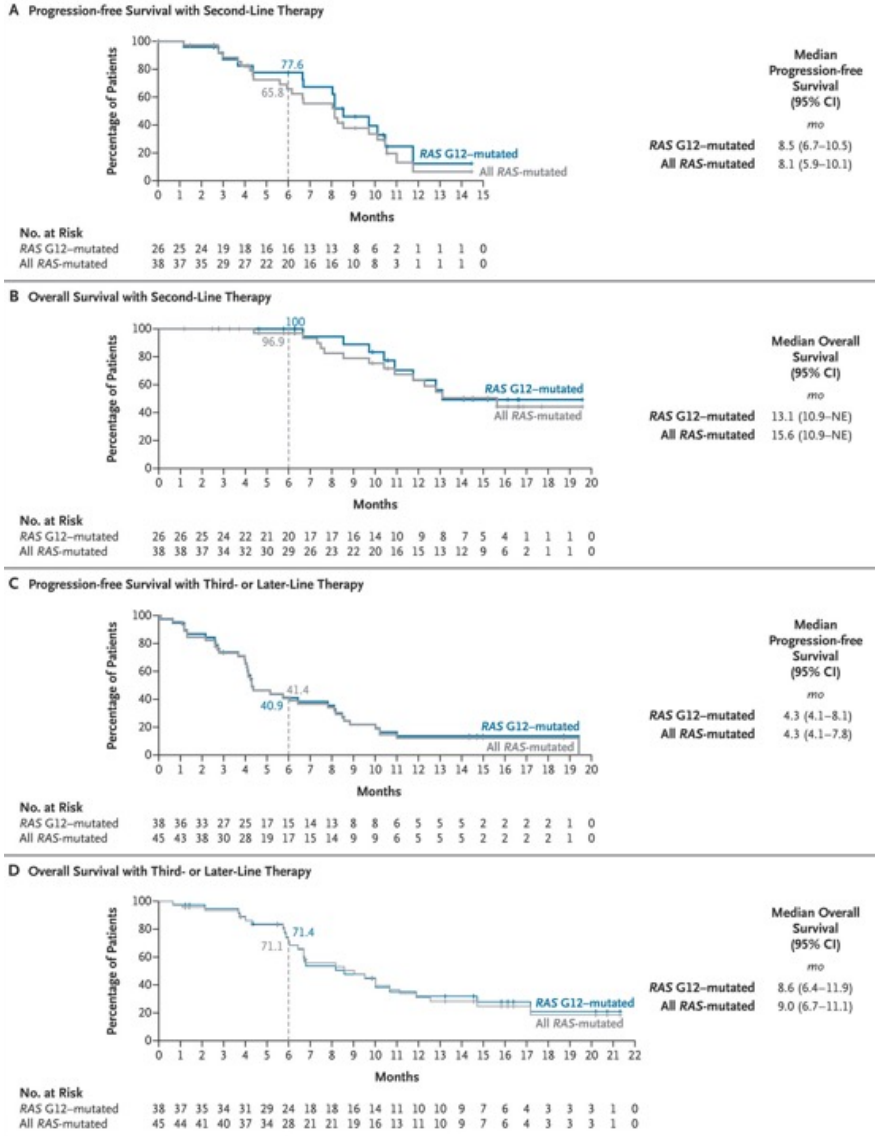

Survival in Patients with *RAS* G12–Mutated and All-*RAS*-Mutated PDAC.

Shown are data for the study patients who received 300 mg of daraxonrasib daily, as reported according to whether they received the drug as second-line therapy (Panels A and B) or third- or later-line therapy (Panels C and D). In these two categories, data are shown regarding the median progression-free survival (Panels A and C) and overall survival (Panels B and D). The two curves indicate whether the patients had tumors with *RAS* G12 mutations or any *RAS* mutations.

Discussion

At 300 mg, daraxonrasib produced objective responses and disease control in patients with *RAS*-mutated PDAC. Although preclinical data suggested greatest activity against *RAS* G12 mutations, the current clinical dataset is too small to establish variant-specific differences. Although direct comparisons cannot be made, the results of this study suggest that across PDAC with varied *RAS* mutations, progression-free and overall survival estimates exceeded those that have been historically reported with second-line chemotherapy. By inhibiting all three *RAS* isoforms, as well as all key *RAS* mutations and wild-type *RAS* in the active, GTP-bound state, daraxonrasib offers comprehensive RAS inhibition as compared with the allele-specific activity of KRAS G12C inhibitors that target only the inactive, GDP-bound state. Daraxonrasib appeared to show a higher response rate and longer survival relative to published results for KRAS G12C inhibitors in PDAC, although cross-trial comparisons are not reliable.

Among patients with previously treated *RAS*-mutated PDAC, daraxonrasib showed antitumor activity and was associated with treatment-related adverse events of grade 3 or higher in one third of patients.

mRNA-Impfstoffe (Boten-RNA-Impfstoffe) stellen eine revolutionäre Technologie dar, die dem Körper nicht den Krankheitserreger selbst, sondern eine genetische "Bauanleitung" liefert.

Funktionsweise

•**Anleitung statt Erreger**: Der Impfstoff enthält synthetische mRNA, die Zellen beibringt, ein spezifisches Protein (Antigen) des Erregers selbst herzustellen.

•**Immunantwort**: Das Immunsystem erkennt dieses Protein als fremd und bildet Antikörper sowie T-Zellen.

•**Abbau**: Die mRNA wird nach kurzer Zeit vom Körper natürlich abgebaut und hinterlässt keine dauerhaften Spuren im Erbgut.

•**Keine DNA-Änderung**: mRNA gelangt nie in den Zellkern, wo die DNA gespeichert ist; eine genetische Veränderung ist biologisch ausgeschlossen.

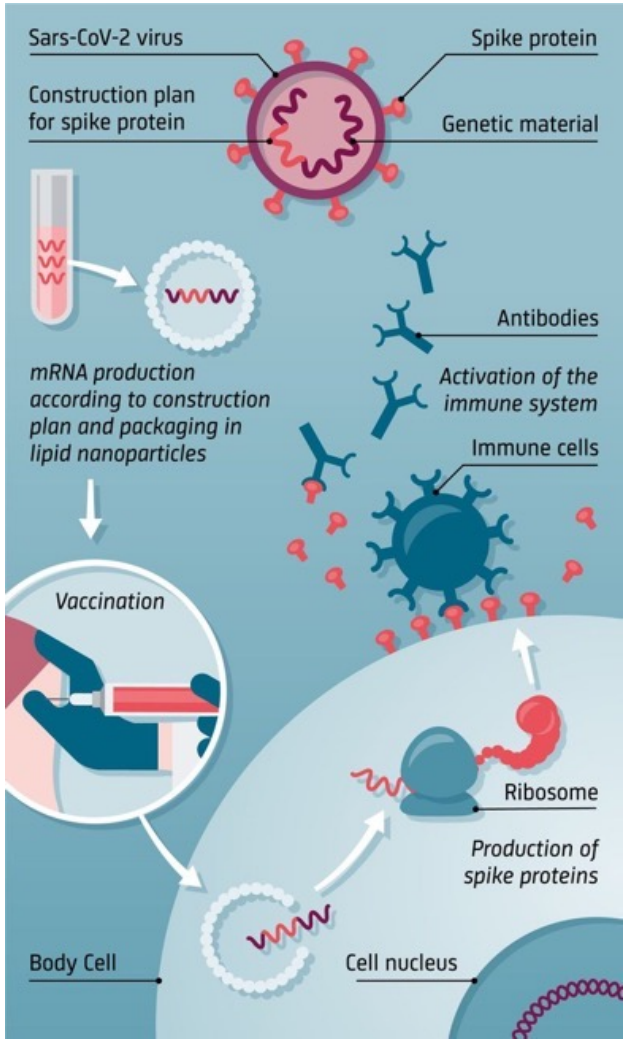

Efficacy and Safety of an mRNA Seasonal Influenza Vaccine in Adults

Seasonal influenza causes substantial illness and death in adults 50 years of age or older, even with current vaccines. An investigational messenger RNA (mRNA)–based vaccine called mRNA-1010 encodes hemagglutinin glycoproteins from World Health Organization–recommended influenza strains.

In this phase 3, double-blind, active-controlled trial, we randomly assigned adults 50 years of age or older to receive trivalent mRNA-1010 (37.5 µg, which includes 12.5 µg of each strain) or a licensed standard-dose comparator. The primary efficacy end point was relative vaccine efficacy against reverse-transcriptase–polymerase-chain-reaction (RT-PCR)–confirmed, protocol-defined influenza-like illness caused by influenza A or B, from at least 14 days after vaccination through the end of the influenza season. Hypothesis testing was conducted hierarchically to assess noninferiority (lower boundary of the 95% confidence interval [CI], >−10%), superiority (lower boundary of the 95% CI, >0%), and a higher level of superiority (lower boundary of the 95% CI, >9.1%).

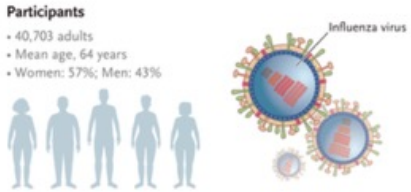

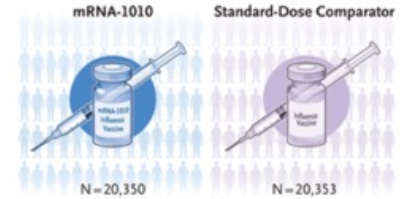

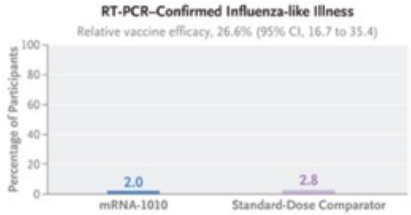

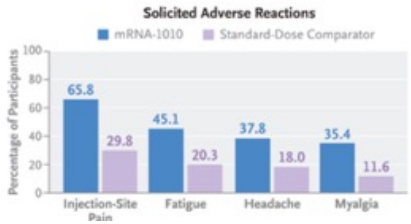

Enhanced (high-dose, adjuvanted, or recombinant-based) influenza vaccines provide greater protection in older adults than standard-dose formulations, although effectiveness varies according to season and match to circulating strains. Most licensed vaccines rely on egg-based platforms. Egg-based production is time-consuming and can introduce egg-adaptive mutations, which reduce antigenic match with circulating strains. A need remains for influenza vaccines that can be rapidly updated to evolving strains and elicit robust protection.

The investigational seasonal influenza vaccine mRNA-1010 encodes surface hemagglutinin (HA) antigens from the three WHO-recommended 2024–2025 strains for cell- or recombinant-based vaccines: A/H1N1, A/H3N2, and B/Victoria. By avoiding egg-based production and enabling rapid strain updates, the messenger RNA (mRNA) platform addresses key limitations of current influenza vaccines and may improve protection in older adults.

The Fluent trial was conducted during the 2024–2025 Northern Hemisphere influenza season to evaluate the relative vaccine efficacy of mRNA-1010 as compared with licensed standard-dose influenza vaccines in preventing laboratory-confirmed influenza-like illness in adults 50 years of age or older. Here, we report the findings from the primary analyses of this pivotal phase 3 trial.

Trial Design and Oversight

This phase 3, double-blind, randomized, active-controlled trial enrolled participants at 301 sites in 11 countries in the Northern Hemisphere. The trial was approved by appropriate institutional review boards and was conducted according to the applicable principles of the International Council for Harmonisation Good Clinical Practice guidelines, the E6(R2) Good Clinical Practice guidelines, the principles of the Declaration of Helsinki, and all local laws or regulations. All the participants provided written informed consent before enrollment. Oversight was provided by an independent data and safety monitoring board.

A sponsor, Moderna, was responsible for overall trial design, site selection, monitoring, and data analysis, which were facilitated by Parexel International.

Trial Participants

Eligible participants were adults 50 years of age or older who were in medically stable condition.

Trial Procedures

The mRNA-1010 vaccine contained mRNAs encoding HA antigens of the WHO-recommended 2024–2025 cell- or recombinant-based influenza strains for the 2024–2025 Northern Hemisphere season. Participants were randomly assigned (in a 1:1 ratio) to receive a single intramuscular injection of mRNA-1010 (37.5-µg trivalent formulation, which includes 12.5 µg of each strain) or a licensed standard-dose inactivated seasonal influenza vaccine,

Efficacy Assessments

The primary efficacy objective was to evaluate the relative vaccine efficacy of mRNA-1010 as compared with a standard-dose comparator against the first episode of protocol-defined influenza-like illness caused by any influenza A or B strain confirmed by a reverse-transcriptase–polymerase-chain-reaction (RT-PCR) assay, beginning at least 14 days after injection through the end of the influenza season. Efficacy end-point events were identified through active surveillance, including twice-weekly e-diary prompts to report respiratory symptoms from day 1 through the end of the influenza season.

Characteristic	mRNA-1010 (N=20,350)	Standard-Dose Comparator (N=20,353)	Total (N=40,703)
Age at enrollment — yr	64.2±8.3	64.2±8.4	64.2±8.3
Age group — no. (%)			
≥50 to <65 yr	10,624 (52.2)	10,615 (52.2)	21,239 (52.2)
≥65 yr	9,726 (47.8)	9,738 (47.8)	19,464 (47.8)
65 to <75 yr	7,372 (36.2)	7,375 (36.2)	14,747 (36.2)
≥75 yr	2,354 (11.6)	2,363 (11.6)	4,717 (11.6)
Sex — no. (%)			
Male	8,834 (43.4)	8,720 (42.8)	17,554 (43.1)
Female	11,516 (56.6)	11,633 (57.2)	23,149 (56.9)
Race or ethnic group — no. (%)†			
White	16,814 (82.6)	16,811 (82.6)	33,625 (82.6)
Black	2,687 (13.2)	2,698 (13.3)	5,385 (13.2)
Asian	496 (2.4)	483 (2.4)	979 (2.4)
Other	252 (1.2)	264 (1.3)	516 (1.3)
Unknown or not reported	101 (0.5)	97 (0.5)	198 (0.5)
Hispanic or Latino ethnic group — no. (%)†			
Yes	2,147 (10.6)	2,067 (10.2)	4,214 (10.4)
No	17,908 (88.0)	17,985 (88.4)	35,893 (88.2)
Unknown or not reported	295 (1.4)	301 (1.5)	596 (1.5)
Geographic region — no. (%)			
North America	14,333 (70.4)	14,340 (70.5)	28,673 (70.4)
Rest of the world‡	6,017 (29.6)	6,013 (29.5)	12,030 (29.6)
Body-mass index§	29.4±6.3	29.5±6.4	29.4±6.4
Influenza vaccination in the previous influenza season — no. (%)			
Received	9,569 (47.0)	9,547 (46.9)	19,116 (47.0)
Not received	10,781 (53.0)	10,806 (53.1)	21,587 (53.0)
Frailty status of participants ≥65 yr of age — no./total no. (%)¶			
Fit	7136/9726 (73.4)	7135/9738 (73.3)	14,271/19,464 (73.3)
Vulnerable	1755/9726 (18.0)	1740/9738 (17.9)	3,495/19,464 (18.0)
Frail	820/9726 (8.4)	843/9738 (8.7)	1,663/19,464 (8.5)
Missing data	15/9726 (0.2)	20/9738 (0.2)	35/19,464 (0.2)
High-risk status — no. (%)‖			
Yes	11,591 (57.0)	11,614 (57.1)	23,205 (57.0)
No	8,759 (43.0)	8,739 (42.9)	17,498 (43.0)

Relative Vaccine Efficacy (Per-Protocol Efficacy Population).

End Point	mRNA-1010 (N=20,179)	Standard-Dose Comparator (N=20,124)	Relative Vaccine Efficacy (95% CI)
	no. of participants (%)		*percent*
Primary end point: first occurrence of RT-PCR–confirmed, protocol-defined influenza-like illness caused by any influenza A or B strain	411 (2.0)	557 (2.8)	26.6 (16.7 to 35.4)†‡
Caused by any influenza A	386 (1.9)	522 (2.6)	26.5 (16.1 to 35.5)§
Caused by influenza A/H1N1	223 (1.1)	315 (1.6)	29.6 (16.4 to 40.7)§
Caused by influenza A/H3N2	158 (0.8)	202 (1.0)	22.2 (4.3 to 36.9)§
Caused by influenza B	25 (0.1)	35 (0.2)	29.1 (−18.5 to 57.5)§
First occurrence of RT-PCR–confirmed, modified CDC-defined influenza-like illness caused by any influenza A or B strain	223 (1.1)	290 (1.4)	23.5 (9.0 to 35.8)†¶
Caused by any influenza A	211 (1.0)	276 (1.4)	24.0 (9.1 to 36.5)§
Caused by influenza A/H1N1	125 (0.6)	172 (0.9)	27.7 (9.0 to 42.6)§
Caused by influenza A/H3N2	83 (0.4)	102 (0.5)	19.1 (−8.1 to 39.5)§
Caused by influenza B	12 (<0.1)	14 (<0.1)	14.8 (−84.3 to 60.6)§

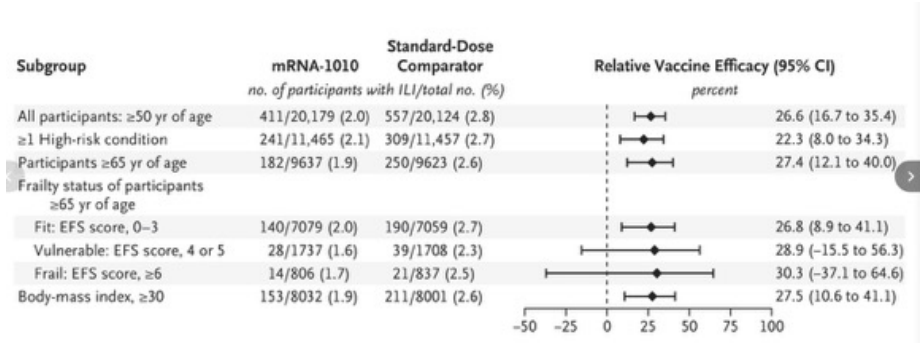

Relative Vaccine Efficacy of mRNA-1010 as Compared with Licensed Influenza Vaccines According to High-Risk Subgroup (Per-Protocol Efficacy Population).

The figure shows estimates of relative vaccine efficacy with 95% confidence intervals for mRNA-1010 as compared with licensed standard-dose influenza vaccines (standard-dose comparator) across prespecified subgroups: participants 50 years of age or older with at least one high-risk medical condition, frailty status among participants 65 years of age or older (categorized as fit, vulnerable, or frail.

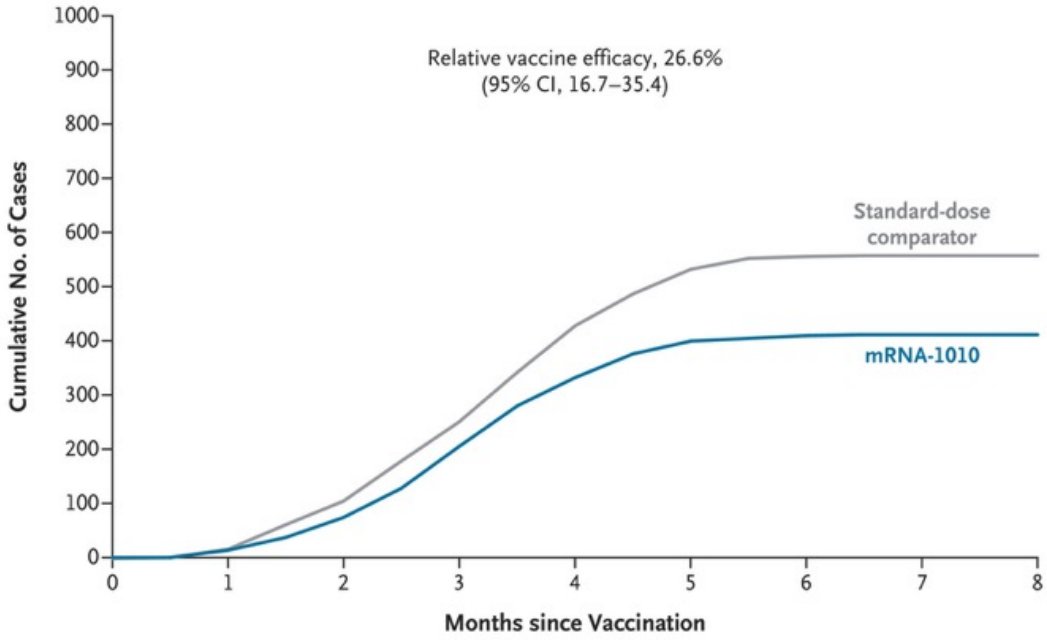

No. at Risk									
Standard-dose comparator	20,124	19,871	19,663	19,383	19,027	18,774	10,098	1932	0
mRNA-1010	20,179	19,930	19,765	19,506	19,151	18,925	10,180	1962	0
Cumulative No. of Events									
Standard-dose comparator	0	16	104	250	428	532	555	557	557
mRNA-1010	0	14	74	205	333	400	409	411	411

First Occurrence of Protocol-Defined Influenza-like Illness Caused by Any Influenza A or B Strain.

Shown are the cumulative case numbers for the first occurrence of RT-PCR–confirmed, protocol-defined influenza-like illness that began at least 14 days after trial vaccination and continued through the end of the influenza season, caused by any influenza A or B strain, regardless of vaccine match. The median follow-up was 6 months. Relative vaccine efficacy was calculated as (1–hazard ratio [mRNA-1010 vs. standard-dose comparator])×100. The relative vaccine efficacy and the 95% confidence interval were based on a stratified Cox proportional-hazards model with the vaccine group as a fixed effect, with adjustment for the randomization stratification factors: age group (50 to <65 years or ≥65 years) and status with respect to influenza vaccination during the previous influenza season (received or not received). Efron's method was used to handle ties.

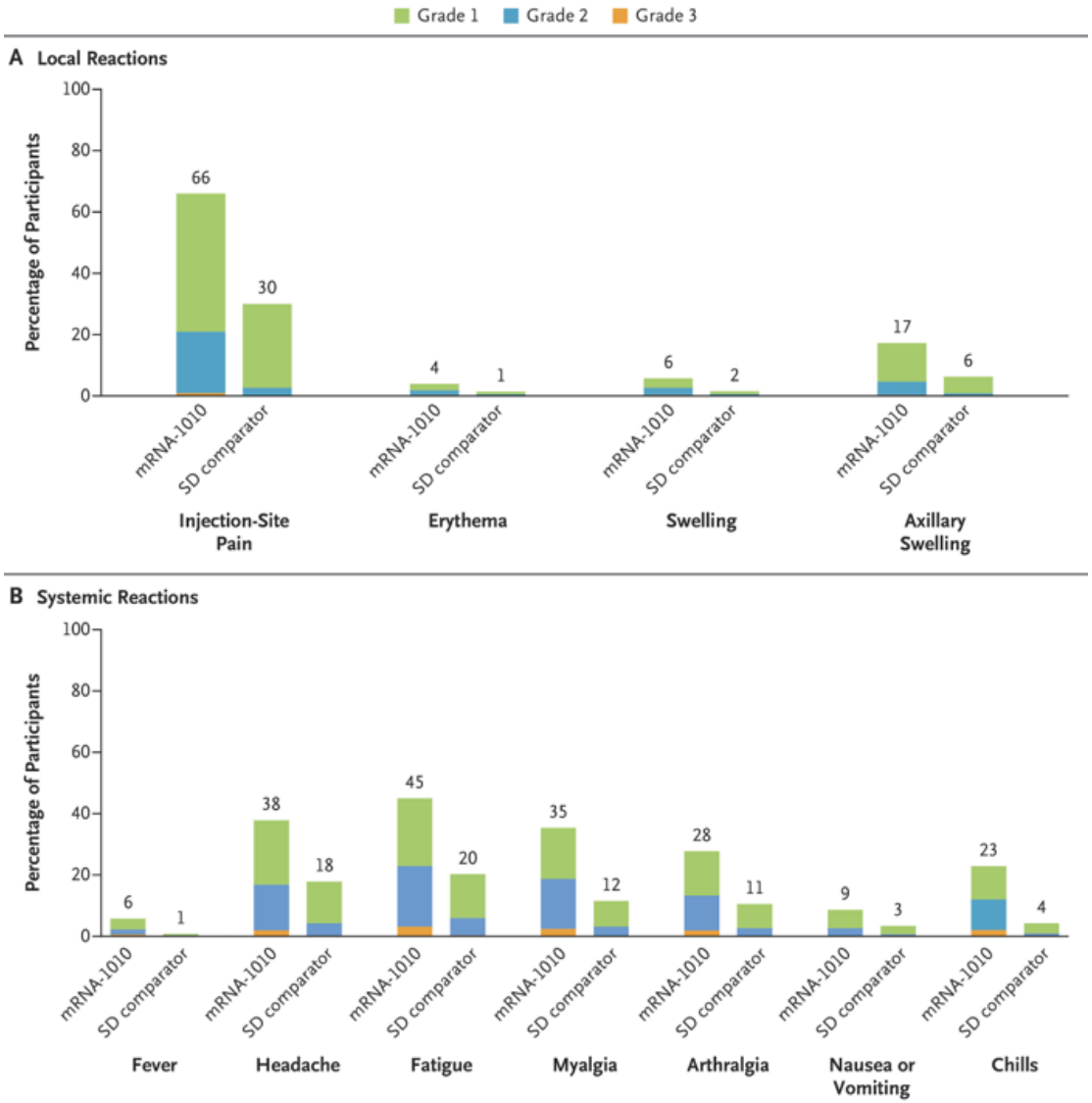

Solicited Local and Systemic Reactions.

Shown are solicited adverse reactions within 7 days after receipt of mRNA-1010 or the standard-dose (SD) comparator. Panel A shows local adverse reactions, and Panel B shows systemic adverse reactions. Percentages are based on the number of exposed participants who submitted data for the event. The toxicity grade is the maximum toxicity grade reported on any day from day 1.

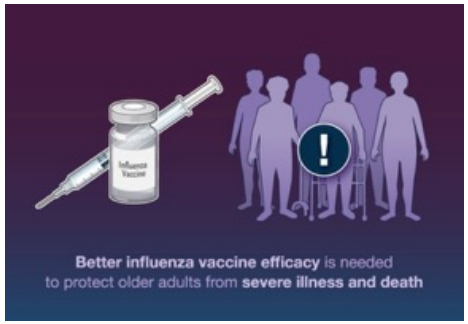
Better influenza vaccine efficacy is needed
to protect older adults from severe illness and death


Fluent Trial
Efficacy and safety
Investigational
mRNA-based
influenza vaccine

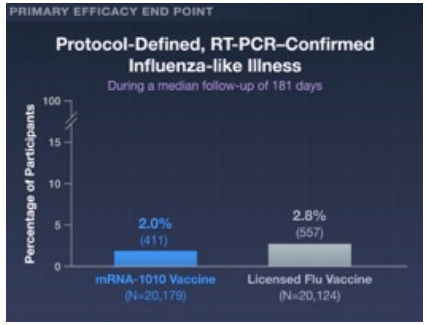
PRIMARY EFFICACY END POINT
Protocol-Defined, RT-PCR–Confirmed
Influenza-like Illness
During a median follow-up of 181 days
Percentage of Participants
100
15
10
5
0
2.0%
(411)
2.8%
(557)
mRNA-1010 Vaccine
(N=20,179)
Licensed Flu Vaccine
(N=20,124)

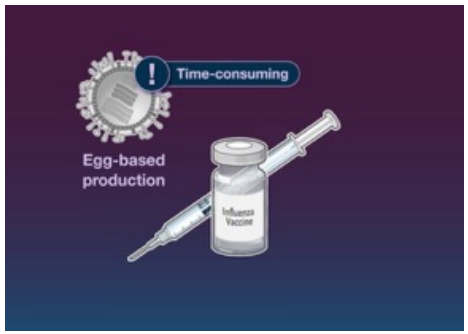
Time-consuming
Egg-based
production

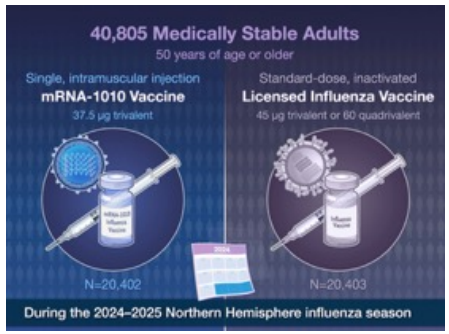
40,805 Medically Stable Adults
50 years of age or older
Single, intramuscular injection
mRNA-1010 Vaccine
37.5 µg trivalent
Standard-dose, inactivated
Licensed Influenza Vaccine
45 µg trivalent or 60 quadrivalent
N=20,402
N=20,403
During the 2024–2025 Northern Hemisphere influenza season

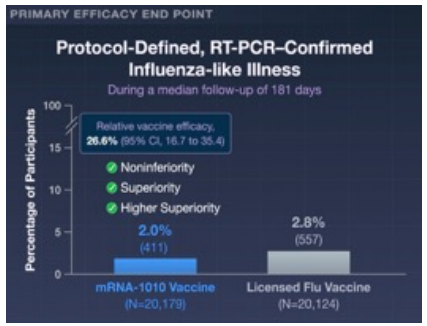
PRIMARY EFFICACY END POINT
Protocol-Defined, RT-PCR–Confirmed
Influenza-like Illness
During a median follow-up of 181 days
Percentage of Participants
100
15
10
5
0
Relative vaccine efficacy,
26.6% (95% CI, 16.7 to 35.4)
Noninferiority
Superiority
Higher Superiority
2.0%
(411)
2.8%
(557)
mRNA-1010 Vaccine
(N=20,179)
Licensed Flu Vaccine
(N=20,124)

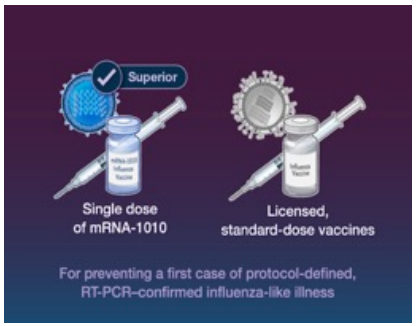
Superior
Single dose
of mRNA-1010
Licensed,
standard-dose vaccines
For preventing a first case of protocol-defined,
RT-PCR–confirmed influenza-like illness

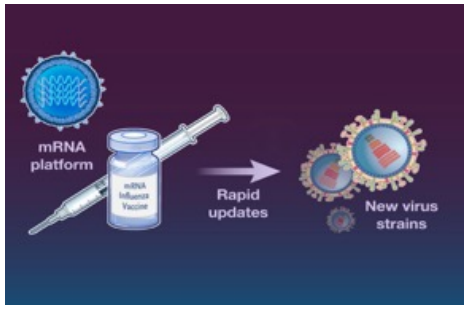
mRNA
platform
Rapid
updates
New virus
strains

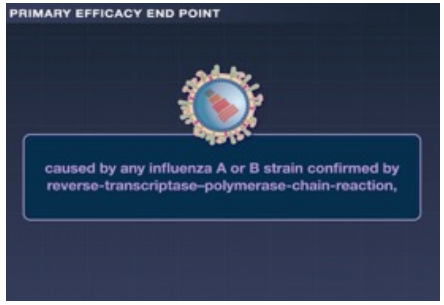
PRIMARY EFFICACY END POINT
caused by any influenza A or B strain confirmed by
reverse-transcriptase–polymerase-chain-reaction,

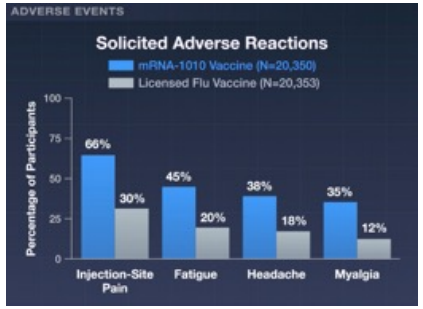
ADVERSE EVENTS
Solicited Adverse Reactions
mRNA-1010 Vaccine (N=20,350)
Licensed Flu Vaccine (N=20,353)
Percentage of Participants
100
75
50
25
0
66%
30%
45%
20%
38%
18%
35%
12%
Injection-Site
Pain
Fatigue
Headache
Myalgia

Skabies (Krätze) ist eine durch **Krätzmilben** verursachte, ansteckende Hautkrankheit. Die winzigen Parasiten graben Gänge in die obere Hautschicht, um dort Eier und Kot abzulegen, was zu einer allergischen Reaktion führt.

Hauptmerkmale

•**Starker Juckreiz**: Besonders intensiv bei Bettwärme in der Nacht.

•**Hautveränderungen**: Feine, dunkle, gewundene Linien (Milbengänge), Bläschen oder kleine rote Knötchen.

•**Betroffene Stellen**: Vor allem Fingerzwischenräume, Handgelenke, Achseln, Genitalbereich und Brustwarzen.

•**Ansteckung**: Meist durch engen, direkten Hautkontakt von mindestens 5–10 Minuten

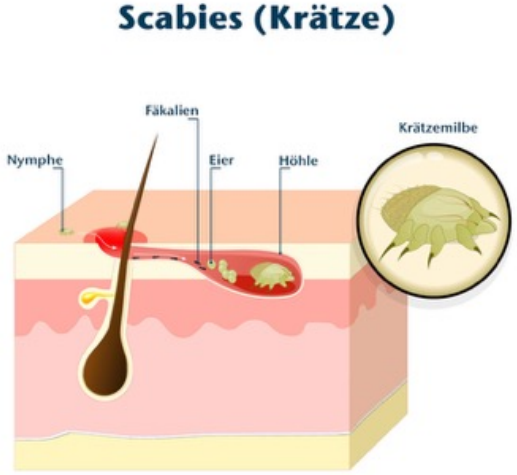

The **discovery and development of ivermectin** won the Nobel Prize in Physiology or Medicine in 2015

Ivermectin ist ein wirksames Medikament zur Bekämpfung von **Parasiten** bei Menschen und Tieren. Es wirkt, indem es das Nervensystem von Parasiten blockiert, was zu deren Lähmung und Tod führt.

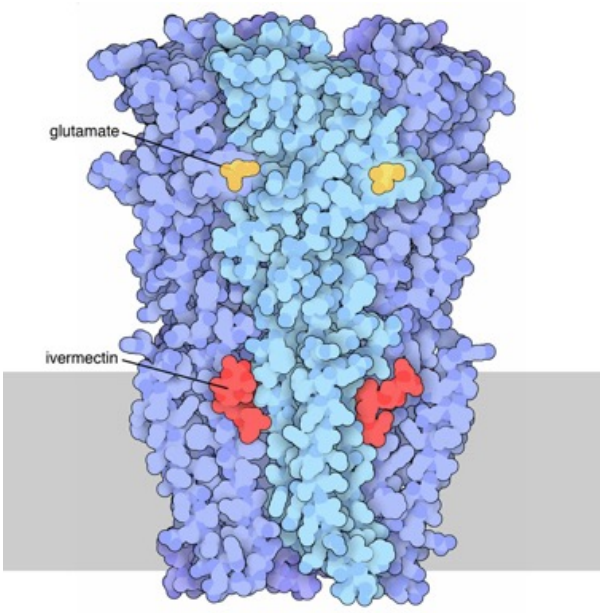

Hauptanwendungsgebiete beim Menschen

In Deutschland ist Ivermectin für folgende Erkrankungen zugelassen:

•**Krätze (Skabies):** Orale Einnahme als Tablette.

•**Rosazea:** Äußerliche Anwendung als Creme bei entzündlichen Hautveränderungen.

•**Wurminfektionen:** Behandlung von Fadenwürmern (z. B. Zwergfadenwurm) und lymphatischer Filariose.

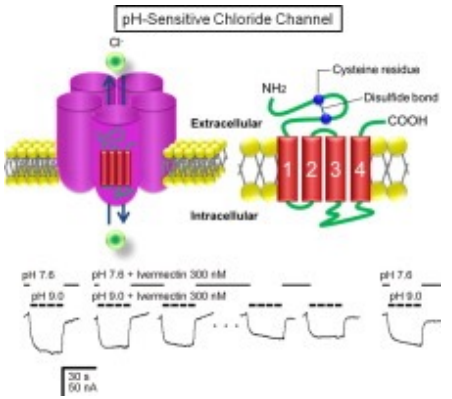

Combined Oral Ivermectin and 5% Permethrin Cream to Treat Severe Scabies

Severe scabies, a rare parasitic skin disease characterized by abundant skin mites, may be life-threatening and poses public health concerns worldwide. A combination of standard-dose oral ivermectin and topical scabicides is recommended for treatment. However, data from randomized clinical trials are lacking, and the probability of cure is uncertain. Ivermectin at higher doses has been effective in the treatment of some parasitic diseases.

We conducted a blinded randomized trial involving adults with severe scabies (i.e., profuse or crusted), as confirmed by parasitologic or dermoscopic assessment. The patients were assigned in a 1:1 ratio to receive oral ivermectin (to be taken with food) at a dose of 400 µg per kilogram of body weight (higher-dose group) or 200 µg per kilogram (standard-dose group) on days 0, 7, and 14, combined with head-to-toe application of 5% permethrin cream on days 0 and 7 and daily application (as recommended) of an emollient cream. The primary end point was cure of severe scabies, which was defined as the absence of mites and mite-related products (i.e., eggs and feces), as confirmed by parasitologic or dermoscopic assessment on days 18 and 21, and the absence of active clinical lesions on physical examination on day 28.

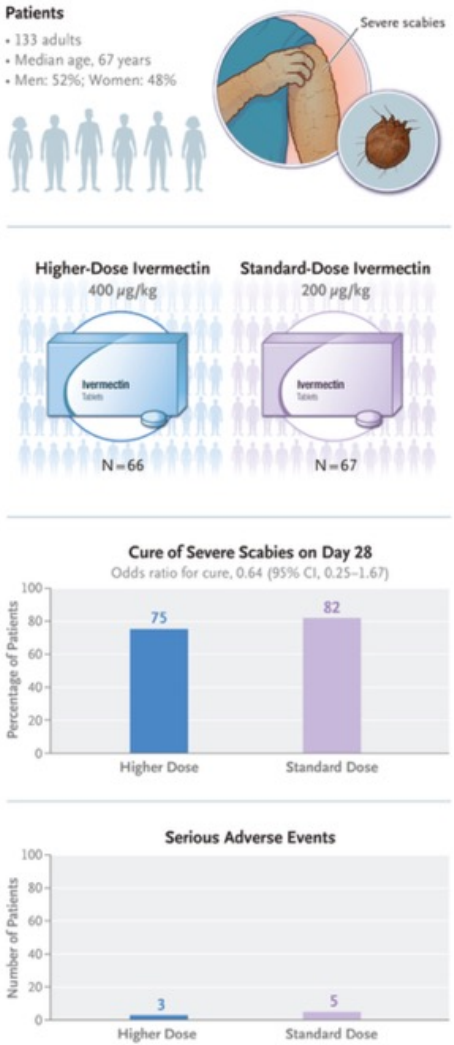

Severe scabies is a rare parasitic skin disease that encompasses profuse and diffuse manifestations of classic scabies and crusted scabies. Clinically, the rash in profuse scabies is erythematous, scaly, and disseminated, involving areas that are not typically affected in classic scabies (e.g., the scalp, head, neck, or back) and potentially engendering erythroderma. Crusted scabies is clinically characterized by the presence of several hyperkeratotic and psoriasiform skin lesions containing dozens to hundreds to thousands of infesting *Sarcoptes scabiei* var. *hominis* mites. Immunosuppression — either iatrogenic (e.g., caused by systemic or topical use of glucocorticoids in patients with transplants or in those with unrecognized scabies-related itch or eczematous lesions, respectively) or noniatrogenic (e.g., caused by underlying human immunodeficiency virus, acquired immunodeficiency syndrome, or human T-cell leukemia virus type 1) — is a risk factor for severe scabies.

Because ivermectin at higher doses has been effective in the treatment of some parasitic diseases, such as head lice and malaria, we conducted a randomized clinical trial involving adults with severe scabies to compare the efficacy and safety of a three-dose regimen of oral ivermectin at a higher dose (400 µg per kilogram of body weight) with those of the standard dose (200 µg per kilogram), combined with two applications of 5% permethrin cream.

Methods

Trial Design and Oversight

The GALE CRUSTED (High Dosage of Oral Ivermectin for Crusted Scabies) trial was a blinded, head-to-head randomized clinical trial that evaluated whether oral ivermectin at a high dose was superior to the standard dose in curing severe scabies; with the patients in both groups receiving 5% permethrin and emollient cream.

Patients were assigned to receive oral ivermectin (to be taken with food) at a dose of 400 µg per kilogram or at the standard 200-µg-per-kilogram dose on days 0, 7, and 14. Because the pharmacist prepared the same number of matched tablets and delivered identical unmarked wallets to both trial groups, the patients and investigators remained unaware of the trial-group assignments.

Patients and Eligibility Criteria

Adults 18 years of age or older with or without immunosuppression (including those with immunosuppression who had previously received topical or systemic glucocorticoids) were eligible to participate if they had severe scabies — either profuse (defined as spreading, erythematous, scaly lesions) or crusted (with at least two hyperkeratotic sites).

End Points

The primary end point was cure of severe scabies, which was defined as the absence of mites and mite-related products, as confirmed by parasitologic or dermoscopic assessment (or both) on days 18 and 21 (a single positive result was considered to indicate treatment failure) and the absence of active clinical scabies lesions on physical examination on day 28.

Demographics

Characteristic	Ivermectin, 400 μg/kg (N=66)	Ivermectin, 200 μg/kg (N=67)
Median age (IQR) — yr	65.5 (49.0–84.0)	68.0 (53.0–85.0)
Age >80 yr		
Yes	19 (29)	26 (39)
No	47 (71)	41 (61)
Sex — no. (%)		
Male	31 (47)	38 (57)
Female	35 (53)	29 (43)
Median body-mass index (IQR)†	24.3 (21.1–27.5)	22.7 (19.9–28.1)
Hospitalization — no. (%)		
Yes	42 (64)	40 (60)
No	24 (36)	27 (40)
Coexisting conditions — no. (%)		
Solid-organ cancer and hematologic disorders		
Yes	13 (20)	12 (18)
No	53 (80)	55 (82)
Neurologic or cognitive impairment		
Yes	29 (44)	27 (40)
No	37 (56)	40 (60)
Median no. of days since the onset of signs or symptoms of scabies (IQR)	81 (42–126)	109 (58–224)
Scabies type — no./total no. (%)‡		
Profuse only	34/66 (52)	44/66 (67)
Crusted only	2/66 (3)	4/66 (6)
Profuse and crusted	30/66 (45)	18/66 (27)

Patients with Cure on Day 28.

Analysis	Ivermectin, 400 μg/kg (N=66)	Ivermectin, 200 μg/kg (N=66)*	Odds Ratio for Cure (95% CI)†
Main analysis			
Patients with cure in the analysis with multiple imputation — %‡	75	82	0.64 (0.25 to 1.67)
Patients with cure in the analysis that included only patients with complete data — no./total no. (%)	35/47 (74)	41/50 (82)	0.64 (0.24 to 1.70)
Sensitivity analysis§			
Patients with cure in the analysis with multiple imputation — %¶	82	83	0.91 (0.35 to 2.35)
Patients with cure in the analysis that included only patients with complete data — no./total no. (%)	43/53 (81)	46/55 (84)	0.84 (0.31 to 2.27)

Subgroup Analyses of Patients with Cure on Day 28.

Variable	No. of Patients	Ivermectin, 400 μg/kg	Ivermectin, 200 μg/kg	Odds Ratio for Cure (95% CI)*
		no. of patients with cure/total no. (%)		
Immunosuppressive drug use				
Yes	20	10/14 (71)	4/6 (67)	1.25 (0.16 to 9.76)
No	77	25/33 (76)	37/44 (84)	0.59 (0.19 to 1.84)
Scabies type†				
Crusted	38	11/21 (52)	13/17 (76)	0.34 (0.08 to 1.39)
Profuse only	59	24/26 (92)	28/33 (85)	2.14 (0.38 to 12.06)
Days since first signs or symptoms of scabies				
>90	41	10/14 (71)	23/27 (85)	0.43 (0.09 to 2.09)
≤90	40	17/24 (71)	13/16 (81)	0.56 (0.12 to 2.60)

Cutaneous Adverse Events Potentially Related to the Combination of Scabicides Used.

Variable	Ivermectin, 400 μg/kg (N=66)	Ivermectin, 200 μg/kg (N=66)††
Patients with any event — no.	14	14
Total no. of events	16	17
Type of adverse event — no.		
Eczema, eczematous lesions, or contact dermatitis	11	7
Erythema or edema	1	2
Itching or burning	2	6
Infection or impetiginization	1	2
Unclear	1	0


Severe Scabies
Rare, contagious, and potentially life-threatening parasitic skin disease


133 Adults with Severe Scabies
Profuse or crusted
Standard Dose
Oral Ivermectin, 200 µg/kg
(N=67)
Higher Dose
Oral Ivermectin, 400 µg/kg
(N=66)
Recommended daily application of an emollient

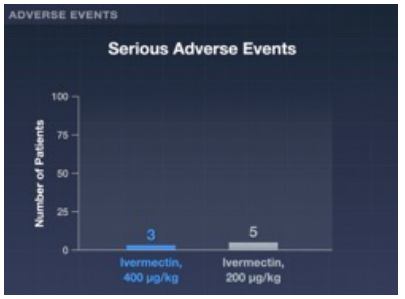
ADVERSE EVENTS
Serious Adverse Events
Number of Patients
100
75
50
25
0
3
5
Ivermectin, 400 µg/kg
Ivermectin, 200 µg/kg


Severe Scabies
Standard dose
Ivermectin
Tablets


PRIMARY END POINT
Cure of Severe Scabies
MONTH


Higher dose
Ivermectin
Tablets
Standard dose
Ivermectin
Tablets
Higher Dose
Oral Ivermectin, 400 µg/kg
Standard Dose
Oral Ivermectin, 200 µg/kg

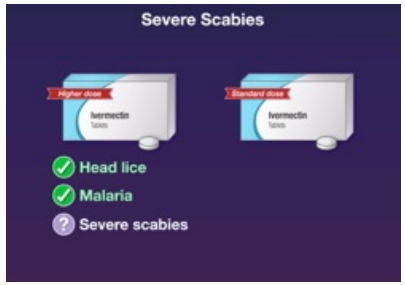
Severe Scabies
Higher dose
Ivermectin
Tablets
Standard dose
Ivermectin
Tablets
Head lice
Malaria
Severe scabies

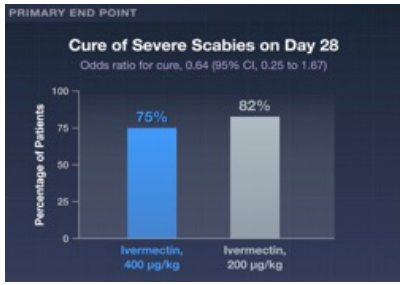
PRIMARY END POINT
Cure of Severe Scabies on Day 28
Odds ratio for cure, 0.64 (95% CI, 0.25 to 1.67)
Percentage of Patients
100
75
50
25
0
75%
82%
Ivermectin, 400 µg/kg
Ivermectin, 200 µg/kg

HBG1 (Hemoglobin Subunit Gamma 1) ist ein menschliches Gen, das für die **A-Gamma-Globin-Kette** kodiert. Diese Kette ist ein wesentlicher Bestandteil des **fetalen Hämoglobins (HbF)**, welches Sauerstoff im Blut von Föten und Neugeborenen transportiert.

Wichtige Fakten zu HBG1:

•**Funktion**: Bildet zusammen mit Alpha-Globin-Ketten das fetale Hämoglobin.

•**Lokalisation**: Befindet sich auf **Chromosom 11** im Beta-Globin-Gencluster.

•**Unterschied zu HBG2**: HBG1 kodiert für Alanin an Position 136, während das fast identische Gen **HBG2** (G-Gamma) dort Glycin besitzt.

•**Entwicklung**: Die Expression findet primär in der fetalen Leber, Milz und im Knochenmark statt und wird nach der Geburt normalerweise durch adultes Hämoglobin ersetzt

HBG1 Kodiert für die beta Kette

In Sichelzell-Anämie ist die beta Kette mutiert

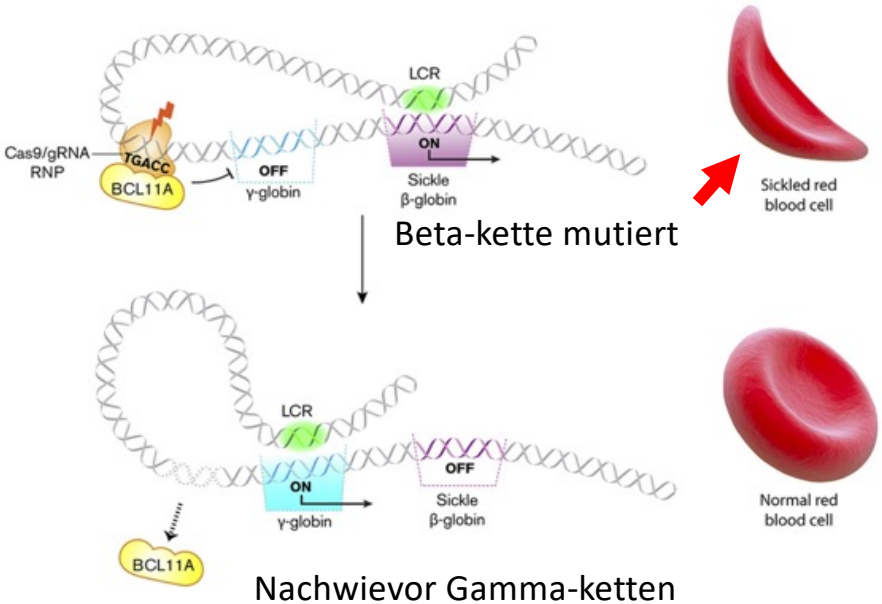

Nachwievor Gamma-ketten anstatt Beta-ketten

HBG2 (Hämoglobin-Untereinheit Gamma-2) ist ein menschliches Gen auf Chromosom 11, das für die Produktion von **fötalem Hämoglobin (HbF)** entscheidend ist

HBG1 Kodiert für die gamma Kette

Biologische Funktion

•**Bestandteil von HbF**: Zusammen mit Alpha-Ketten bildet das HBG2-Protein das fötale Hämoglobin.

•**Sauerstofftransport**: HbF hat eine höhere Affinität zu Sauerstoff als das Hämoglobin von Erwachsenen, was die Versorgung des Fötus im Mutterleib sichert.

•**Entwicklung**: Es wird vorrangig in der fötalen Leber, Milz und im Knochenmark exprimiert und nach der Geburt normalerweise durch adultes Hämoglobin (HbA) ersetzt.

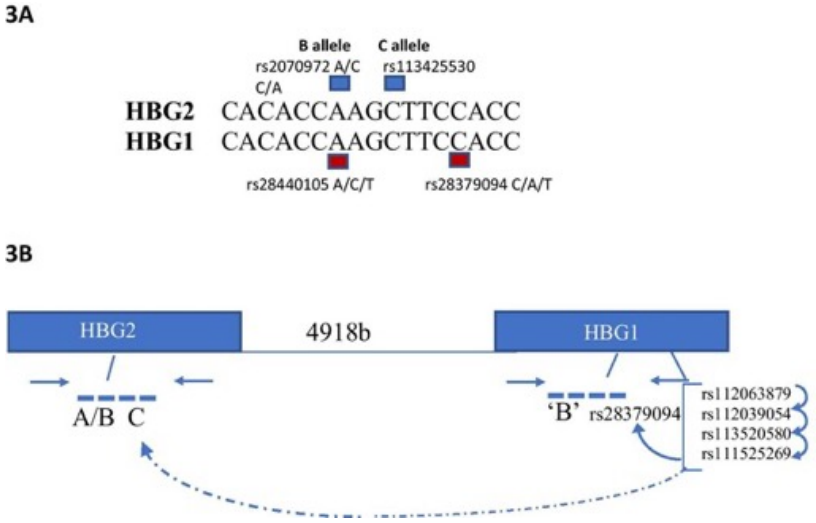

Risto-cel (vollständiger Name: **Ristoglogene autogetemcel**) ist eine experimentelle Zelltherapie zur Behandlung der schweren **Sichelzellkrankheit**.

Die wichtigsten Fakten zur Therapie

•**Einmalige Behandlung**: Es handelt sich um eine autologe Stammzelltransplantation, bei der patienteneigene Zellen außerhalb des Körpers genetisch verändert werden.

•**Wirkmechanismus**: Durch Base-Editing wird das BCL11A-Gen so beeinflusst, dass der Körper wieder gesundes, nicht-sichelndes Hämoglobin produziert (macht HbF anstatt HbA).

•**Aktueller Status**: Die Therapie befindet sich in klinischen Studien (Phase 1/2 BEACON-Studie).

•**Ergebnisse**: Erste Daten zeigen eine deutliche Reduktion schmerzhafter Gefäßverschlüsse (VOCs) und eine Normalisierung der Blutwerte bei den behandelten Patienten.

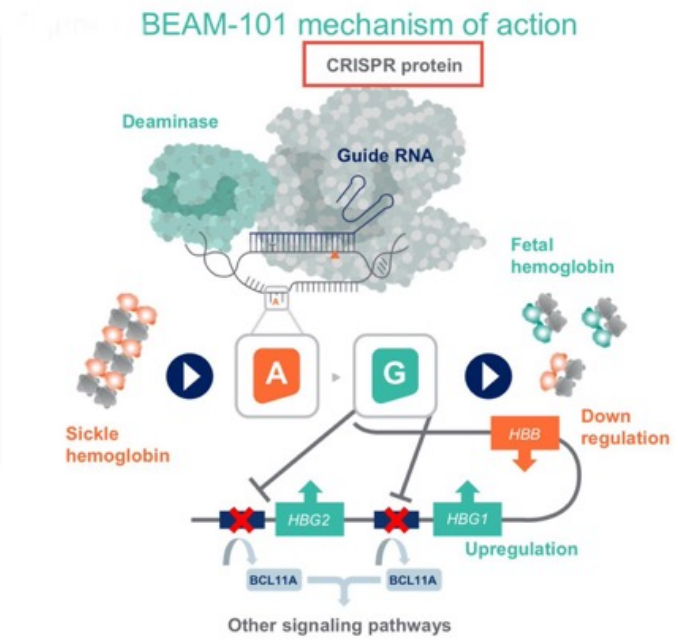

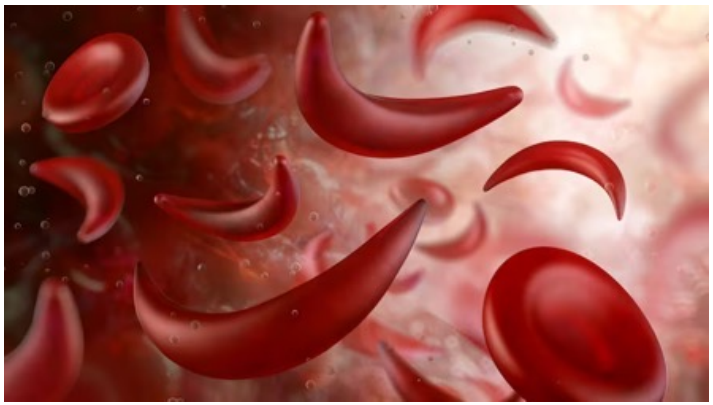

Base Editing of *HBG1* and *HBG2* Promoters for Sickle Cell Disease

Sickle cell disease is characterized by chronic hemolytic anemia and recurrent severe vaso-occlusive crises. Ristoglogene autogetemcel (risto-cel) includes autologous CD34+ hematopoietic stem and progenitor cells that have been base-edited to target the *HBG1* and *HBG2* promoters and inhibit BCL11A binding without altering BCL11A expression, yielding a switch in hemoglobin production from sickle hemoglobin (HbS) to antisickling fetal hemoglobin (HbF).

In this phase 1–2 study, we enrolled patients 12 to 35 years of age with sickle cell disease who had had at least four severe vaso-occlusive crises in the 2 years before enrollment. After myeloablative conditioning with pharmacokinetically guided administration of busulfan, patients received a single infusion of risto-cel (at a dose of ≥3.0×10^6 viable CD34+ cells per kilogram of body weight). The primary efficacy end point was freedom from severe vaso-occlusive crises for 12 consecutive months, starting later than 60 days after the last red-cell transfusion. This interim analysis was unplanned; here, we describe safety, editing, engraftment, and hemoglobin production and the number of severe vaso-occlusive crises starting later than 60 days after the last red-cell transfusion.

Conclusions

Treatment with risto-cel was followed by rapid engraftment and durable expression of HbF and reduction in HbS. These data support further investigation of risto-cel to treat sickle cell disease.

Ristoglogene autogetemcel (BEAM-101; risto-cel) is an investigational genetically modified cell therapy consisting of ex vivo base-edited autologous CD34+ hematopoietic stem and progenitor cells (HSPCs) that are designed to increase the production of antisickling fetal hemoglobin (HbF) and decrease the production and levels of circulating HbS. HbF is the dominant hemoglobin during fetal development and early infancy. The fetal-to-adult globin switch is mediated by transcriptional repressor BCL11A, which binds to regulatory sites within the *HBG1* and *HBG2* promoters and silences γ-globin expression, thereby reducing the production of HbF soon after birth. Sustained pancellular expression of HbF into adulthood confers antisickling effects and is observed in persons with hereditary persistence of fetal hemoglobin (HPFH) who coinherit the sickle mutation. Among patients with sickle cell disease, HbF levels of 10 to 20% are associated with improved childhood survival, whereas levels approaching those seen in persons with HPFH (30 to 40%) are linked to a markedly attenuated disease course. Families with homozygous deletional HPFH, resulting from large deletions in the β-globin gene cluster and characterized by constitutively elevated HbF level, have HbF values ranging from 60 to 100%, and no adverse clinical effects have been described in the literature. Protection against red-cell sickling is achieved under normal conditions at a concentration of 10 pg of HbF per F cell (a red cell that expresses detectable levels of fetal hemoglobin).

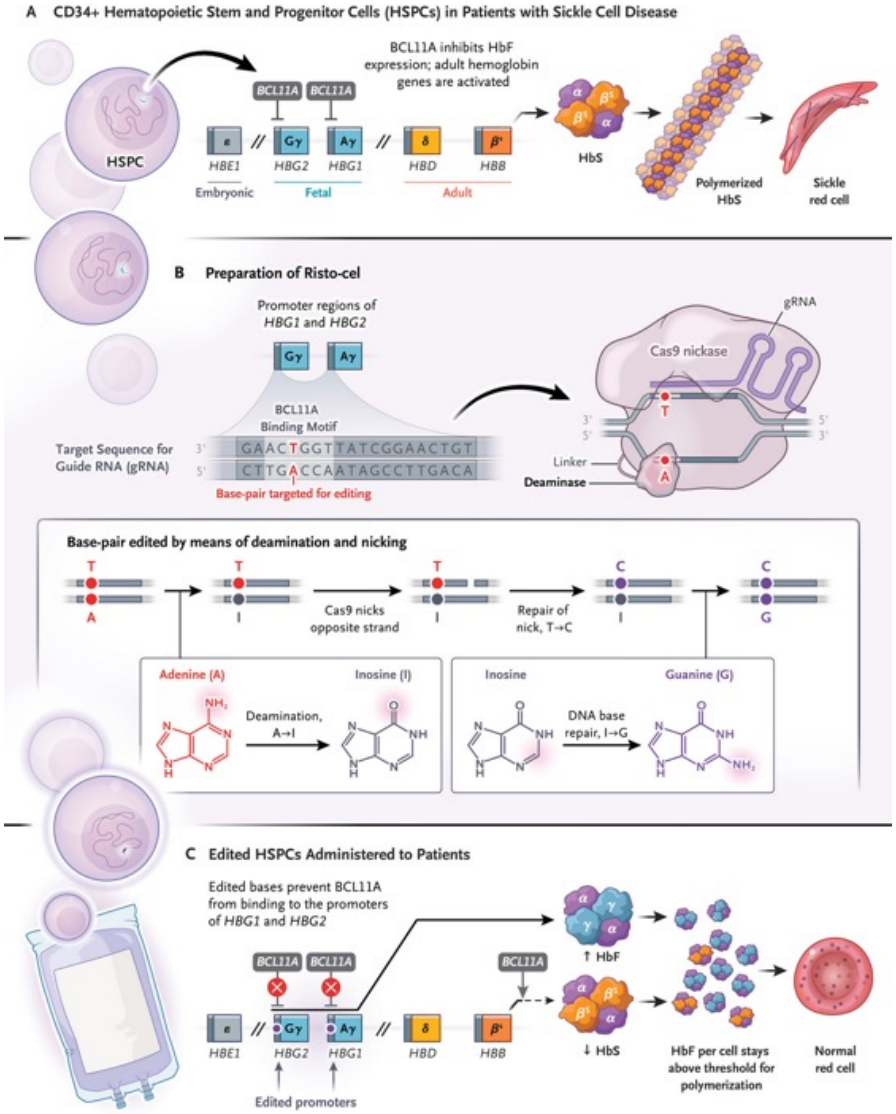

Mechanism of Action of Risto-cel.

Ristoglogene autogetemcel (risto-cel) introduces precise edits at the *HBG1* and *HBG2* promoter regions to inhibit BCL11A binding, thereby promoting the expression of antisickling fetal hemoglobin (HbF). This targeted approach preserves overall BCL11A expression, avoiding disruption of its broader biologic functions.[20,45,46] Cas9 denotes clustered regularly interspaced short palindromic repeats–associated protein 9, and HbS sickle hemoglobin.

Demographics

Characteristic	Patients (N = 31)
Age — yr	
Mean	22.8±4.7
Range	16–34
Sex — no. (%)	
Male	16 (52)
Female	15 (48)
Genotype — no. (%)†	
β^S/β^S	28 (90)
β^S/β^0	1 (3)
β^S/β^+	2 (6)
Race — no. (%)‡	
Black	25 (81)
White	1 (3)
Not reported	4 (13)
Other	1 (3)
Previous hydroxyurea use — no. (%)	31 (100)
Median no. of investigator-reported sVOCs in the 2-yr baseline period (range)	7 (4–60)

Mobilization, Collection, and Transplantation Characteristics (Treated Population).

Variable	Patients (N = 31)
Median no. of stem-cell collection cycles (range)	1 (1–5)
Total median no. of collection days for risto-cel manufacture (range)	3 (1–13)
Cumulative AUC for busulfan (range) — hr·mg/liter	71.0 (61.0–86.1)
Median risto-cel dose infused (range) — $\times 10^{-6}$ viable CD34+ cells/kg	6.2 (3.2–23.4)
Duration of follow-up after risto-cel infusion — mo	
Mean	6.6±5.1
Range	0.3–20.4
Median no. of days to last red-cell transfusion after risto-cel infusion (range)†	14 (1–26)
Neutrophil engraftment — days‡	
Median time to neutrophil engraftment (range)	17.5 (12–30)
Median duration of severe neutropenia (range)§	7 (1–17)
Platelet engraftment	
Median time to platelet engraftment (range) — days¶	19 (11–53)
Platelet count ≥50,000/μl — no. (%)	6 (19)
Did not receive a platelet transfusion — no. (%)	9 (29)
No. of patients with transplantation-related death within 100 days after risto-cel infusion	0

Adverse Events after Risto-cel Infusion.

Event	Patients (N = 31)
Any adverse event related to risto-cel†	3 (10)
Most common adverse events	
Stomatitis	24 (77)
Febrile neutropenia	22 (71)
Decreased appetite	10 (32)
Hypokalemia	10 (32)
Skin hyperpigmentation	10 (32)
Adverse events of grade ≥3 occurring in ≥2 patients	
Febrile neutropenia	17 (55)
Stomatitis	15 (48)
Decreased appetite	9 (29)
Platelet count decreased	6 (19)
Anemia	5 (16)
Neutrophil count decreased	4 (13)
Hypokalemia	3 (10)
Nausea	3 (10)
White-cell count decreased	3 (10)
Acute kidney injury	2 (6)
Hematuria	2 (6)
Hypoxia	2 (6)
Laryngeal inflammation	2 (6)
Pharyngeal inflammation	2 (6)
Pyrexia	2 (6)
Serious adverse events occurring in ≥2 patients	
Pain	2 (6)
Acute kidney injury	2 (6)
Death	1 (3)
Any adverse event leading to study discontinuation	0

Investigator-Reported Severe Vaso-occlusive Crises after Treatment with Risto-cel (Treated Population).

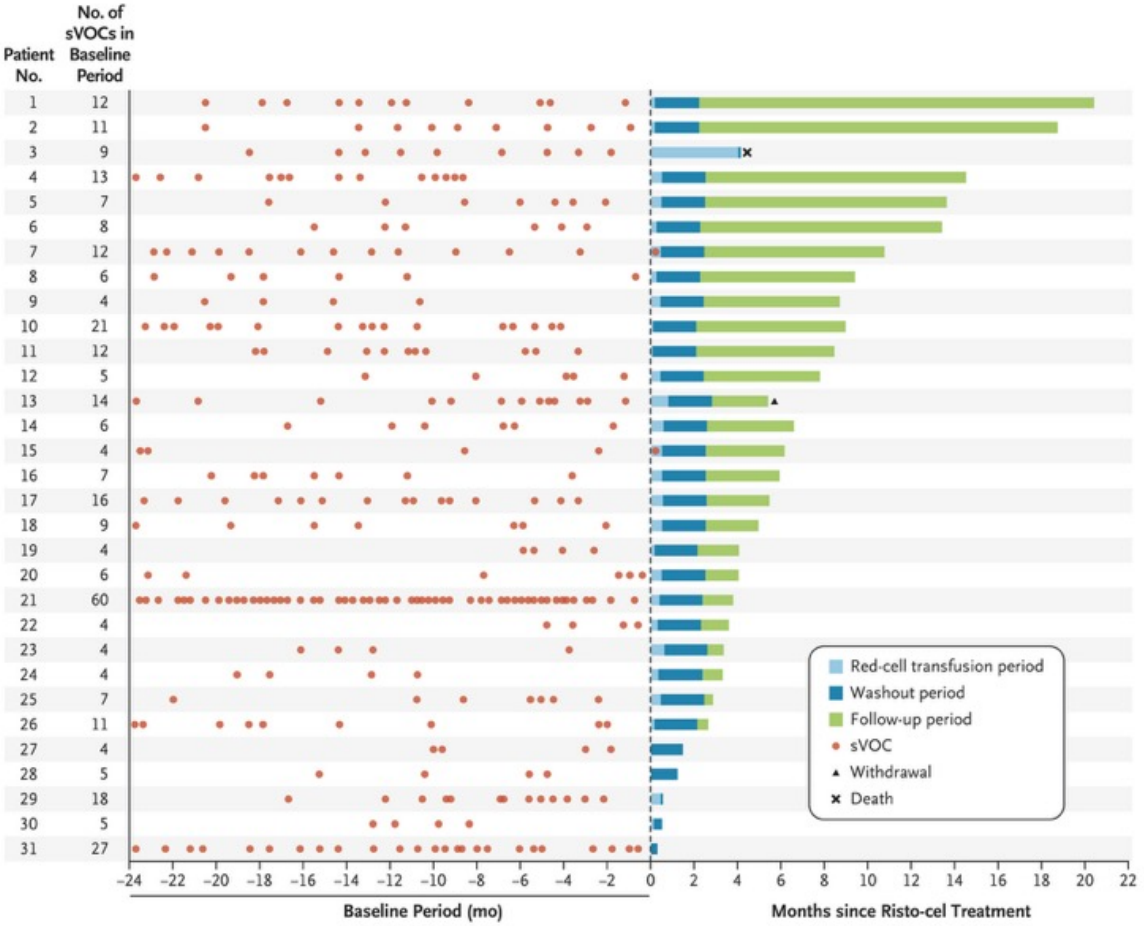

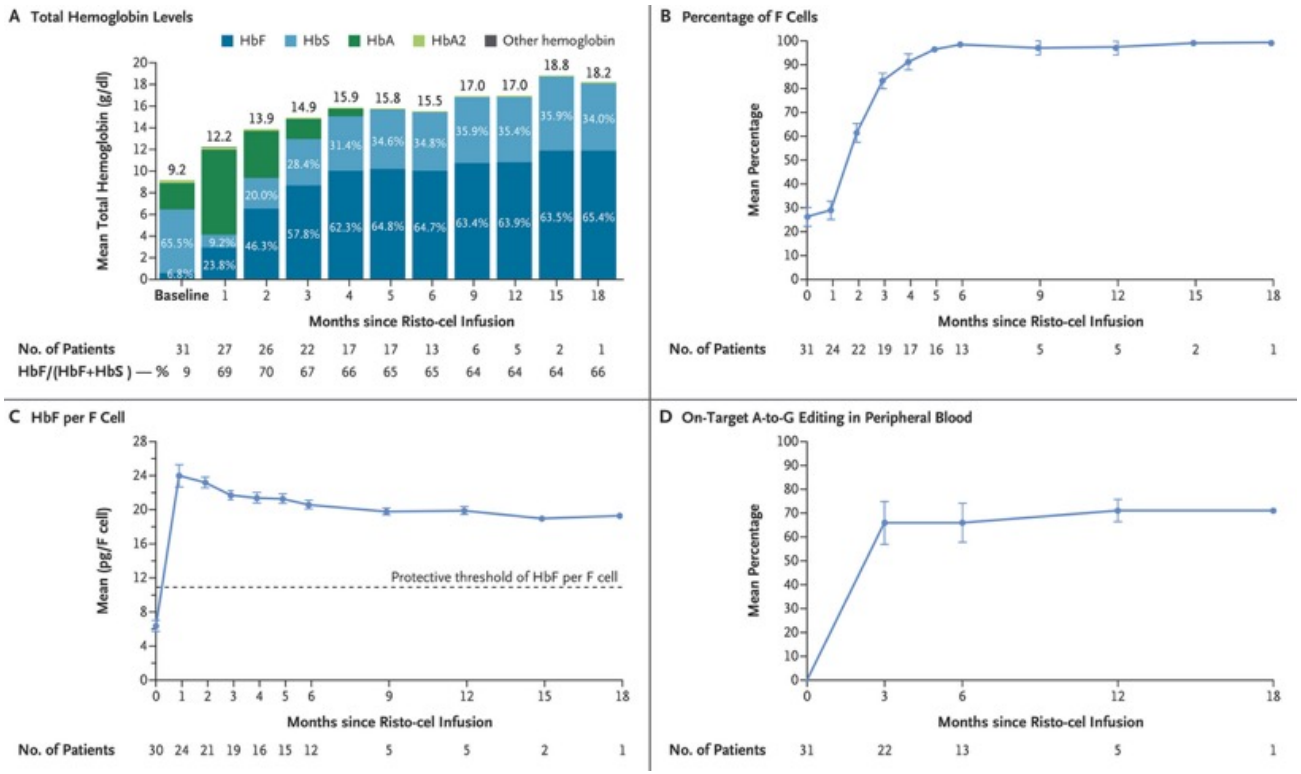

Changes in Total Hemoglobin Levels, Pancellular HbF Distribution, and Peripheral Blood Editing.

Shown are the mean total hemoglobin levels (Panel A), the mean percentage of F cells (red cells that contain HbF) (Panel B), the mean HbF level per F cell (Panel C), and on-target A-to-G editing in peripheral blood (Panel D). In Panel A, the fractions of endogenous HbF (calculated as HbF÷[HbF+HbS]) are expressed as percentages. HbA denotes adult hemoglobin, and HbA2 minor adult hemoglobin. In Panel B and D, I bars indicate the standard deviation. The dashed line in Panel C indicates the protective threshold of HbF per F cell, defined as the level of HbF per F cell that inhibits deoxygenated HbS polymerization (10 pg).[20] In Panel C, I bars indicate the standard error.

Discussion

In this ongoing study (BEACON), one-time treatment with risto-cel in 31 patients with up to 20 months of follow-up was followed by rapid engraftment and durable expression of HbF of more than 60% and reduction in HbS to less than 40%. One patient died from idiopathic pneumonia syndrome. Adverse events were generally consistent with busulfan conditioning, autologous hematopoietic stem-cell transplantation, and underlying sickle cell disease, a finding that underscores the importance that treating physicians ensure patient understanding of the overall risks of busulfan conditioning and transplantation and continue to counsel them throughout the study to avoid risk factors (such as smoking, vaping, and alcohol use) that could further elevate the risks of pulmonary and liver toxic effects that have been associated with busulfan conditioning. Because this study is ongoing, the primary efficacy end point cannot be evaluated yet; as of the data-cutoff date for this analysis, no participant has had an investigator-reported severe vaso-occlusive crisis after engraftment.

Patients had rapid, robust, and pancellular HbF expression after treatment with risto-cel. Sickling kinetics decreased to levels similar to those of sickle cell trait reference samples. The resolution of anemia, sickling, and hemolysis that was seen in all patients is consistent with improved red-cell health and function. The BEACON study, however, is limited by the single-group design, a narrow age range for enrollment, the exclusion of patients with a history of stroke, restriction to a United States–based population, and limited applicability to the specific genotypes and age groups studied; the current analysis is limited by a short duration of follow-up.

Beta-amyloid (\(A\beta\)) is a peptide that plays a crucial role in normal brain function, including regulating synaptic plasticity, supporting neuron growth and repair, and defending against oxidative stress. While infamous for aggregating into plaques in Alzheimer's disease, in its soluble form, it serves as a normal metabolic product involved in protection against pathogens and maintaining the blood-brain barrier.

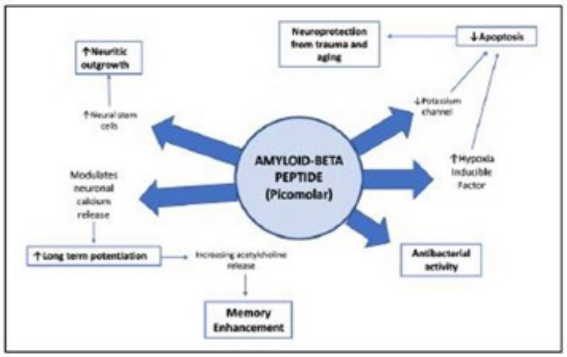

Disclosures: The authors declare there are no conflicts

Key Physiological Functions

•**Synaptic Modulation:** It helps regulate the strength of connections between neurons (synaptic plasticity), which is vital for memory and learning.

•**Neuroprotection & Repair:** It acts as a defense mechanism, with its production increasing in response to injury or stress to protect brain cells.

•**Immune Response:** It is believed to act as an antimicrobial peptide, defending the brain against infections and toxins.

•**Vascular Regulation:** It helps repair leaks in the blood-brain barrier and regulate blood flow.

Role in Disease (Pathology)

The pathology arises when the production of \(A\beta\) exceeds its clearance rate, causing it to misfold and aggregate.

•**Oligomers & Plaques:** Soluble \(A\beta\) converts into toxic soluble oligomers and eventually insoluble plaques.

•**Neurotoxicity:** These aggregates interfere with synaptic function, cause inflammation, and eventually lead to neuronal death, contributing to Alzheimer's disease.

•**Age Factor:** While present throughout life, the ability to break down \(A\beta\) decreases with age, leading to accumulation.

Cerebral Amyloid Angiopathy (CAA) und die Alzheimer-Krankheit (AD) sind eng verwandte Erkrankungen, die beide durch die Ablagerung von **Amyloid-Beta-Proteinen** (Amyloid beta) im Gehirn gekennzeichnet sind. Während sie oft gemeinsam auftreten, unterscheiden sie sich grundlegend darin, *wo* sich dieses Protein ansammelt.

- **Ablagerungsort**:
- **Alzheimer**: Amyloid bildet "Plaques" im **Hirngewebe** (Parenchym).
- **CAA**: Amyloid lagert sich in den **Wänden der kleinen Blutgefäße** des Gehirns ab.
- **Protein-Varianten**:
- Alzheimer ist primär mit der längeren Form **Aβ42** assoziiert.
- CAA besteht überwiegend aus der kürzeren Form **Aβ40**.
- **Primäre Symptome**:
- **Alzheimer**: Gedächtnisverlust und fortschreitender kognitiver Abbau.
- **CAA**: Erhöhtes Risiko für **Hirnblutungen** (hämorrhagischer Schlaganfall) und Mikroblutungen.

These are not quite the same

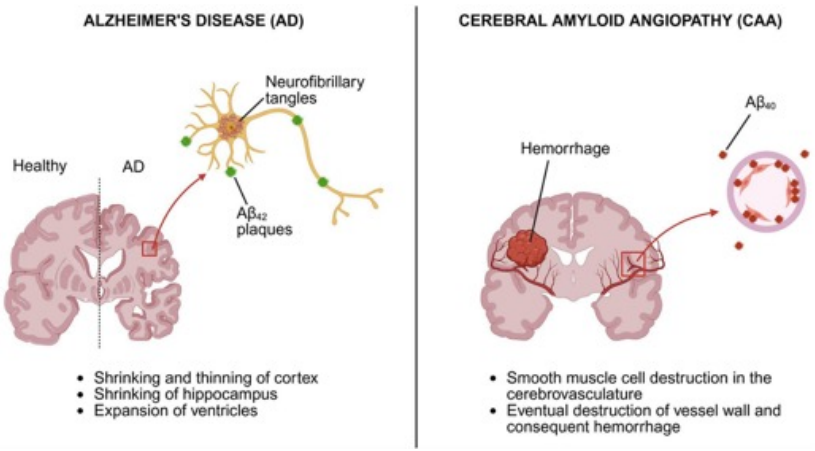

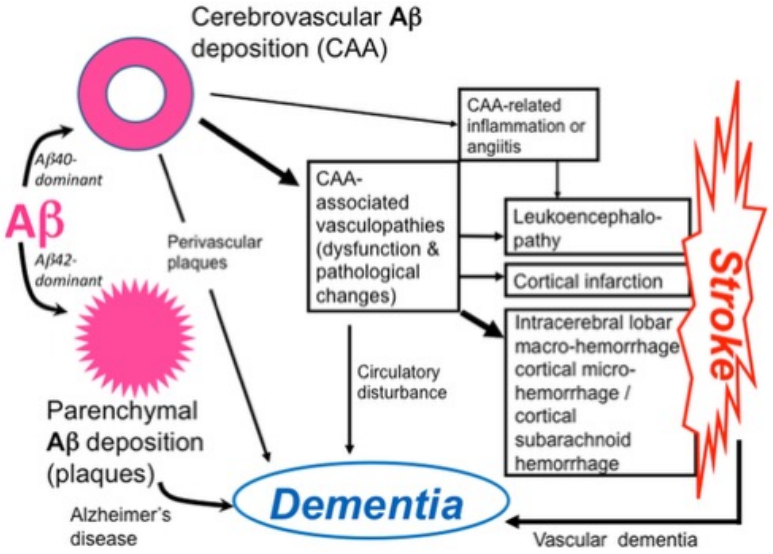

Cerebral Amyloid Angiopathy

Summary

Cerebral amyloid angiopathy is a major cause of hemorrhagic stroke, a frequent contributor to age-related cognitive impairment, and a key component in adverse responses to beta-amyloid (Aβ) immunotherapy. Defined by pathological deposition of Aβ in the small blood vessels of the brain, cerebral amyloid angiopathy is most often diagnosed on the basis of magnetic resonance imaging studies showing multiple hemorrhages or leptomeningeal blood products within or overlying the cerebral cortex. The disorder typically manifests as hemorrhagic stroke or as a contributing factor to cognitive decline and, less commonly, with transient focal neurologic symptoms or a cerebral inflammatory autoimmune syndrome. The high risk of recurrent hemorrhagic strokes associated with cerebral amyloid angiopathy poses a particular challenge in patients with indications for antithrombotic therapy and dictates a carefully individualized weighing of risks and benefits. Ongoing research is focused on tools to aid in risk prediction, early diagnostic markers, and identification of key pathogenic steps as targets for disease-modifying therapies.

Pathogenesis and Epidemiology

The Aβ fibril deposits that characterize cerebral amyloid angiopathy differ from those in Alzheimer's disease in that they are primarily localized to cerebral blood-vessel walls rather than brain tissue and are characterized by a predominance of the shorter Aβ40 isoform rather than the longer Aβ42 isoform. The pathological changes range from trace Aβ deposits surrounding arteriolar smooth-muscle cells (mild cerebral amyloid angiopathy, Figure 1A) to full replacement of the arteriolar media (moderate cerebral amyloid angiopathy, Figure 1A) and, ultimately, to fragmentation of the vessel wall (severe cerebral amyloid angiopathy, Figure 1B). Amyloid is predominantly deposited in leptomeningeal and cortical arterioles, but it may appear in cerebral capillaries, otherwise sparing cerebral veins, venules, larger arteries, and deep penetrating arterioles in the basal ganglia, thalamus, and brain stem. Deposits are absent in vessels outside the central nervous system. Intracerebral hemorrhage occurs at the severe pathological stage[3] and is likely to be the result of vascular remodeling that leads to replacement of Aβ-laden vessel-wall segments with fibrin and other plasma components, blood–brain barrier leakage, and accumulation of activated astrocytes and perivascular microglia or macrophages.

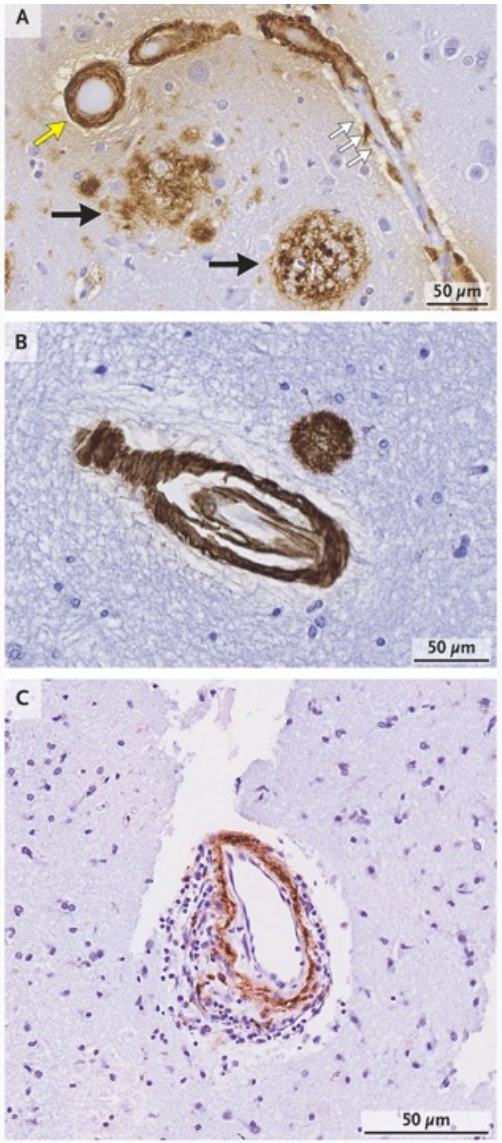

Neuropathological Features of Cerebral Amyloid Angiopathy.

The vessels in Panel A show both mild cerebral amyloid angiopathy, characterized by beta-amyloid (Aβ) deposits (white arrows) alternating with unaffected vessel segments, and moderate cerebral amyloid angiopathy, characterized by complete replacement of the vessel wall with Aβ (yellow arrow). Segment-to-segment variation in the severity of cerebral amyloid angiopathy within a brain is typical. The section also shows Aβ-containing senile plaques (black arrows). Panel B shows severe cerebral amyloid angiopathy, with concentric splitting of the Aβ-laden vessel wall creating a vessel-within-vessel appearance. The vessel segment in Panel C shows inflammation related to cerebral amyloid angiopathy, with an infiltration of mononuclear inflammatory cells surrounding an Aβ-positive segment. Anti-Aβ immunohistochemical staining was used for the sections in all three panels, with hematoxylin counterstaining. These neuropathological images are courtesy of Drs. Susanne van Veluw and Francesco Bax.

Cerebral Amyloid Angiopathy

- Cerebral amyloid angiopathy, the deposition of beta-amyloid peptide in small blood vessels of the brain, is a common age-associated disease that, when advanced, can cause vessel breakdown and bleeding.
- The major clinical manifestations of cerebral amyloid angiopathy are hemorrhagic strokes that frequently recur and smaller brain injuries that contribute to progressive cognitive decline.
- Cerebral amyloid angiopathy can be diagnosed with high specificity on the basis of magnetic resonance imaging showing multiple bleeds or microbleeds confined to the cortex or leptomeninges, as well as other, nonhemorrhagic lesions in the white matter.
- Decisions regarding antithrombotic treatment for patients with both cerebral amyloid angiopathy and a defined indication for anticoagulation require an individualized balancing of risks and benefits, which includes consideration of the patient's risk of future hemorrhagic strokes.
- Cerebral amyloid angiopathy can trigger a cerebral autoimmune inflammatory syndrome, a condition mimicking the amyloid-related imaging abnormalities identified as the major adverse effect of Alzheimer's disease immunotherapy.
- The priorities for improving prevention of cerebral amyloid angiopathy–related hemorrhage are the development of methods for early detection and candidate treatments for blocking the cascade of pathogenic steps.

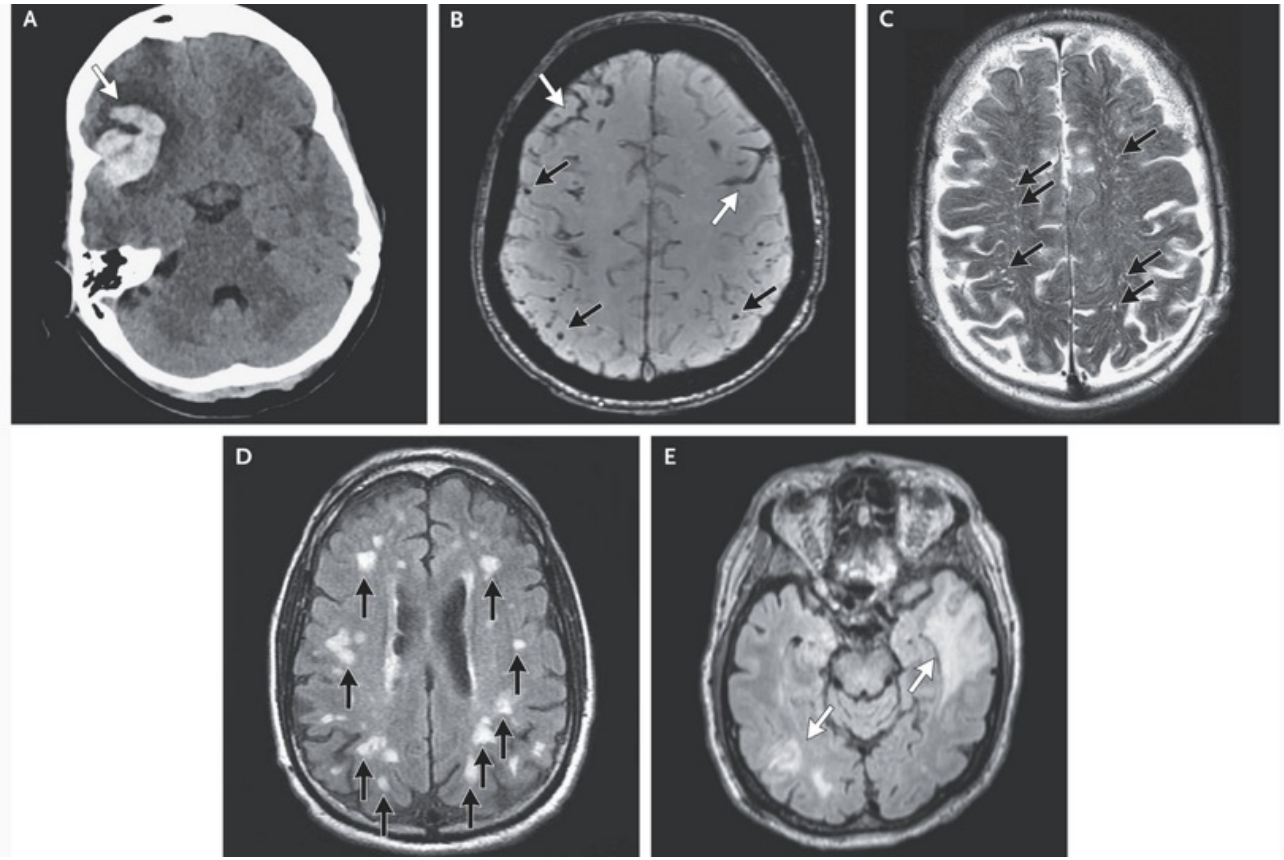

Neuroimaging Features of Cerebral Amyloid Angiopathy.

The computed tomographic scan in Panel A shows an acute right frontal lobar intracerebral hemorrhage, with subarachnoid extension and a fingerlike projection (arrow), features that are characteristic of cerebral amyloid angiopathy. In Panel B, magnetic resonance imaging with T2*-weighted images shows two foci of cortical superficial siderosis (white arrows) and multiple lobar cerebral microbleeds (black arrows). Panels C and D show the two types of nonhemorrhagic white-matter lesions incorporated into the Boston criteria for the diagnosis of cerebral amyloid angiopathy: severe (>20 in a hemisphere) visible perivascular spaces in the centrum semiovale seen on T2-weighted images (Panel C, arrows) and a multispot pattern of white-matter hyperintensities (>10 small, circular or ovoid lesions in the subcortical white matter of both hemispheres) on fluid-attenuated inversion recovery (FLAIR) images (Panel D, arrows). Panel E shows two FLAIR-hyperintense lesions in juxtacortical left frontal and right temporo-occipital white matter (arrows), which are characteristic of inflammation related to cerebral amyloid angiopathy, in a patient with a biopsy-confirmed diagnosis of this disorder.

Boston Criteria, Version 2.0, for Probable Cerebral Amyloid Angiopathy.

Age ≥50 years

Clinical presentation with spontaneous intracerebral hemorrhage, cognitive decline, or transient focal neurologic symptoms

One of the following:

- Two or more of the following lobar hemorrhagic lesions on T2*-weighted MRI: intracerebral hemorrhages, cerebral microbleeds, foci of cortical superficial siderosis, or convexity subarachnoid hemorrhage
- One of the above lobar hemorrhagic lesions plus either of the following nonhemorrhagic white-matter features: severe perivascular spaces in the centrum semiovale or white-matter hyperintensities in a multispot pattern

Absence of spontaneous hemorrhagic lesions on T2*-weighted MRI in deep-brain regions atypical of cerebral amyloid angiopathy: basal ganglia, thalamus, and brain stem

Absence of other direct causes of intracranial hemorrhage: severe head trauma, hemorrhagic transformation of ischemic strokes, arteriovenous malformation, hemorrhagic tumor, central nervous system vasculitis, and aneurysmal subarachnoid hemorrhage

Conclusions and Future Directions

A neuroimaging-based diagnosis of cerebral amyloid angiopathy can inform decisions about blood-pressure control and judicious use or avoidance of antithrombotic therapies. Similar considerations of risks and benefits apply to the incorporation of cerebral amyloid angiopathy markers into decisions about whether to initiate immunotherapy in patients with Alzheimer's disease.

The limited treatment options for cerebral amyloid angiopathy highlight the importance of identifying new approaches to disease modification. The decades-long pathogenic pathway and insidious effects on physiological properties of blood vessel, cognitive function, and intracerebral hemorrhage risk provide a long time window for slowing progression, but only if the early pathogenic steps can be detected and blocked. Potential approaches to slowing the progression of cerebral amyloid angiopathy include reducing Aβ production, enhancing Aβ clearance, and protecting vessels from destructive remodeling triggered by Aβ. Data on blocking production of Aβ may emerge from an ongoing phase 2 trial (ClinicalTrials.gov number, NCT06393712) of a C16-conjugated short interfering RNA targeted to APP, a trial involving persons with symptomatic sporadic cerebral amyloid angiopathy as well as those with presymptomatic or symptomatic Dutch-type cerebral amyloid angiopathy. Determining how and when cerebral amyloid angiopathy can be slowed will inform future progress in developing treatments for this small-vessel brain disease.

Cerebral Amyloid Angiopathy

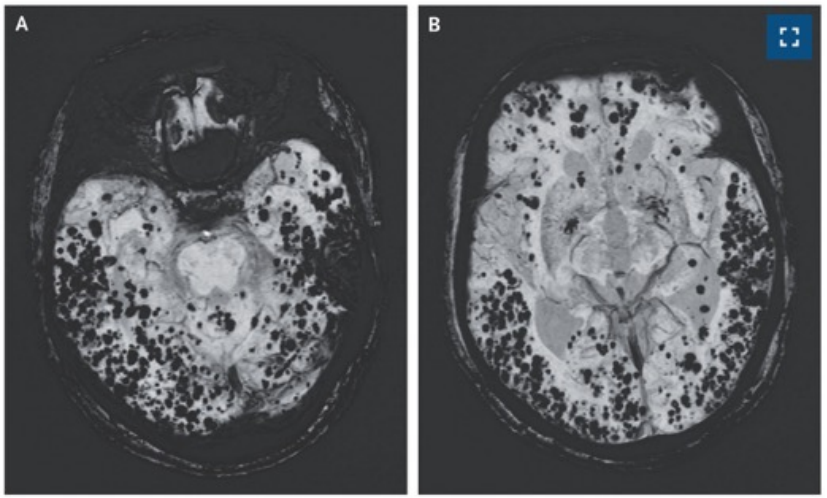

An 86-year-old man presented to the neurology clinic with a 2-year history of progressive memory loss and gait instability. Recent computed tomography of the head had shown mild cerebral atrophy. Neurologic examination was notable for a slow gait with a narrow base of support, as well as moderate-to-severe cognitive impairment on multiple tests. Magnetic resonance imaging with the use of susceptibility-weighted methods showed more than 500 hypointense, round foci throughout the lobar regions, with relative sparing of deep structures, findings consistent with the pattern of cerebral microbleeds seen in cerebral amyloid angiopathy (Panels A and B, susceptibility-weighted imaging sequence). Cerebral amyloid angiopathy is characterized by abnormal deposition of beta-amyloid (Aβ) peptides in the walls of small and medium cerebral blood vessels. Clinical manifestations include acute lobar intracerebral hemorrhage, dementia, and transient focal neurologic episodes. Further diagnostic testing was performed in this patient as part of a clinical trial. Positron-emission tomography showed diffuse cortical amyloid deposition. Analysis of the cerebrospinal fluid showed decreased levels of Aβ42 and Aβ40 proteins and a normal ratio of the two proteins. Exome sequencing was negative for variants associated with cerebral amyloid angiopathy, which is sporadic in most patients. Treatment with supportive care was advised. During the 3 years after diagnosis, the patient had worsening cognitive decline.

Erythema Multiforme

A previously healthy 22-year-old man presented to the emergency department with a 5-day history of painful lesions on his hands, feet, and mouth, with accompanying fever and malaise. Two months earlier, he had had a similar episode. His temperature was 39.1°C. On physical examination, hemorrhagic crusting of the lips, an ulceration at the right commissure of the mouth, and shallow erosions on the tongue, palate, and buccal mucosa were observed (Panel A). Target lesions with central vesicles were also found on the palms (Panel B) and soles. Polymerase-chain-reaction testing of a swab sample from the lip ulceration was positive for herpes simplex virus (HSV) type 1. Testing was negative for human immunodeficiency virus and syphilis. A diagnosis of erythema multiforme associated with HSV infection was made. Erythema multiforme is an acute, immune-mediated mucocutaneous reaction that is most commonly triggered by infection. It may also be idiopathic or associated with medication. It can be accompanied by systemic symptoms in severe cases and may have a recurring course, as in this patient. Owing to discomfort associated with oral intake, the patient was treated with systemic glucocorticoids, along with therapeutic and then prophylactic antiviral therapy. Three weeks after presentation, the lesions had abated and had not recurred (Panels C and D).

Immune Interference

A 62-year-old man was admitted to the hospital for malaise, anorexia, rash, and diffuse lymphadenopathy. Fatigue and anorexia had begun 6 months earlier. Four months before admission, a pruritic rash developed on the back and during the next several days spread to the abdomen, arms, and legs. The rash did not resolve with topical glucocorticoids, antihistamines, or antibiotics (cephalosporin followed by fluoroquinolone). One month before admission, he completed a course of antibiotics and underwent a cervical-lymph-node biopsy at another hospital. The specimen showed granulation tissue with infiltration of lymphocytes, plasma cells, neutrophils, and a small population of atypical T cells but was inconclusive. No microbiologic studies were performed on the specimen.

The patient had lost 11 kg in the past 6 months. He reported no fever, night sweats, or cough. His medical history was notable only for coronavirus disease 2019 (Covid-19) 1 year earlier. He was taking no medications or herbal supplements. He had smoked one pack of cigarettes daily for 42 years and drank 12 ounces of beer twice per week. He was an office worker and enjoyed gardening. He was born in Kyushu, the southernmost of the four main islands of Japan, and later resided near Tokyo.

He appeared fatigued. The axillary temperature was 36.8°C, the pulse 108 beats per minute, the blood pressure 112/66 mm Hg, the respiratory rate 12 breaths per minute, and the oxygen saturation 95% while he was breathing ambient air. Multiple tender lymph nodes, each between 1.0 and 1.5 cm in diameter, were noted, bilaterally in the cervical, axillary, and inguinal regions. Cardiopulmonary and abdominal examinations were normal; there was no hepatosplenomegaly. Erythematous papules and pustules were present on the trunk, arms, and legs, including the palms and soles.

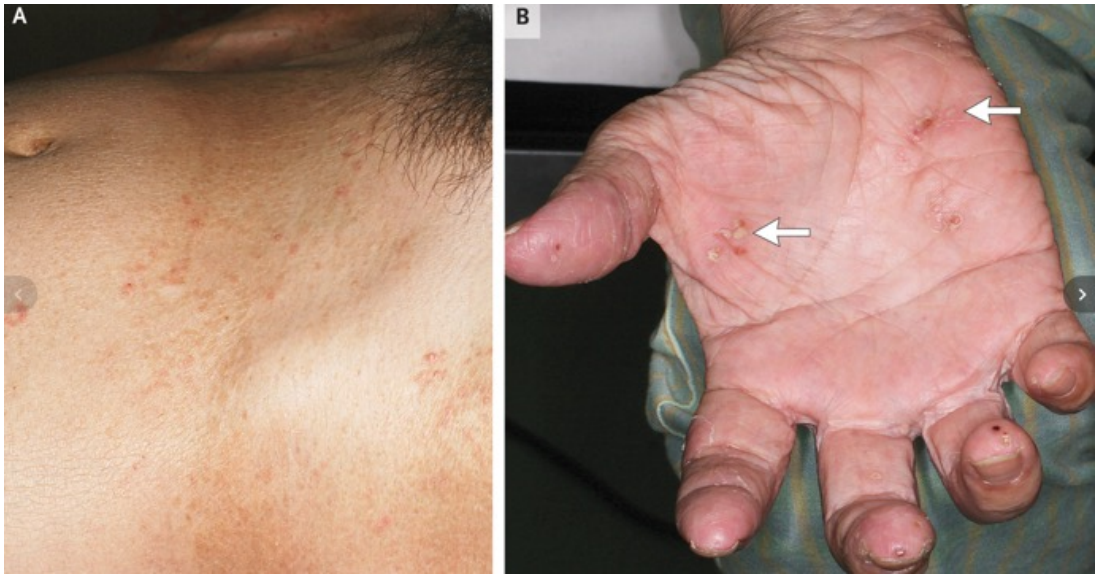

Skin Changes.

Panel A shows erythematous papules and pustules on the lower abdomen and right lateral side of the waist. Panel B shows pustules (arrows) and crust on the right palm.

The white-cell count was 30,800 per microliter, with 83% neutrophils, 6% lymphocytes, 3% monocytes, and 5% eosinophils. The hemoglobin level was 9.7 g per deciliter with a platelet count of 676,000 per microliter. The erythrocyte sedimentation rate was 117 mm per hour (reference value, <10). The C-reactive protein (CRP) level was 11.3 mg per deciliter (reference value, <0.14). The aspartate aminotransferase level was 30 U per liter (reference range, 13 to 30), the alanine aminotransferase level was 44 U per liter (reference range, 10 to 42), and the lactate dehydrogenase level was 190 U per liter (reference range, 124 to 222). These results were similar to those obtained 1 month earlier at the outside facility.

The IgG, IgM, and IgA levels were normal. Testing for antinuclear antibodies was negative, as was testing for rapid plasma reagin and serum HIV antibodies. The CD4+ T-cell count was 1197 per microliter (reference range, 344 to 1290). Tests for EBV DNA in peripheral-blood mononuclear cells and CMV antigenemia were both negative. Testing for anti–HTLV-1 antibody was negative. The T-SPOT.TB (T-SPOT) interferon-γ release assay was negative. Acid-fast bacilli stains of the sputum were negative. Two sets of blood cultures were sterile. A chest radiograph was normal.

Contrast-enhanced computed tomography (CT) showed diffuse lymphadenopathy, with one left cervical lymph node having internal necrosis. Whole-body positron-emission tomography revealed hypermetabolic lymph nodes in cervical, supraclavicular, axillary, intrathoracic, mediastinal, periaortic, and mesenteric regions (Figure 2), available with the full text of this article at NEJM.org). An excisional biopsy of a left supraclavicular lymph node revealed replacement of the lymph follicle by lymphocytes, plasma cells, and neutrophils, along with a small population of atypical plasma cells. There were no granulomas. Flow cytometry and immunostaining did not suggest lymphoma, Castleman's disease, or IgG4-related disease. Ziehl–Neelsen and Giemsa staining showed no microorganisms.

An abdominal skin biopsy revealed epidermal pustular dermatitis (neutrophilic infiltrate with spongiosis). No atypical cells were identified. Cultures of the biopsy specimens yielded no growth of bacteria or fungi.

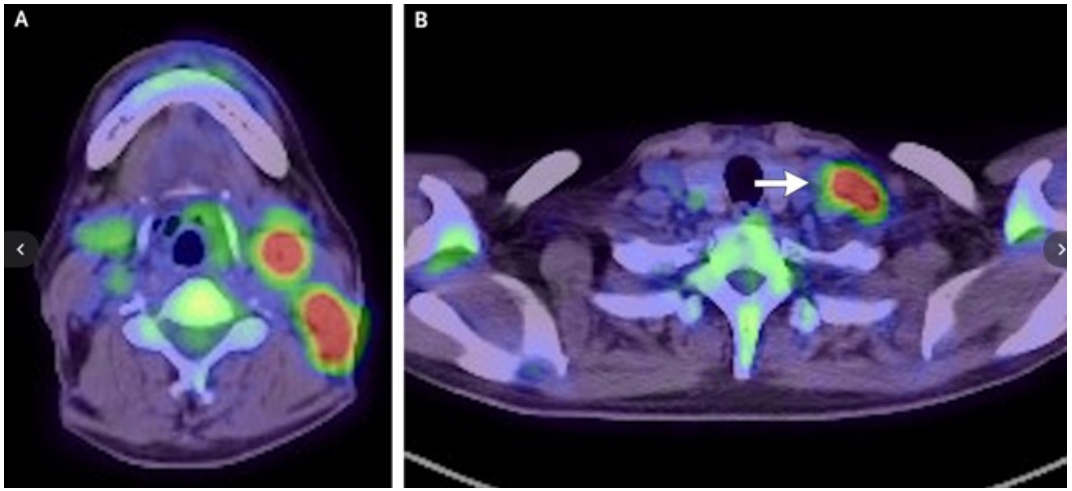

Whole-Body Positron-Emission Tomography (PET).

Whole-body PET showed hypermetabolic lymph nodes in the cervical (Panel A), supraclavicular (Panel B), axillary, intrathoracic, periaortic, and mesenteric regions. The arrow in Panel B indicates a biopsied lymph node.

After 6 days, acid-fast bacilli were detected on mycobacterial blood culture and were later identified as *Mycobacterium abscessus*. Culture from a biopsy of the left axillary lymph node subsequently grew *M. abscessus*. A second interferon-γ release assay, QuantiFERON-TB Gold Plus (QFT), was indeterminate, owing to a lack of response in the mitogen tube (a positive control that confirms that the patient's immune system is capable of mounting an interferon-γ response).

Neutralizing autoantibodies against interferon-γ were detected at a titer of 768 enzyme-linked immunosorbent assay (ELISA) units (EU) (reference range, 5 to 50; 1 EU=1.0 µg per milliliter) in a serum dilution of 1:1000. Anti–interferon-γ autoantibody syndrome was diagnosed.

After 4 weeks of intravenous antibiotic therapy (azithromycin, amikacin, and imipenem), the rash and lymphadenopathy abated. On the basis of susceptibility testing, the regimen was switched to oral azithromycin and sitafloxacin.

One month later, the rash and lymphadenopathy recurred (Figure 3). The patient was afebrile, and blood and skin mycobacterial cultures were negative. Cultures of a left axillary lymph node grew *M. abscessus* with an increase of four times in macrolide minimum inhibitory concentration (MIC) as compared with the original strain. After the administration of imipenem, tigecycline, and clarithromycin, the rash resolved, and the lymphadenopathy decreased.

Skin Changes on the Second Admission.

Exanthematous pustulosis was observed on the palms.

Surveillance CT performed 4 weeks later showed regression of the lymphadenopathy but multiple new hepatic lesions. CT performed 2 weeks after the initial surveillance CT revealed further enlargement of these hepatic lesions, despite further reductions in lymphadenopathy and in the rash and an increase in the energy level. A liver biopsy showed necrosis and clusters of epithelioid cells suggestive of granulomas. Cultures from the specimen were negative.

A paradoxical reaction to antimicrobial treatment was diagnosed. The antimicrobial regimen was continued without administration of glucocorticoids. After 6 weeks of intravenous therapy, the regimen was switched to oral treatment with clarithromycin, sitafloxacin, and clofazimine. At 2 months of follow-up, the liver lesions had resolved and the patient had gained 2 kg and returned to work.

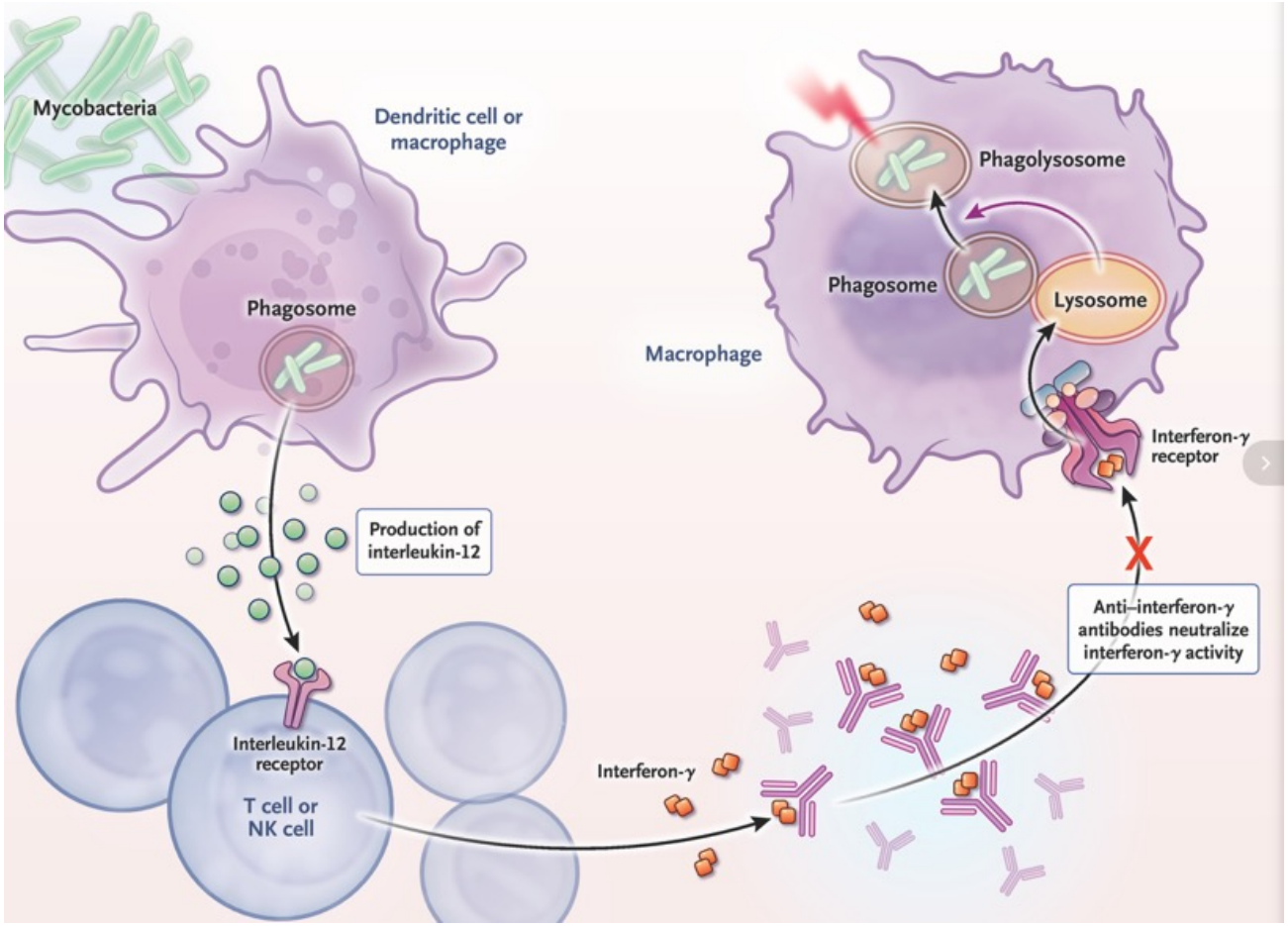

Cell-Mediated Defense Mechanism against Mycobacteria.

After the recognition and internalization of nontuberculous mycobacteria, macrophages and dendritic cells form a phagosome and produce interleukin-12. Interleukin-12 subsequently induces interferon-γ production by T cells and natural killer (NK) cells. Interferon-γ activates macrophages, promoting the fusion of phagosomes with lysosomes to form phagolysosomes, which enables them to kill and degrade the pathogen. Anti–interferon-γ autoantibodies neutralize interferon-γ activity, thereby disrupting the interleukin-12–interferon-γ axis.

Paradoxical reactions commonly emerge or intensify during immune reconstitution in immunocompromised patients but can also occur in persons who are immunocompetent. This patient had impaired interferon-γ responsiveness but intact cell-mediated immunity, including CD4+ T cells, which were capable of reacting to the increased quantity of mycobacterial antigens. Treatment failure, including drug resistance, must be ruled out before diagnosis of a paradoxical reaction. Clinical improvement often occurs with observation alone. In patients with severe symptoms, glucocorticoids or tumor necrosis factor α antagonists may be considered.

This case illustrates how the discovery of a particular infection (in this case, *M. abscessus* in a patient without known immunocompromise) can point to a specific immunodeficiency syndrome (in this case, anti–interferon-γ autoantibody syndrome). It also highlights that clinical worsening in the context of treatment does not necessarily imply treatment failure but rather may indicate a paradoxical reaction, which reflects the dynamic interplay between mycobacteria and the immune system. These two manifestations illustrate both interference with the immune system and its overzealous response.

Eine Darmspiegelung (Koloskopie) gilt als der „Goldstandard“ für die Darmkrebsvorsorge. Sie ist die einzige Methode, die Krebs nicht nur erkennt, sondern durch die Entfernung von Vorstufen (Polypen) aktiv verhindern kann.

Warum die Koloskopie wichtig ist

•**Prävention:** Ärzte können Polypen während der Untersuchung direkt entfernen, bevor diese bösartig werden.

•**Vollständigkeit:** Der gesamte Dickdarm wird mit einer Kamera gründlich untersucht.

•**Genauigkeit:** Sie ist der empfindlichste verfügbare Test zur Früherkennung

Long-term effects of colonoscopy screening on colorectal cancer incidence and mortality: a multicountry, population-based randomised controlled trial

Summary

Background We previously reported the 10-year effects of colonoscopy screening on colorectal cancer incidence and mortality. Here, we report the effects after 13 years of follow-up.

Methods In this multicountry, population-based randomised controlled trial, 84 583 men and women aged 55–64 years at enrolment from Norway, Poland, and Sweden were randomly allocated (1:2) to colonoscopy screening or no screening and analysed. The primary outcomes were colorectal cancer incidence and mortality after 10–15 years of follow-up in intention-to-screen analyses, with first analysis after 10 years, and repeated every other year or at longer intervals. This trial is registered with ClinicalTrials.gov, NCT00883792, and is ongoing.

Findings At 13 years of follow-up, colorectal cancer incidence was 375 colorectal cancers (1·46%) of 28 217 individuals in the screening group and 912 colorectal cancers (1·80%) of 56 366 individuals in the no-screening group. The risk ratio (RR) was 0·81 (95% CI 0·71–0·90) in intention-to-screen analyses and 0·55 (0·33–0·81) in per-protocol analyses. The risk for proximal colorectal cancer was 129 (0·51%) in the screening group versus 283 (0·56%) in the no-screening group (RR 0·91 [0·71–1·09]), and the risk for distal colorectal cancer was 224 (0·87%) in the screening group versus 563 (1·11%) in the no-screening group (RR 0·79 [0·65–0·89]; interaction p<0·0001). In men, the colorectal cancer risk was 214 (1·69%) of 14 154 in the screening group and 541 (2·19%) of 28 247 in the no-screening group (RR 0·77 [0·64 to –0·88]); in women, the risk was 161 (1·24%) of 14 063 in the screening group versus 371 (1·43%) of 28 119 in the no-screening group (RR 0·87 [0·70 to 1·02]; interaction p<0·0001). Colorectal cancer mortality was 106 (0·41%) of 28 217 in the screening group and 236 (0·47%) of 56 366 in the no-screening group (intention-to-screen RR 0·88 [0·68–1·08], per-protocol RR 0·70 [0·26–1·25]). The observed colorectal cancer mortality in the non-screening group (0·47%) was substantially lower than expected at the time of designing the trial (0·82%).

Interpretation One colonoscopy significantly reduced colorectal cancer incidence but not mortality over 13 years. Colorectal cancer mortality was lower in both study groups than when the trial was designed.

	Poland (n=54 527)	Norway (n=26 413)	Sweden (n=3643)
Group			
Attender	6002 (11·0%)	5354 (20·3%)	485 (13·3%)
Non-attender	12 181 (22·3%)	3461 (13·1%)	734 (20·1%)
Control	36 344 (66·7%)	17 598 (66·6%)	2424 (66·5%)
Sex			
Female	27 329 (50·1%)	13 194 (50·0%)	1659 (45·5%)
Male	27 198 (49·9%)	13 219 (50·0%)	1984 (54·5%)
Age at enrolment			
<60 years	28 791 (52·8%)	12 524 (47·4%)	1782 (48·9%)
≥60 years	25 736 (47·2%)	13 889 (52·6%)	1861 (51·1%)

Data are n (%). Discrepancies in numbers of analysed individuals between this analysis and the previously published 10-year follow-up study can be found in the appendix (p 28).

Table 1: **Characteristics of trial participants**

	Screening group (n=28 217)		No-screening group (n=56 366)		Risk difference, % (95% CI)	Risk ratio (95% CI)
	Number of events	13-year risk, % (95% CI)	Number of events	13-year risk, % (95% CI)		
Intention-to-screen analysis						
Colorectal cancer	375	1·46% (1·32–1·62)	912	1·80% (1·69–1·92)	−0·34% (−0·54 to −0·17)	0·81 (0·71–0·90)
Death from colorectal cancer	106	0·41% (0·34–0·50)	236	0·47% (0·42–0·54)	−0·06% (−0·16 to 0·04)	0·88 (0·68–1·08)
Death from any cause	4506	16·30% (15·87–16·74)	9017	16·34% (16·03–16·65)	−0·04% (−0·56 to 0·51)	1·00 (0·97–1·03)
Per-protocol analysis						
Colorectal cancer	..	1·00% (0·63–1·41)	..	1·80% (1·69–1·91)	−0·80% (−1·24 to −0·33)	0·55 (0·33–0·81)
Death from colorectal cancer	..	0·33% (0·13–0·55)	..	0·47% (0·42–0·53)	−0·14% (−0·37 to 0·11)	0·70 (0·26–1·25)

Table 2: **Primary and secondary endpoints in intention-to-screen and per-protocol analyses**

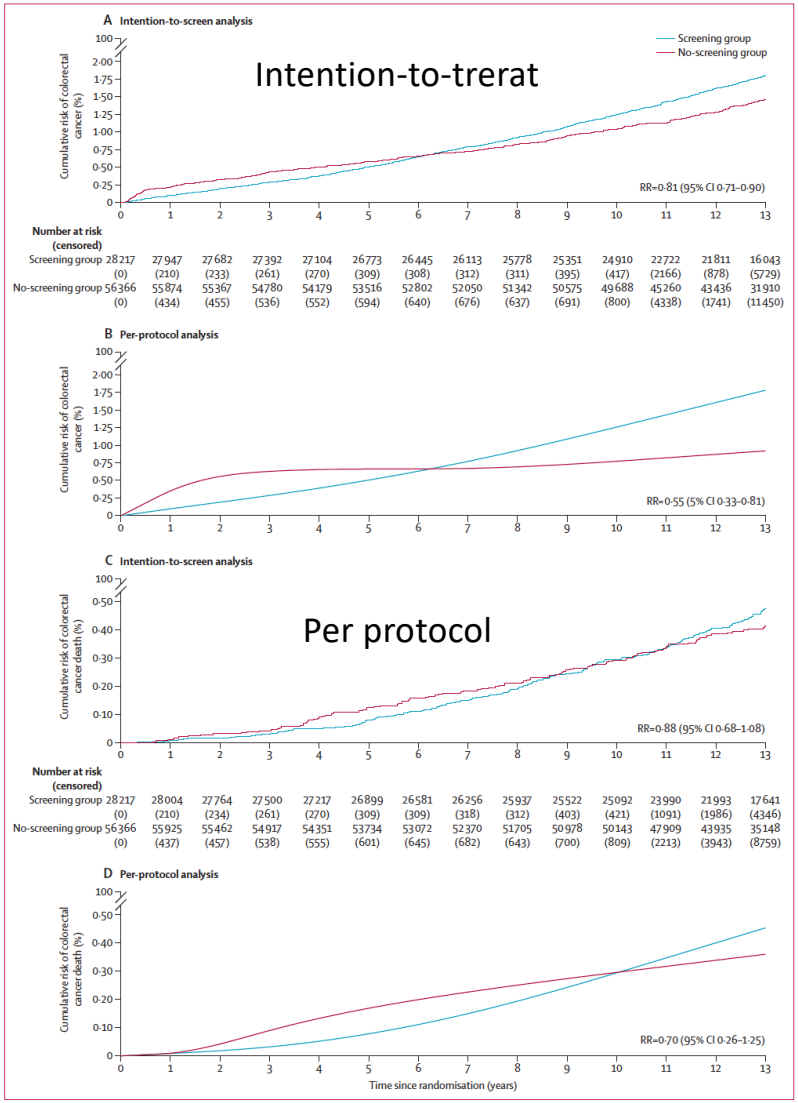

Figure 1: **Cumulative colorectal cancer incidence and mortality at 13 years in intention-to-screen and per-protocol analyses**
Colorectal cancer incidence in intention-to-screen analysis (A) and per-protocol analysis (B). Colorectal cancer death in intention-to-screen analysis (C) and per-protocol analysis (D). Risk curves based on per-protocol estimations were smoothed with restricted cubic splines with knots at 0·5, 1, 3, 7, and 11 years of follow-up. RR=risk ratio.

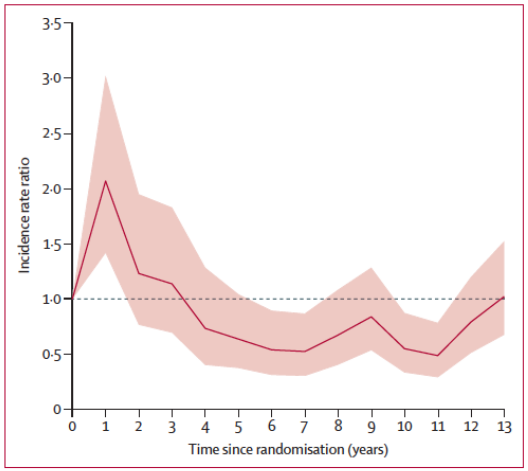

Figure 2: **Yearly rate ratios for colorectal cancer incidence in the screening group compared with the no-screening group, intention-to-screen analysis**
Shading indicates 95% CIs. The dotted line indicates similar incidence rate ratio in the two groups.

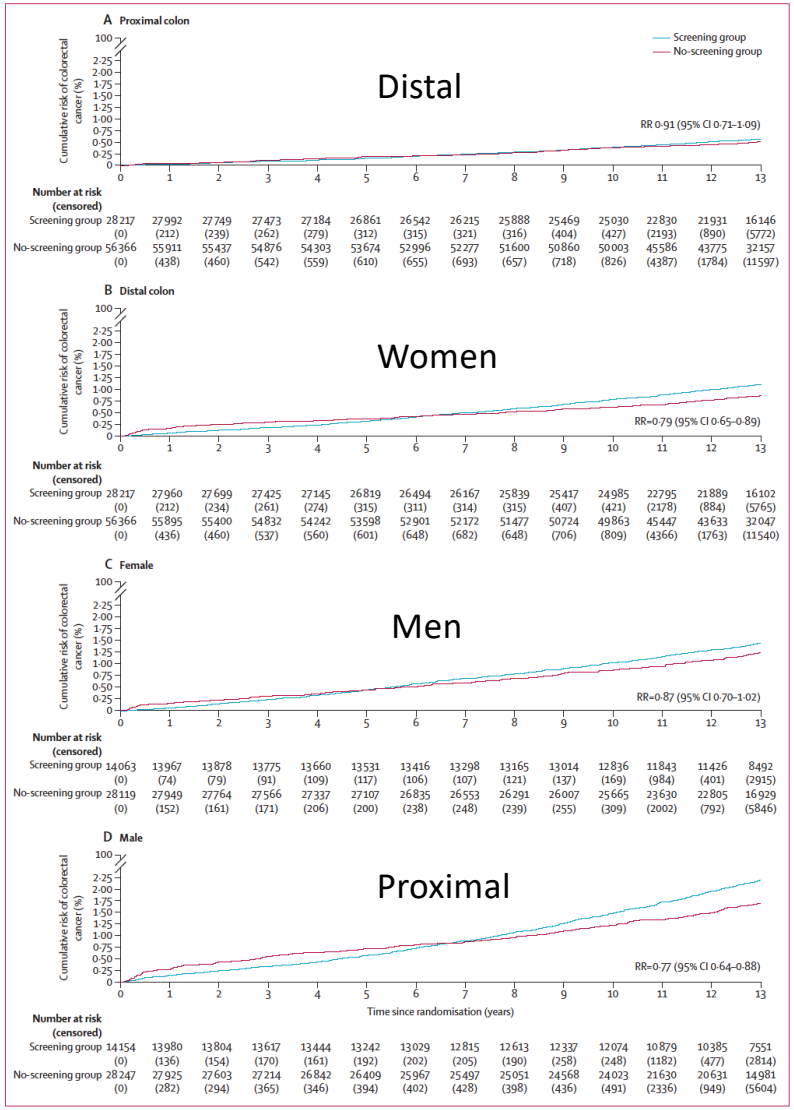

***Figure 3*: Cumulative colorectal cancer incidence at 13 years in intention-to-screen analysis according to cancer location and sex**
Proximal colorectal cancer incidence* (A), distal colorectal cancer incidence* (B), colorectal cancer incidence in female participants (C), and colorectal cancer incidence in male participants (D).
*Proximal colorectal cancer: location proximal for the descending colon. Distal colorectal cancer: location in the descending colon, sigmoid colon, or rectum.

Implications of all the available evidence

According to these new results, a single colonoscopy reduces colorectal cancer risk by 0·3% to 0·8% over 13 years. The study reveals that the risk of colorectal cancer death is significantly lower than was expected when the trial started even without screening, and that screening does not provide additional reduction of an already low risk for colorectal cancer mortality with longer follow-up than 10 years. These data might help to guide policies at the population level, where screening benefits must be weighed against other expenditures that promote public health.

Es gibt derzeit zwei von der Weltgesundheitsorganisation (WHO) empfohlene Impfstoffe gegen Malaria: RTS,S/AS01 (Mosquirix) und den neueren R21/Matrix-M. Diese Impfstoffe sind primär für Kinder in afrikanischen Gebieten mit hohem Übertragungsrisiko vorgesehen und dienen nicht als Reiseimpfung für Touristen.

Das primäre Zielantigen der aktuell zugelassenen und am weitesten fortgeschrittenen Malaria-Impfstoffe ist das **Circumsporozoitenprotein (CSP)**.

Dieses Protein befindet sich auf der Oberfläche der **Sporozoiten**, dem Stadium des Parasiten *Plasmodium falciparum*, das durch den Mückenstich in die Blutbahn des Menschen gelangt. Die Impfung soll verhindern, dass diese Sporozoiten die Leberzellen infizieren.

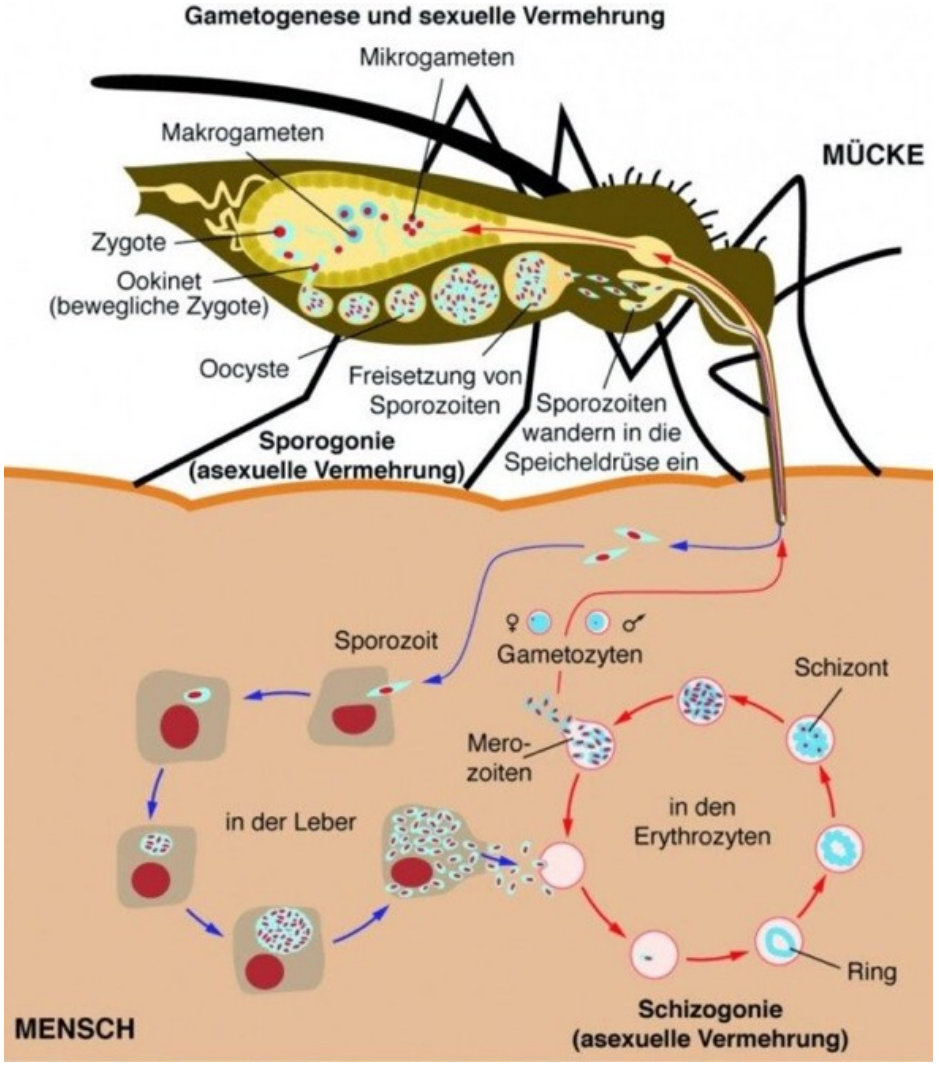

RTS,S/AS01 (Handelsname **Mosquirix**) ist der weltweit erste von der WHO empfohlene Malaria-Impfstoff (seit 2021). Er richtet sich gegen *Plasmodium falciparum*, den tödlichsten Malaria-Erreger, und wird primär bei Kindern in Subsahara-Afrika eingesetzt. Der Impfstoff zeigt eine moderate Wirksamkeit von ca. \(56\ \%\) und erfordert vier Dosen für einen wirksamen Schutz.

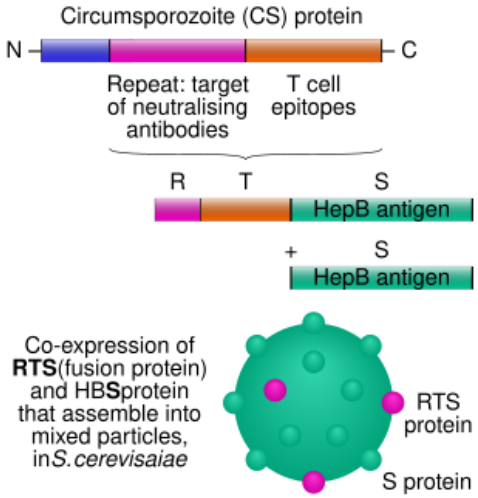

Wichtige Fakten zu Mosquirix:

•**Entwicklung & Zulassung:** Entwickelt von GSK (GlaxoSmithKline) und der PATH Malaria Vaccine Initiative, mit Förderung durch die Bill & Melinda Gates Foundation.

•**Wirkmechanismus:** Es handelt sich um einen rekombinanten Impfstoff, der ein Protein des Malaria-Parasiten mit Hepatitis-B-Oberflächenantigen kombiniert.

•**Zielgruppe:** Kinder ab 5 Monaten in Regionen mit moderater bis hoher Übertragungsrate.

•**Impfschema:** Drei Dosen im ersten Lebensjahr, eine vierte Auffrischungsdosis im Alter von ca. 24 Monaten.

•**Wirksamkeit:** In Studien wurde eine Senkung der schweren Malariafälle um über \(30\ \%\) i Pilotregionen beobachtet.

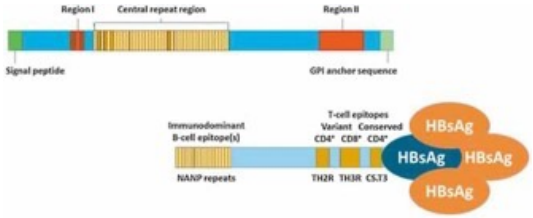

•**Sicherheit:** Der Impfstoff gilt als sicher und gut verträglich.

Impact of introducing RTS,S/AS01$_E$ malaria vaccine on mortality in young children in Ghana, Kenya, and Malawi: an observational evaluation of a cluster-randomised implementation programme

Summary

Background Malaria vaccines have been added to immunisation schedules in 25 sub-Saharan African countries, with the expectation that deaths in young children would be prevented. The introduction of the RTS,S/AS01$_E$ malaria vaccine (RTS,S) in Ghana, Kenya, and Malawi in 2019 was evaluated over 4 years to show the impact on mortality in young children and to monitor severe malaria admissions, vaccine uptake, and safety. Favourable evidence on safety and impact on severe malaria admissions during the first 2 years contributed to WHO's recommendations on malaria vaccines. Here, we report the primary analysis of the impact on mortality at 46 months.

Methods Clusters of administrative units (districts in Ghana, subcounties in Kenya, and groups of immunisation clinics in Malawi), each with an estimated annual birth cohort of about 4000 children, were randomly assigned 1:1 to introduce the RTS,S malaria vaccine in 2019 (implementation areas), or to implement later (comparison areas). RTS,S was delivered in a four-dose schedule, at age 6, 7, 9, and 24 months in Ghana and Kenya, and at age 5, 6, 7, and 22 months in Malawi. Surveillance for post-neonatal mortality in children younger than 5 years was established throughout by a network of 26 000 local reporters who notified deaths in their community. The families were then visited at home by study staff to confirm details and complete a verbal autopsy. Surveillance for severe malaria and other conditions was strengthened in 18 sentinel hospitals serving part of the study area and maintained for 46 months. Uptake of RTS,S and other vaccines was monitored by the Expanded Programme on Immunisation in each country and independently through three household coverage surveys, at baseline, and at about 18 months and 30 months after introduction of RTS,S. The primary outcome of this impact evaluation was mortality due to any cause, except injury, in children eligible to receive three doses of RTS,S. Mortality rate ratios were estimated by comparing the ratio of deaths among vaccine-eligible age groups to deaths in non-eligible age groups between implementation and comparison areas. This evaluation is registered on ClinicalTrials.gov (NCT03806465) and is complete.

Vaccine given for 4 doses

Findings 158 clusters (66 in Ghana, 46 in Kenya, and 46 in Malawi) were selected and randomly assigned; 79 areas served as implementation areas and 79 as comparison areas. By the end of the 46-month evaluation period, 1 289 504 children had received the first dose of RTS,S, 1 158 850 had received the second dose, 1 068 039 had received a third dose, and 436 527 had received a fourth dose. Coverage assessed in 2022 was 82·8% (95% CI 80·7–84·9) for the first dose, 71·1% (68·8–73·5) for the third dose, and 39·9% (36·9–42·9) for the fourth dose. Excluding deaths due to injury, there were 5576 deaths in implementation areas versus 6152 in comparison areas in children eligible to have received the third dose of RTS,S, and 7534 versus 7044 deaths among non-eligible children. The mortality rate ratio was 0·87 (95% CI 0·77–0·97; p=0·016).

Interpretation Introduction of the RTS,S malaria vaccine in routine immunisation programmes was associated with a significant reduction in mortality in young children, averting about one in eight deaths, in areas with moderate coverage of three doses of the vaccine and low uptake of the fourth dose. These results highlight the urgency to accelerate the deployment of malaria vaccines in areas of Africa where malaria continues to be a leading cause of child mortality.

Reduced mortality (somewhat)

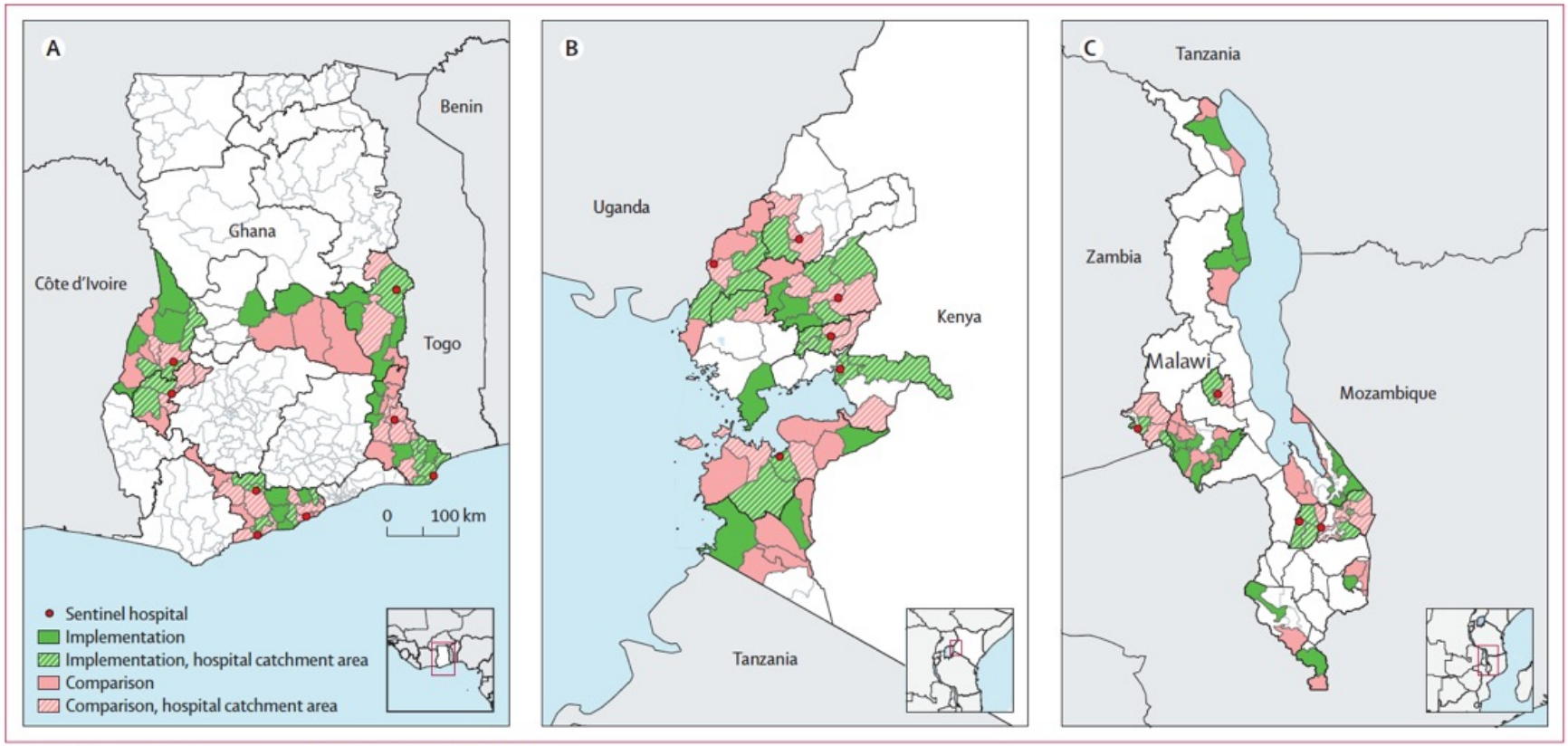

Figure 1: **Maps of evaluation areas in Ghana, Kenya, and Malawi**

Areas shaded green are clusters randomly assigned to RTS,S implementation beginning in 2019, while areas shaded pink, randomised to implement later, served as comparison areas. The 158 clusters comprised 66 districts in Ghana, 46 subcounties in Kenya, and the catchment areas of 46 groups of immunisation clinics in Malawi. Mortality surveillance was maintained throughout all 158 clusters. Sentinel hospitals, indicated by red dots, served part of the evaluation areas. Diagonal hatching indicates the 77 clusters out of the 158 that were defined as sentinel hospital catchment clusters, based on a review of paediatric admissions before randomisation. RTS,S=RTS,S/AS01E malaria vaccine.

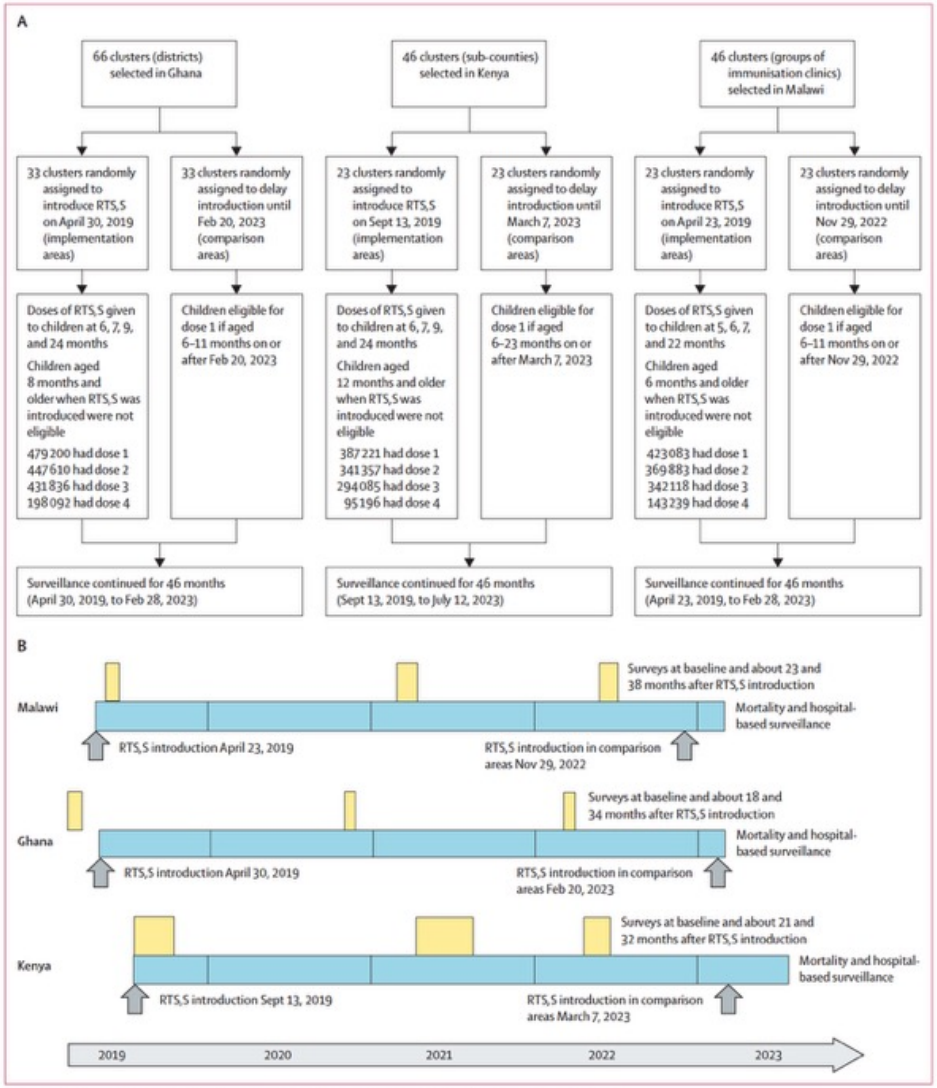

Figure 2: Random assignment to implementation and comparison areas (A), and evaluation timelines (B)
RTS,S=RTS,S/AS01E malaria vaccine.

	Pooled estimates		Ghana		Kenya		Malawi	
	Implementation areas	Comparison areas	Implementation areas	Comparison areas	Implementation areas	Comparison areas	Implementation areas	Comparison areas
Clusters, n	79	79	33	33	23	23	23	23
Mean surviving infants per cluster in 2018, n (SD)	4596 (1690·0)	4727 (1648·3)	3898 (1725·3)	4052 (1753·1)	5509 (1649·0)	5467 (1579·1)	4684 (1211·2)	4956 (1164·9)
Children aged 12–23 months, n	2493	2564	1079	1176	644	694	770	694
Home-based vaccine record	2129/2493 (85·4%)	2256/2564 (87·7%)	926/1079 (85·6%)	1062/1176 (89·7%)	553/644 (86·2%)	588/694 (85·3%)	650/770 (84·4%)	606/694 (85·8%)
BCG	1954/2129 (92·5%)	2103/2256 (93·7%)	860/926 (92·0%)	1000/1062 (94·6%)	533/553 (95·5%)	572/588 (95·2%)	561/650 (86·7%)	531/606 (87·1%)
Penta-3	2110/2301 (91·1%)	2233/2419 (94·4%)	875/926 (93·3%)	1015/1062 (96·0%)	584/630 (91·8%)	613/674 (91·4%)	651/745 (87·5%)	605/683 (88·5%)
OPV-3	2000/2295 (90·5%)	2119/2411 (93·2%)	852/926 (90·5%)	973/1062 (92·4%)	536/622 (85·4%)	564/667 (84·9%)	612/747 (81·2%)	582/682 (85·5%)
PCV-3	2077/2291 (90·8%)	2217/2405 (94·8%)	879/926 (94·0%)	1015/1062 (96·0%)	553/622 (88·8%)	602/660 (91·6%)	645/743 (86·7%)	600/683 (87·8%)
Rota-2	2087/2294 (91·4%)	2228/2405 (95·2%)	877/926 (94·3%)	1025/1062 (96·9%)	563/624 (89·3%)	607/659 (91·9%)	647/744 (87·3%)	596/684 (86·7%)
Measles-1	2029/2310 (88·0%)	2144/2425 (88·9%)	841/926 (90·2%)	971/1062 (90·8%)	553/632 (85·5%)	609/677 (90·6%)	635/752 (85·4%)	564/686 (82·5%)
Fully vaccinated	1651/2129 (74·7%)	1773/2256 (78·0%)	734/926 (77·2%)	847/1062 (80·3%)	438/553 (76·4%)	476/588 (81·0%)	479/650 (73·1%)	450/606 (74·8%)
Vitamin A in the previous 6 months	1221/2301 (50·0%)	1217/2429 (49·4%)	494 /926 (50·9%)	529/1062 (48·4%)	290/638 (43·1%)	308/688 (45·6%)	437/737 (58·0%)	380/679 (54·7%)
Children aged 24–35 months (Ghana and Kenya), 21–32 months (Malawi), n	2344	2280	896	891	665	652	783	737
Measles-2	1537/2272 (69·1%)	1498/2229 (67·3%)	744/896 (82·8%)	730/891 (80·2%)	315/624 (48·1%)	312/619 (50·8%)	478/752 (63·4%)	456/719 (66·0%)
Children aged 5–48 months, n	8789	8783	3881	3887	2430	2518	2478	2378
Slept under insecticide-treated nets the previous night	6858/8788 (87·4%)	6870/8782 (84·8%)	2521/3881 (63·4%)	2453/3887 (59·8%)	2094/2430 (85·6%)	2218/2518 (88·9%)	2243/2477 (90·3%)	2199/2377 (91·9%)
MUAC <13·5 cm	1224/8789 (11·3%)	1251/8783 (13·1%)	623/3881 (17·1%)	665/3887 (17·7%)	145/2430 (5·8%)	161/2518 (6·6%)	456/2478 (18·5%)	425/2378 (17·6%)
Malaria positive by RDT	2081/8754 (24·2%)	1812/8746 (18·5%)	805/3881 (20·7%)	831/3887 (20·4%)	642/2400 (26·4%)	502/2488 (18·6%)	634/2473 (28·1%)	479/2371 (16·7%)
Sought care for fever*	582/799 (73·0%)	536/763 (72·6%)	209/287 (74·5%)	178/253 (76·6%)	185/252 (71·6%)	183/256 (71·8%)	188/260 (71·9%)	175/254 (67·7%)

Data are n/N (%) unless otherwise specified. Percentages are survey weighted, hence may not equal the value calculated from numerator and denominator. Baseline surveys were conducted from Feb 25 to March 18, 2019 (Ghana), July 15 to Dec 16, 2019 (Kenya), and May 6 to June 19, 2019 (Malawi). Coverage of routine vaccinations in the first year of life was estimated in children aged 12–23 months. In Ghana, estimates are based on the home-based record only; in Kenya and Malawi, estimates are based on documented status from the home-based record, or caregiver recall if a home-based record was not available. Coverage of the second dose of measles vaccine was estimated in a 12-month age range, starting 6 months after the recommended age for the second dose, which was 18 months in Ghana and Kenya, and 15 months in Malawi. Fully vaccinated was defined as having received BCG at birth, three doses of OPV (excluding the birth dose), three doses of pentavalent vaccine, and one dose of measles vaccine. Children who received IPV at 14 weeks in place of OPV-3 were considered to be fully vaccinated for polio. IPV=inactivated polio virus. Measles-1=first dose of measles vaccine. Measles-2=second dose of measles vaccine. MUAC=mid-upper arm circumference. OPV-3=third dose of oral polio vaccine (excluding birth dose). PCV-3=third dose of pneumococcal vaccine. Penta-3=third dose of pentavalent vaccine. RDT=rapid diagnostic test. Rota-2=second dose of rotavirus vaccine. *Care-seeking for fever was assessed in children who had fever in the 2 weeks before the survey, according to the caregiver (this was 34·0% in implementation areas and 28·1% in comparison areas, pooled).

***Table*: Characteristics of children in implementation and comparison areas at baseline**

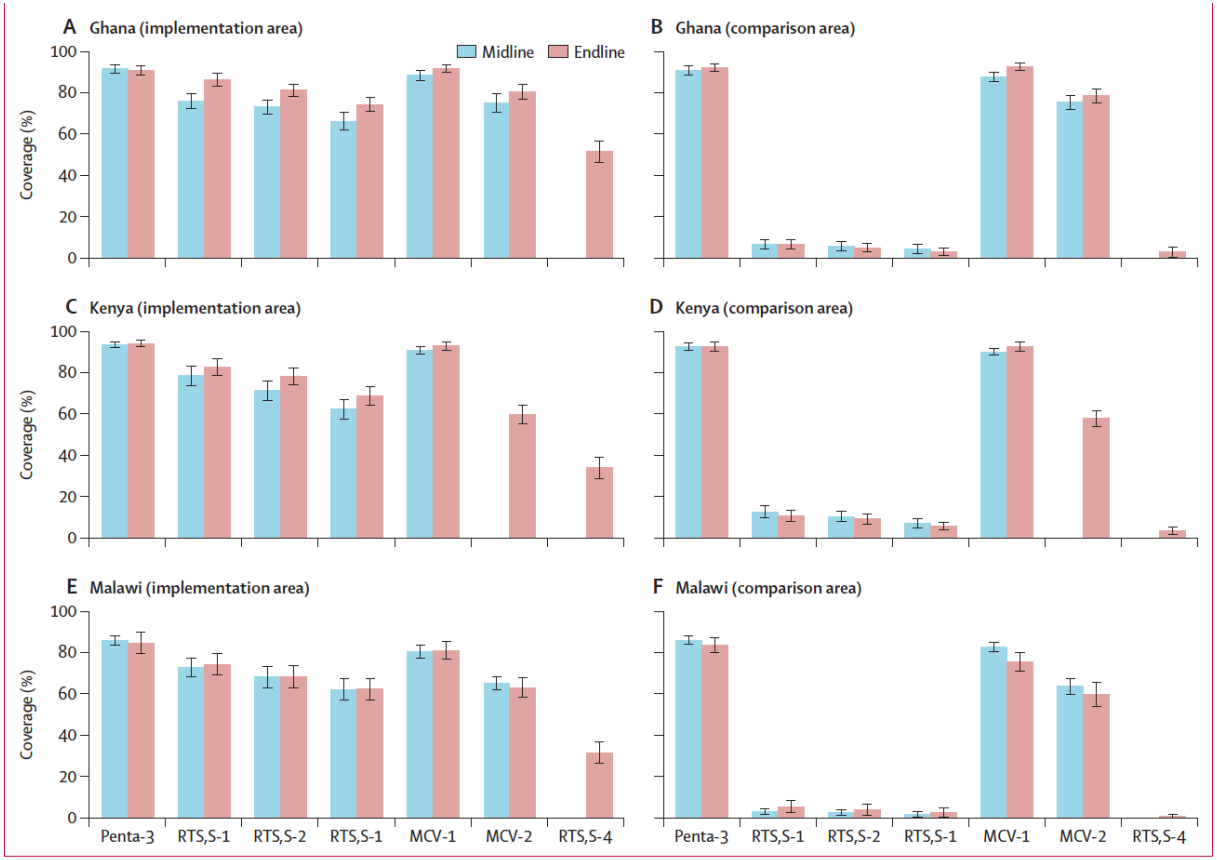

Figure 3: **Coverage of RTS,S and other childhood vaccines by dose in implementation and comparison clusters at midline and endline household surveys**
Vaccination coverage was estimated in surveys about 18 months after introduction of RTS,S (midline) and about 30 months after introduction (endline) in RTS,S implementation and comparison areas. The error bars are 95% CIs. Penta-3 was given at 14 weeks, RTS,S-1 at 6 months (Ghana and Kenya) and 5 months (Malawi), RTS,S-2 at 7 months (Ghana and Kenya) and 6 months (Malawi), RTS,S-3 at 9 months (Ghana and Kenya) and 7 months (Malawi), MCV-1 at 9 months, and MCV-2 at 15 months (Malawi) or 18 months (Ghana and Kenya). Penta-3, RTS,S doses 1–3, and MCV-1 coverages were estimated among children aged 12–23 months. MCV-2 and RTS,S dose 4 coverages were estimated among children aged 30–40 months in Ghana, 30–36 months in Kenya, and 28–39 months in Malawi. Coverage is according to home-based record (HBR) or caregiver recall if HBR was not available. Tests of interaction showed coverage of RTS,S dose 3 was similar across countries at midline ($F_{2,237}$=1·09, p=0·34), but at endline coverage differed with respect to dose 3 ($F_{2,235}$=7·44, p=0·0007) and dose 4 ($F_{2,234}$=17·88, p<0·0001), with coverage higher in Ghana. MCV-1=first dose of measles-containing vaccine. MCV-2=second dose of measles-containing vaccine. Penta-3=third dose of pentavalent vaccine. RTS,S-1=first dose of RTS,S/AS01$_E$ malaria vaccine. RTS,S-2=second dose of RTS,S/AS01$_E$ malaria vaccine. RTS,S-3=third dose of RTS,S/AS01$_E$ malaria vaccine. RTS,S-4=fourth dose of RTS,S/AS01$_E$ malaria vaccine.

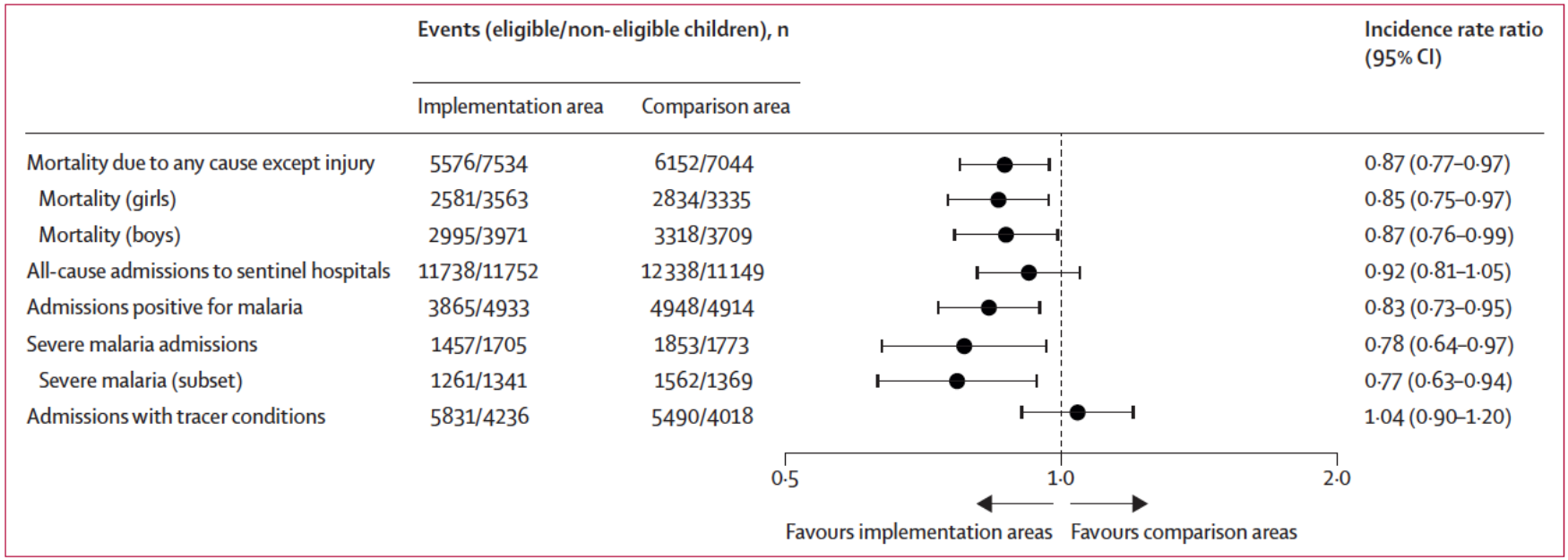

Figure 4: **Estimates of the association of RTS,S introduction with all-cause mortality (excluding deaths due to injury) and with admissions to hospital for any cause and with severe malaria**

Incidence rate ratios refer to children eligible to have received the third dose of RTS,S. Deaths were captured through mortality surveillance throughout the evaluation areas. Hospitalisation data were captured through sentinel hospital surveillance in part of the evaluation areas (hatched areas in figure 1). Severe malaria followed standardised case definitions; the subset refers to patients with severe malaria in whom lumbar puncture was performed in cases of coma to rule out meningitis. Tracer conditions are hospitalisations due to conditions unlikely to be influenced by RTS,S introduction (admissions from any cause, excluding those with a positive malaria test, with anaemia, or meningitis). RTS,S=RTS,S/AS01$_E$ malaria vaccine.

Implications of all the available evidence

There is an extensive body of evidence showing that current malaria vaccines are safe and effective. Malaria vaccines have been introduced in 25 countries—Ghana, Kenya, and Malawi in 2019; Central African Republic, Côte d'Ivoire, Burkina Faso, Liberia, Cameroon, Benin, Sierra Leone, South Sudan, Mozambique, Niger, Chad, the Democratic Republic of the Congo, Sudan, and Nigeria in 2024; Burundi, Uganda, Mali, Guinea, Ethiopia, Togo, and Zambia in 2025; and Guinea-Bissau in 2026, with more countries planning introductions. In many areas where malaria vaccines are most urgently needed, vaccine delivery is often constrained by weak health systems, mistrust, and conflict. Operational research is needed to address these implementation challenges; however, our findings show that substantial reductions in deaths among young children are possible even when only moderate levels of malaria vaccine coverage can be achieved.

Der Systemische Lupus erythematodes (SLE) ist eine chronische, meist in Schüben verlaufende Autoimmunerkrankung aus der Gruppe der Kollagenosen, die nahezu jedes Organsystem betreffen kann. Das Immunsystem greift fälschlicherweise gesundes Gewebe an, oft betroffen sind Haut, Gelenke, Nieren und Blutgefäße. Frauen im Alter von 20 bis 40 Jahren sind am häufigsten betroffen.

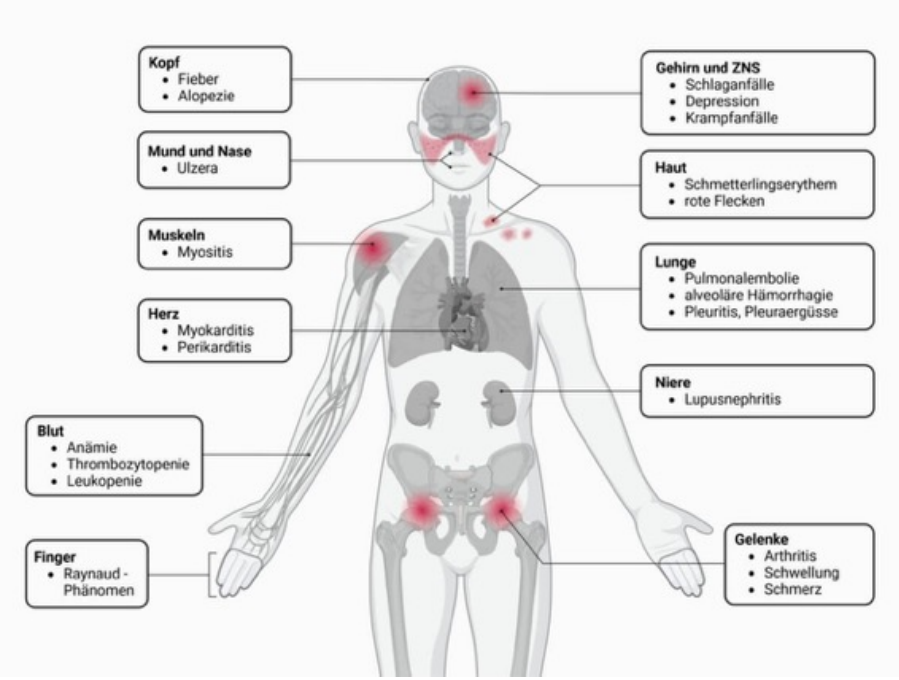

Therapie

Lupus ist bisher nicht heilbar, aber mit modernen Medikamenten gut behandelbar. Ziel ist die Unterdrückung der Entzündung und Vermeidung von Organschäden.

- **Basistherapie:** Hydroxychloroquin.
- **Schubtherapie:** Kortison (Prednisolon).
- **Immunsuppressiva:** Azathioprin, Cyclophosphamid.
- **Biologicals:** Belimumab.
- **Prävention:** Konsequenter UV-Schutz (Sonnencreme LSF 50+).

Toll-like-Rezeptoren (TLRs) sind ein entscheidender Teil deines **angeborenen Immunsystems**. Als sogenannte Pattern-Recognition Receptors (PRRs) fungieren sie wie biologische „Sensoren“, die fremde Eindringlinge anhand ihrer charakteristischen Oberflächenstrukturen (PAMPs) erkennen.

Kernfunktionen

•**Frühwarnsystem**: Sie erkennen Moleküle von Bakterien, Viren und Pilzen.

•**Unterscheidung**: Sie helfen dem Körper, zwischen „selbst“ (eigenem Gewebe) und „nicht selbst“ (Erregern) zu unterscheiden.

•**Signalgebung**: Bei Kontakt lösen sie eine Kaskade aus, die Entzündungsstoffe (**Zytokine**) freisetzt und das Immunsystem aktiviert.

•**Brücke**: Sie verbinden die schnelle, unspezifische angeborene Abwehr mit der gezielten, adaptiven Immunantwort.

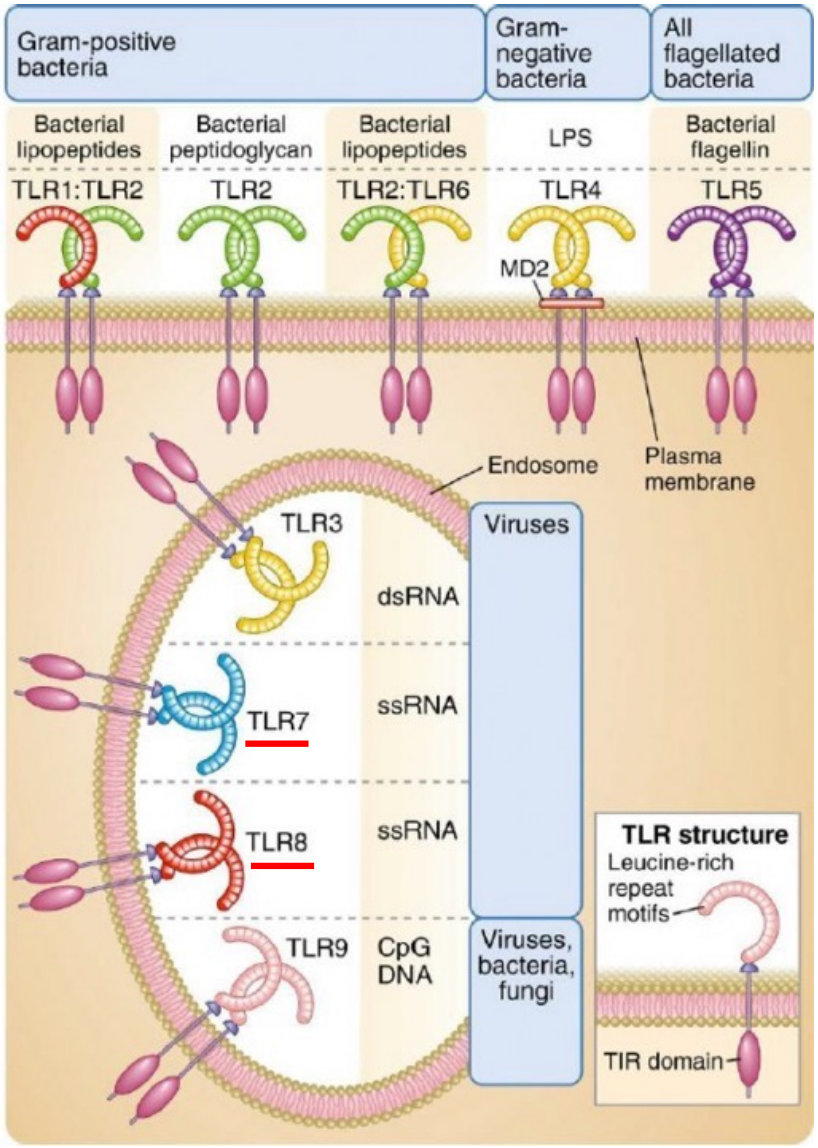

Enpatoran, a Toll-like receptor 7/8 inhibitor, in moderate-to-severe systemic lupus erythematosus: findings from Cohort B of a multicentre, international, double-blind, placebo-controlled dose-finding phase 2 trial

Summary

Background Toll-like receptors (TLR) 7 and 8 (TLR7/8) are activators of innate and adaptive immunity contributing to lupus pathogenesis. In Cohort B of WILLOW, a phase 2, randomised, placebo-controlled, double-blind, basket, dose-finding study, enpatoran, an oral small molecule inhibitor of TLR7/8, was evaluated in participants with active systemic lupus erythematosus (SLE).

Methods Participants were eligible if they were aged 18–75 years with moderate-to-severe SLE, with or without cutaneous manifestations, had a disease duration of at least 6 months, and were receiving a stable dose of medication before the screening period. Participants were recruited from 132 centres in 22 countries. In Part 1, participants were randomly allocated in a 1:2 ratio to receive either placebo or 100 mg enpatoran, both twice-daily. Following the enrolment of 60 participants, Part 2 was activated and additional participants were randomly allocated in a 1:1:1:1 ratio to 25 mg, 50 mg, or 100 mg of enpatoran or placebo, all twice-daily, for 24 weeks. Random allocation was stratified by region, biomarker status, and hybrid Safety of Estrogens in Lupus Erythematosus National Assessment–SLE Disease Activity Index score. The primary objective was to evaluate the dose–response relationship of enpatoran, using British Isles Lupus Assessment Group-based Composite Lupus Assessment (BICLA) response rate at week 24, based on multiple comparison procedure–modelling analysis. Study visits were scheduled from week 0 to week 24, followed by a 2-week safety follow-up period for participants who chose not to enter the long-term extension. From weeks 2 to 12, glucocorticoid doses were tapered to a prednisone-equivalent dose of no more than 5 mg/day, as clinically tolerated. Adverse events were monitored continuously throughout the study; safety parameters (including physical examination, vital signs, and routine chemistry and haematology) were assessed at all study visits. The trial was registered at ClinicalTrials.gov (NCT05162586) and a long-term extension study is ongoing.

Findings Between May 4, 2022, and Feb 6, 2024, participants were screened for eligibility for WILLOW cohorts A and B; 715 participants were screened and 354 were randomly allocated and included in the Cohort B safety population (95 to placebo, 71 to 25 mg enpatoran, 74 to 50 mg enpatoran, and 114 to 100 mg enpatoran). One patient allocated to the placebo group was found to be ineligible and was excluded from the full analysis set for the efficacy analyses. 335 (95%) of 353 participants were female, 18 (5%) were male, and median age was 41 years (IQR 33–51). At week 24, the study did not meet its primary objective of identifying a statistically significant dose–response relationship for enpatoran in BICLA response rate (p=0·14). BICLA response rates at week 24 were higher with all doses of enpatoran (25 mg: 41 [58%] of 71; odds ratio [OR] *vs* placebo 2·2 [95% CI 1·1–4·0], 50 mg: 36 [49%] of 74; OR 1·5 [95% CI 0·8–2·8], and 100 mg: 56 [49%] of 114; OR 1·6 [95% CI 0·9–2·8]) versus placebo (37 [39%] of 94). The most common treatment-emergent adverse event was diarrhoea, in four (6%) of 71, two (3%) of 74, and two (2%) of 114 participants in the 25 mg, 50 mg, and 100 mg enpatoran groups, respectively, and seven (7%) of 95 participants in the placebo group. Serious adverse events were reported in one (1%) of 71, three (4%) of 74, five (4%) of 114, and three (3%) of 95 participants treated with 25 mg, 50 mg, and 100 mg enpatoran and placebo, respectively.

Interpretation In this study of participants with moderate-to-severe SLE, enpatoran improved BICLA response rates versus placebo; however, the primary objective of a statistically significant dose-dependent effect on disease activity based on BICLA response was not met. Enpatoran was well tolerated across all dose groups.

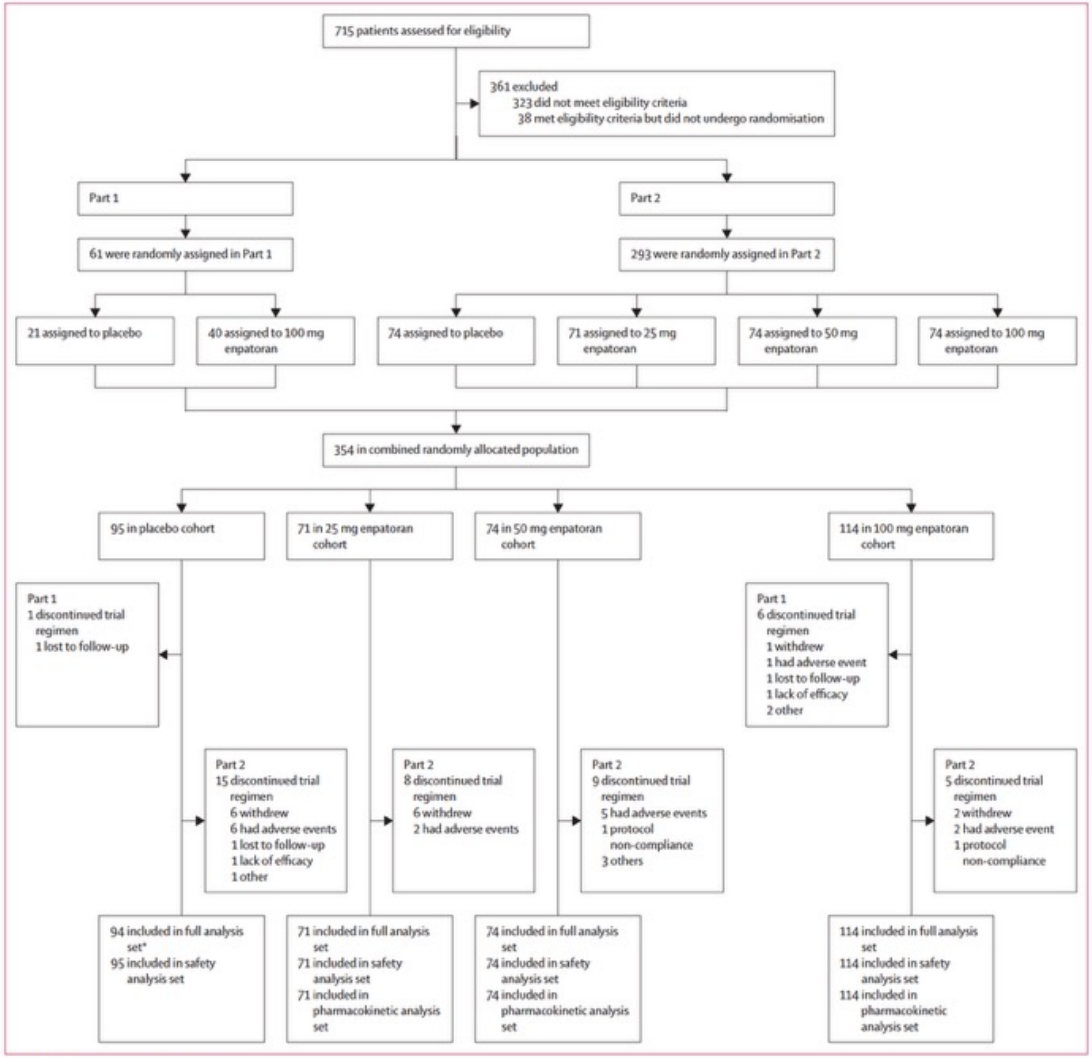

***Figure 1*: WILLOW Cohort B trial profile**

BILAG=British Isles Lupus Assessment Group. *One participant who was randomised to placebo was excluded from the full analysis set for the efficacy analyses as they entered Cohort B incorrectly owing to an error in recording BILAG at screening.

	Placebo (n=94)*	25 mg enpatoran (n=71)	50 mg enpatoran (n=74)	100 mg enpatoran (n=114)	Total (n=353)
Median age, years (IQR)	40 (34-51)	41 (32-49)	39 (29-48)	44 (36-53)	41 (33-51)
Sex					
Female	87 (93%)	69 (97%)	69 (93%)	110 (96%)	335 (95%)
Male	7 (7%)	2 (3%)	5 (7%)	4 (4%)	18 (5%)
Race†					
American Indian or Alaska Native	27 (29%)	22 (31%)	18 (24%)	28 (25%)	95 (27%)
Asian	26 (28%)	16 (23%)	20 (27%)	27 (24%)	89 (25%)
Black or African American	3 (3%)	6 (8%)	6 (8%)	3 (3%)	18 (5%)
White	35 (37%)	24 (34%)	29 (39%)	51 (45%)	139 (39%)
More than one race	1 (1%)	0	0	2 (2%)	3 (1%)
Other	2 (2%)	3 (4%)	1 (1%)	3 (3%)	9 (3%)
Geographic region					
North America and Europe	17 (18%)	14 (20%)	16 (22%)	33 (29%)	80 (23%)
Asia	21 (22%)	15 (21%)	18 (24%)	21 (18%)	75 (21%)
Central/South America and rest of world	56 (60%)	42 (59%)	40 (54%)	60 (53%)	198 (56%)
Time since SLE diagnosis, years (SD)	10·2 (7·8)	7·0 (6·9)	9·8 (7·8)	9·6 (6·6)	9·4 (7·3)
Diagnosis of SLE and CLE	59 (63%)	45 (63%)	43 (58%)	69 (61%)	216 (61%)
Biomarker status at baseline					
IFN-GS high	67 (71%)	54 (76%)	50 (68%)	83 (73%)	254 (72%)
IFN-GS low	27 (29%)	17 (24%)	24 (32%)	31 (27%)	99 (28%)
Hybrid SLENA-SLEDAI					
Hybrid SELENA-SLEDAI total, mean (SD)	11 (3·3)	11 (2·9)	10 (2·8)	11 (3·0)	11 (3·0)
<10	33 (35·1)	20 (28·2)	23 (31·1)	34 (29·8)	110 (31·2)
≥10	61 (64·9)	51 (71·8)	51 (68·9)	80 (70·2)	243 (68·8)
Hybrid SELENA-SLEDAI mucocutaneous score >0	91 (97%)	71 (100%)	71 (96%)	113 (99%)	346 (98%)
Hybrid SELENA-SLEDAI musculoskeletal score >0	89 (95%)	64 (90%)	69 (93%)	104 (91%)	326 (92%)
BILAG severity					
Mild (no BILAG A and no more than one B)	4 (4%)	3 (4%)	3 (4%)	7 (6%)	17 (5%)
Moderate (at least two BILAG B and no A)	55 (59%)	45 (63%)	43 (58%)	62 (54%)	205 (58%)
Severe (at least one BILAG A)	35 (37%)	23 (32%)	28 (38%)	45 (39%)	131 (37%)
CLASI-A total score					
Mild (0–9)	69 (73%)	52 (73%)	48 (65%)	78 (68%)	247 (70%)
Moderate (10–20)	21 (22%)	14 (20%)	24 (32%)	30 (26%)	89 (25%)
Severe (≥21)	4 (4%)	5 (7%)	2 (3%)	6 (5%)	17 (5%)
Concomitant therapy					
Systemic glucocorticoids	78 (83%)	63 (89%)	66 (89%)	94 (82%)	301 (85%)
≥10 mg dose‡	51 (54%)	34 (48%)	36 (49%)	59 (52%)	180 (51%)
Immunosuppressants	50 (53%)	42 (59%)	46 (62%)	66 (58%)	204 (58%)
Antimalarials	80 (85%)	60 (85%)	60 (81%)	97 (85%)	297 (84%)

Data are n (%) unless otherwise stated. BILAG=British Isles Lupus Assessment Group-based Composite Lupus Assessment. CLASI-A=Cutaneous Lupus Disease Area and Severity Index-Activity. CLE=cutaneous lupus erythematosus. IFN-GS=interferon gene signature. SLE=systemic lupus erythematosus. SELENA-SLEDAI=Safety of Estrogens in Lupus Erythematosus National Assessment-SLE Disease Activity Index. *One participant who was randomly allocated to placebo was excluded from the full analysis set for the efficacy analyses as they entered Cohort B incorrectly owing to an error in recording BILAG at screening. †Includes 172 of 353 participants who identified as Hispanic or Latino (47 [50%] of 94 in the placebo group; 37 [52%] of 71 in the 25 mg enpatoran group; 37 [50%] of 74 in the 50 mg enpatoran group, and 51 [45%] of 114 in the 100 mg enpatoran group). ‡Daily prednisone-equivalent dose.

Table 1: **Baseline characteristics in the full analysis set for the efficacy analyses**

	Placebo (n=94)*	25 mg enpatoran (n=71)	50 mg enpatoran (n=74)	100 mg enpatoran (n=114)	Total (n=353)
Median age, years (IQR)	40 (34-51)	41 (32-49)	39 (29-48)	44 (36-53)	41 (33-51)
Sex					
Female	87 (93%)	69 (97%)	69 (93%)	110 (96%)	335 (95%)
Male	7 (7%)	2 (3%)	5 (7%)	4 (4%)	18 (5%)
Race†					
American Indian or Alaska Native	27 (29%)	22 (31%)	18 (24%)	28 (25%)	95 (27%)
Asian	26 (28%)	16 (23%)	20 (27%)	27 (24%)	89 (25%)
Black or African American	3 (3%)	6 (8%)	6 (8%)	3 (3%)	18 (5%)
White	35 (37%)	24 (34%)	29 (39%)	51 (45%)	139 (39%)
More than one race	1 (1%)	0	0	2 (2%)	3 (1%)
Other	2 (2%)	3 (4%)	1 (1%)	3 (3%)	9 (3%)
Geographic region					
North America and Europe	17 (18%)	14 (20%)	16 (22%)	33 (29%)	80 (23%)
Asia	21 (22%)	15 (21%)	18 (24%)	21 (18%)	75 (21%)
Central/South America and rest of world	56 (60%)	42 (59%)	40 (54%)	60 (53%)	198 (56%)
Time since SLE diagnosis, years (SD)	10·2 (7·8)	7·0 (6·9)	9·8 (7·8)	9·6 (6·6)	9·4 (7·3)
Diagnosis of SLE and CLE	59 (63%)	45 (63%)	43 (58%)	69 (61%)	216 (61%)
Biomarker status at baseline					
IFN-GS high	67 (71%)	54 (76%)	50 (68%)	83 (73%)	254 (72%)
IFN-GS low	27 (29%)	17 (24%)	24 (32%)	31 (27%)	99 (28%)
Hybeid SLENA-SLEDAI					
Hybrid SELENA-SLEDAI total, mean (SD)	11 (3·3)	11 (2·9)	10 (2·8)	11 (3·0)	11 (3·0)
<10	33 (35·1)	20 (28·2)	23 (31·1)	34 (29·8)	110 (31·2)
≥10	61 (64·9)	51 (71·8)	51 (68·9)	80 (70·2)	243 (68·8)
Hybrid SELENA-SLEDAI mucocutaneous score >0	91 (97%)	71 (100%)	71 (96%)	113 (99%)	346 (98%)
Hybrid SELENA-SLEDAI musculoskeletal score >0	89 (95%)	64 (90%)	69 (93%)	104 (91%)	326 (92%)
BILAG severity					
Mild (no BILAG A and no more than one B)	4 (4%)	3 (4%)	3 (4%)	7 (6%)	17 (5%)
Moderate (at least two BILAG B and no A)	55 (59%)	45 (63%)	43 (58%)	62 (54%)	205 (58%)
Severe (at least one BILAG A)	35 (37%)	23 (32%)	28 (38%)	45 (39%)	131 (37%)
CLASI-A total score					
Mild (0–9)	69 (73%)	52 (73%)	48 (65%)	78 (68%)	247 (70%)
Moderate (10–20)	21 (22%)	14 (20%)	24 (32%)	30 (26%)	89 (25%)
Severe (≥21)	4 (4%)	5 (7%)	2 (3%)	6 (5%)	17 (5%)
Concomitant therapy					
Systemic glucocorticoids	78 (83%)	63 (89%)	66 (89%)	94 (82%)	301 (85%)
≥10 mg dose‡	51 (54%)	34 (48%)	36 (49%)	59 (52%)	180 (51%)
Immunosuppressants	50 (53%)	42 (59%)	46 (62%)	66 (58%)	204 (58%)
Antimalarials	80 (85%)	60 (85%)	60 (81%)	97 (85%)	297 (84%)

Data are n (%) unless otherwise stated. BILAG=British Isles Lupus Assessment Group-based Composite Lupus Assessment. CLASI-A=Cutaneous Lupus Disease Area and Severity Index-Activity. CLE=cutaneous lupus erythematosus. IFN-GS=interferon gene signature. SLE=systemic lupus erythematosus. SELENA-SLEDAI=Safety of Estrogens in Lupus Erythematosus National Assessment-SLE Disease Activity Index. *One participant who was randomly allocated to placebo was excluded from the full analysis set for the efficacy analyses as they entered Cohort B incorrectly owing to an error in recording BILAG at screening. †Includes 172 of 353 participants who identified as Hispanic or Latino (47 [50%] of 94 in the placebo group; 37 [52%] of 71 in the 25 mg enpatoran group; 37 [50%] of 74 in the 50 mg enpatoran group, and 51 [45%] of 114 in the 100 mg enpatoran group). ‡Daily prednisone-equivalent dose.

Table 1: **Baseline characteristics in the full analysis set for the efficacy analyses**

	Placebo (n=94)	25 mg enpatoran (n=71)	50 mg enpatoran (n=74)	100 mg enpatoran (n=114)
Primary efficacy outcome at week 24 (full analysis set)				
Detection of enpatoran dose-response relationship in BICLA response based on MCP-Mod* (parts 1 and 2 combined), p-value	..	..	..	0·14
BICLA response rate at week 24 (supplementary analysis)				
Response rate	37 (39%)	41 (58%)	36 (49%)	56 (49%)
Percentage difference in response rate (95% CI)	..	18 (3 to 33)	9 (−6 to 24)	10 (−4 to 23)
OR (95% CI)	..	2·2 (1·1 to 4·0)	1·5 (0·8 to 2·8)	1·6 (0·9 to 2·8)
p-value versus placebo†	..	0·0088	0·10	0·052
Subgroup analyses of BICLA response rate at week 24				
IFN-GS high (≥0·71) at baseline				
Response rate	31% (21 to 44)	61% (47 to 74)	52% (37 to 66)	49% (38 to 61)
Percentage difference in response rate (95% CI)	..	30% (12 to 46)	21% (3 to 38)	18% (2 to 33)
OR (95% CI)	..	3·4 (1·6 to 7·3)	2·4 (1·1 to 5·1)	2·1 (1·1 to 4·2)
p-value versus placebo	..	0·0013	0·026	0·027
High glucocorticoid use (daily prednisone-equivalent dose ≥10 mg) at baseline				
Response rate	37% (24 to 52)	68% (50 to 83)	61% (44 to 77)	53% (39 to 66)
Percentage difference in response rate (95% CI)	..	30% (9 to 49)	24% (2 to 43)	15% (−4 to 33)
OR (95% CI)	..	3·52 (1·4 to 8·8)	2·7 (1·1 to 6·4)	1·9 (0·9 to 4·0)
p-value versus placebo	..	0·0071	0·03	0·11
Secondary efficacy outcomes at week 24 (full analysis set)‡				
BICLA response and glucocorticoid reduction§				
Response rate	16/51 (31%)	20/34 (59%)	20/36 (56%)	28/59 (48%)
OR (95% CI)	..	3·3 (1·3 to 8·2)	2·8 (1·1 to 6·7)	2·1 (1·0 to 4·6)
p-value versus placebo (one-sided)	..	0·0056	0·013	0·034
Percentage difference in response rate (95% CI)¶	..	28% (6 to 47)	24% (3 to 44)	16% (−2 to 33)
SRI-4 response§				
Response rate	50/94 (53%)	44/71 (62%)	48/74 (65%)	77/114 (68%)
OR (95% CI)	..	1·5 (0·8 to 2·8)	1·7 (0·9 to 3·2)	1·9 (1·1 to 3·5)
p-value versus placebo (one-sided)	..	0·11	0·052	0·012
Percentage difference in response rate (95% CI)¶	..	9% (−7 to 24)	12% (−3 to 26)	14% (1 to 27)
Attainment of LLDAS§				
Response rate	23/94 (25%)	21/71 (30%)	32/74 (43%)	35/114 (31%)
OR (95% CI)	..	1·3 (0·6 to 2·6)	2·5 (1·3 to 4·9)	1·5 (0·8 to 2·8)
p-value versus placebo (one-sided)	..	0·24	0·0039	0·11
Percentage difference in response rate (95% CI)¶	..	5% (8 to 19)	19% (4 to 33)	6% (−6 to 18)
Attainment of remission (DORIS criteria)§‖				
Response rate	10/94 (11%)	7/71 (10%)	8/74 (11%)	20/114 (18%)
OR (95% CI)	..	0·9 (0·3 to 2·6)	1·1 (0·4 to 2·9)	2·0 (0·9 to 4·6)
p-value versus placebo (one-sided)	..	0·56	0·44	0·049
Percentage difference in response rate (95% CI)¶	..	−1 (−10 to 10)	0 (−9 to 11)	7 (−3 to 16)
Clinically meaningful glucocorticoid reduction§				
Number of participants with response	36/51 (71%)	28/34 (82%)	27/36 (75%)	41/59 (69%)
OR (95% CI)	..	2·1 (0·7 to 6·3)	1·2 (0·4 to 3·2)	0·9 (0·4 to 2·2)
p-value versus placebo (one-sided)	..	0·09	0·37	0·56
≥50% reduction in tender and swollen (28-joint) count				
Number of participants with response	53/77 (69%)	39/54 (72%)	45/58 (78%)	68/86 (79%)
Change from baseline in PGA of SLE disease activity				
Mean (SD)	−0·9 (0·6)	−1·0 (0·6)	−1·1 (1·0)	−1·1 (0·6)

(Table 2 continues on next page)

(Continued from previous page)

	Placebo (n=94)	25 mg enpatoran (n=71)	50 mg enpatoran (n=74)	100 mg enpatoran (n=114)
Change from baseline in FACIT-Fatigue score**				
Participants, n	79	63	65	101
Least squares mean (95% CI)	2·4 (0·4 to 4·4)	4·8 (2·5 to 7·0)	3·6 (1·4 to 5·8)	5·1 (3·3 to 6·9)
Least squares mean difference (95% CI)	..	2·3 (−0·5 to 5·2)	1·2 (−1·7 to 4·0)	2·6 (0·1 to 5·2)
Exploratory subgroup analysis at week 24 (CLASI-A score ≥8 at screening and baseline)				
Change from baseline to week 24 in CLASI-A score**				
Participants, n	41	29	38	54
Least squares mean (95% CI)	−45·2 (−55·4 to −34·9)	−59·5 (−71·5 to −47·4)	−75·6 (−86·2 to −65·0)	−73·5 (−82·3 to −64·7)
Least squares mean difference (95% CI)	..	−14·3 (−29·8 to 1·2)	−30·4 (−44·7 to −16·2)	−28·3 (−41·5 to −15·2)
Attainment of remission at week 24				
CLASI-A 0 to 1	7 (17%)	6 (21%)††	13 (34%)	15 (28%)
CLASI-A 0 to 3	12 (29%)	12 (41%)††	23 (61%)	29 (54%)
CLASI-A 0 to 1 and CLA-IGA 0 to 1	5 (12%)	6 (21%)††	11 (29%)	15 (28%)
SRI-4 response rate at week 24 (post-hoc analysis)‡‡				
Response rate	20 (49%)††	18 (62%)††	27 (71%)	36 (67%)
OR (95% CI)	..	1·7 (0·7 to 4·7)	2·7 (1·1 to 7·0)	2·1 (0·9 to 5·0)
p-value versus placebo (one-sided)	..	0·13	0·02	0·039
Percentage difference in response rate (95% CI)	..	13% (−11 to 35)	22% (1 to 42)	18% (−2 to 37)

Unless otherwise stated, data are n (%) for response rates, % (95% CI) for subgroup analyses of BICLA response at week 24, n/N (%) for secondary efficacy outcomes, and differences in response rates are given as percentages versus placebo (95% CI). BILAG=British Isles Lupus Assessment Group-based Composite Lupus Assessment. CLASI-A=Cutaneous Lupus Erythematosus Disease Area and Severity Index-Activity. CLA-IGA=Cutaneous Lupus Activity-Investigator's Global Assessment. CLE=cutaneous lupus erythematosus. DORIS=Definition of Remission in SLE. FACIT=Functional Assessment of Chronic Illness Therapy. IFN-GS=interferon gene signature score. LLDAS=lupus low disease activity state. MCP-mod=multiple comparison procedure-modelling. MMRM=mixed-model with repeated measures. OR=odds ratio. PGA=Physician Global Assessment. SRI-4=SLE Responder Index-4. SLE=systemic lupus erythematosus. SELENA-SLEDAI=Safety of Estrogen in Lupus Erythematosus National Assessment-SLE Disease Activity Index. *MCP-Mod adjusted for baseline hybrid SELENA–SLEDAI total score, region, and biomarker status. †Combined p-value from weighted inverse normal method. Treatment effect statistically significant if p≤0·025. ‡Except BICLA response plus clinically meaningful glucocorticoid reduction, which were assessed in participants receiving ≥10 mg/day prednisone equivalent dose of glucocorticoid at baseline. §ORs, 95% CIs, and p-values based on logistic regression with stratification factors of region, biomarker status, and SELENA-SLEDAI score as independent variables. 95% CI for ORs were calculated using the Wald method. ¶95% CI for difference in response rate calculated using non-stratified Miettinen–Nurminen method. ‖If remission attainment was not evaluable, it was considered not attained. **Estimates and 95% CIs based on a an MMRM of the change from baseline, with region, biomarker status, treatment, and analysis visit as classification variables, baseline score and baseline hybrid SELENA-SLEDAI total score as covariates, and treatment by analysis visit interaction. ††Data missing for one participant. ‡‡ORs, 95% CI, and p-values were based on a logistic model with treatment group, baseline hybrid SELENA-SLEDAI total score, region, and biomarker status as independent variables. Crude percentage differences in response rate and 95% CI were computed using the non-stratified Miettinen–Nurminen method.

Table 2: **Primary and secondary efficacy outcomes (full analysis set) and exploratory subgroup analysis in participants with SLE and cutaneous manifestations (CLASI-A score ≥8 at screening and baseline)**

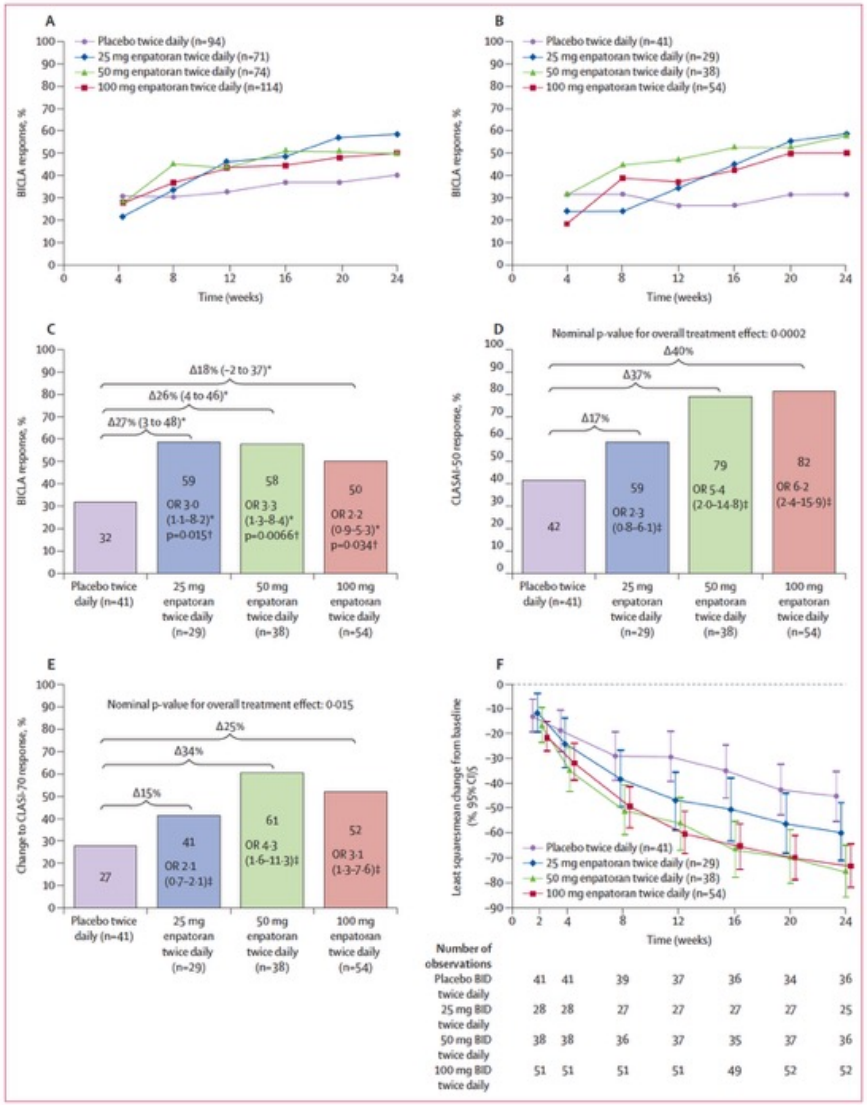

Figure 2: **BICLA response and cutaneous responses over time and at week 24**

(A) BICLA response over time in the full analysis set (n=353). (B–F) Outcomes in the subgroup of participants with SLE and cutaneous manifestations (CLASI-A score ≥8 at screening and baseline [n=162]), including BICLA response over time (B), BICLA response at week 24 (C), CLASI-50 response at week 24 (D), CLASI-70 response at week 24 (E), and percentage change from baseline in CLASI-A total score over time (F). BICLA=British Isles Lupus Assessment Group-based Composite Lupus Assessment. CLASI-A=Cutaneous Lupus Erythematosus Disease Area and Severity Index-Activity. OR=odds ratio. SELENA-SLEDAI=Safety of Estrogens in Lupus Erythematosus National Assessment-Systemic Lupus Erythematosus Disease Activity Index. *95% CIs were calculated using the Clopper-Pearson method, and the Miettinen-Nurminen method for the between-group differences; ORs and 95% CI are based on a logistic model with treatment group, baseline hybrid SELENA-SLEDAI total score, region, and biomarker status as independent variables. †Nominal p-value, one-sided. ‡ORs for between-group differences were based on a logistic model adjusted for region, biomarker status, baseline CLASI-A score, and hybrid SELENA-SLEDAI total scores, with Clopper-Pearson 95% CIs and p-values based on the likelihood ratio χ^2 test. §Least-square means and 95% CIs based on mixed-model with repeated measures modelling of change from baseline in CLASI-A total score until week 24, with region, biomarker status, treatment, and analysis visit as classification variables, baseline CLASI-A total score and baseline hybrid SELENA-SLEDAI total score as covariates, and treatment by analysis visit interaction.

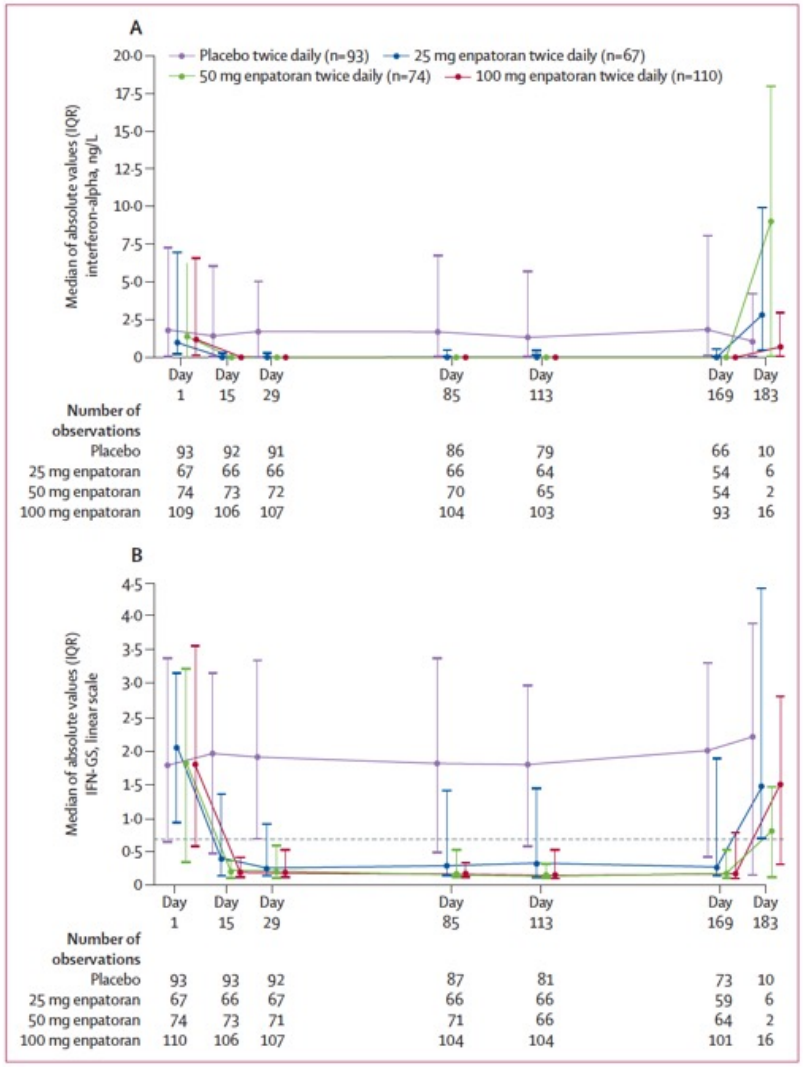

Figure 3: Changes from baseline in interferon-alpha (A) and IFN-GS levels (B)
IFN-GS=interferon gene signature.

	Placebo (n=95)	25 mg enpatoran (n=71)	50 mg enpatoran (n=74)	100 mg enpatoran (n=114)
Any adverse event	61 (64%)	43 (61%)	47 (64%)	70 (61%)
Any treatment-related adverse event	19 (20%)	13 (18%)	19 (26%)	22 (19%)
Grade ≥3 adverse event	6 (6%)	1 (1%)	3 (4%)	5 (4%)
Grade ≥4 adverse event	1 (1%)	0	0	0
Serious adverse event	3 (3%)	1 (1%)	3 (4%)	5 (4%)
Adverse event leading to study drug discontinuation	6 (6%)	2 (3%)	5 (7%)	3 (3%)
Adverse event leading to death	0	0	0	0
Any adverse event of special interest*	3 (3%)	1 (1%)	0	3 (3%)
Adverse events with an incidence of ≥5% in any group†				
Gastrointestinal disorders				
Diarrhoea	7 (7%)	4 (6%)	2 (3%)	2 (2%)
Infections and infestations				
Upper respiratory tract infection	6 (6%)	7 (10%)	9 (12%)	8 (7%)
Urinary tract infection	9 (9%)	2 (3%)	5 (7%)	11 (10%)
Nasopharyngitis	4 (4%)	2 (3%)	6 (8%)	10 (9%)
Influenza	6 (6%)	5 (7%)	2 (3%)	5 (4%)
Asymptomatic bacteriuria	2 (2%)	4 (6%)	3 (4%)	2 (2%)
Herpes zoster	2 (2%)	2 (3%)	2 (3%)	2 (2%)
Laboratory investigations				
Lymphocyte count decreased	5 (5%)	1 (1%)	2 (3%)	1 (1%)
Nervous system disorders				
Headache	4 (4%)	2 (3%)	7 (10%)	3 (3%)

Data are number of participants (%). *Adverse events considered to be of special interest were severe infections (grade ≥3), seizure (any grade), clinically significant cardiac arrythmia, or serotonin syndrome. †Headings and subheadings are the system organ classes and preferred terms, respectively, in the Medical Dictionary for Regulatory Activities version 27.1.

Table 3: Adverse events in the safety population

Implications of all the available evidence

Although the primary objective of identifying a statistically significant dose–response relationship was not met, systemic disease activity reduction was observed across enpatoran dose groups, evidenced by improved British Isles Lupus Assessment Group-based Composite Lupus Assessment (BICLA) response rates at week 24 versus placebo. Moreover, clinically meaningful treatment benefits of enpatoran were demonstrated across multiple prespecified secondary and exploratory clinical and biomarker outcomes. Rates of attainment of the composite endpoint of BICLA response plus clinically meaningful glucocorticoid reductions improved across all enpatoran groups compared with placebo. The effect of enpatoran on type I interferon activity was demonstrated by a rapid reduction in IFN-GS emerging as early as week 2, maintained until the end of treatment. Enpatoran was well tolerated, with rates of treatment-emergent adverse events similar to placebo and consistent with previous clinical studies. Overall, these findings highlight the role of TLR7/8 activation in the IFN pathway in SLE, and the role of TLR7/8 inhibition in attenuating cutaneous and systemic disease activity in SLE, supporting further investigation of enpatoran in phase 3 trials.

Implementing sustainable liver health in Europe: a second EASL–*Lancet* Commission

Key messages

- Mortality from cirrhosis has remained persistently high in the WHO European region since 2000, with liver cancer mortality increasing by more than 50%, and the cost of liver disease to the combined economies of the EU27+4 (EU member states, plus Norway, Iceland, the UK, and Switzerland) being now estimated at €55 billion per year
- Consumption of alcohol and unhealthy foods are key drivers for liver-related mortality in Europe, and eliminating risk factors related to health behaviour would almost halve the burden of liver diseases in the EU27+4
- Liver disease is closely linked to broader health and longevity harms, which is exemplified by the fact that, in the WHO European region, three-quarters of the alcohol-attributable disability-adjusted life-years lost are due to non-liver-related primary causes, particularly other non-communicable diseases
- Our modelling of viral hepatitis shows that 25% of migrants with chronic hepatitis B and 44% with chronic hepatitis C come from low endemicity countries and would therefore be excluded from testing under current international guidelines
- The European Beating Cancer Plan emphasises the importance of early detection and prevention, yet has overlooked surveillance strategies specific to liver cancer
- The current digital marketing ecosystem and social media algorithms amplify structural determinants of liver health and promote behaviours related to alcohol and unhealthy food consumption in children and adolescents
- The absence of transparency of medicine pricing across Europe exemplifies the extensive health policy and legislative heterogeneity in this region, and joint procurement initiatives and pricing cooperation would strengthen the negotiating capacity of European countries
- Early detection of progressive liver disease requires integrated care pathways, including primary care, endocrinolology, psychiatry, and peer-led initiatives, supported by precision diagnostics with an emphasis on non-invasive liver fibrosis assessments, artificial intelligence-driven risk stratification, and updated educational models that account for relevant multimorbidity
- Building upon democratic values of solidarity and equity, the EU and national governments should update and harmonise health-related policies based on the evidence presented in this report and associated recommendations, and develop standardised liver health indicators to drive transparent monitoring of outcomes

What to do

Recommendations

- Integrate pathways of care for liver disease with other chronic disease pathways, managing multi-morbidity.
- Recognise steatotic liver disease as a preventable non-communicable disease within the core non-communicable disease framework, and invest in equitable prevention and care strategies.
- Develop and implement a European liver health education and training framework.
- Integrate mental health support and anti-stigma approaches into liver disease prevention and care services.
- Strengthen and implement primary and secondary prevention programmes for liver cancer.
- Enforce Europe-wide regulations on digital advertising and marketing of alcohol and unhealthy foods and drinks, particularly algorithm-driven marketing targeting those under 18 years.
- Implement legislation to require mandatory health warnings on alcohol-containing beverages, at the point of purchase and consumption.
- Implement policies and interventions to address the health needs of migrants across Europe, with a strong focus on viral hepatitis elimination.
- Provide publicly accessible guidance frameworks for structuring market entry agreements for medicines that balance equitable access with sustainable pricing.
- Encourage voluntary joint procurement initiatives and pricing cooperation among EU member states to strengthen their negotiating capacity, particularly for high-cost or high-uncertainty drugs.
- Exclude the alcohol industry and their agents from the formulation of public health policy, and from interactions with policy makers, health and public health leaders, and from alcohol harm reduction activities.
- Align taxation of alcohol and unhealthy foods to the economic burden they impose, including costs incurred by health-care systems, law enforcement, the justice system, and social services.

Possible effects of GLP-1 agonists were recognized

Conclusion

This EASL–*Lancet* Commission report is published against the backdrop of an escalating and unsustainable burden of liver disease in Europe. Evidence-based policy implementation by national governments and the EU to reduce this burden has been inadequate. Our recommendations (table 6) present substantial opportunities to advance policy in key areas, including alcohol regulation, childhood protection from marketing, and harmonisation of the European health-related policy landscape. Importantly, these same measures would also deliver major co-benefits by reducing the burden of other NCDs, including cardiovascular disease and cancer. Responsible entities named in table 6, in particular, medical societies such as EASL, WHO, relevant EU bodies, and European states, should urgently initiate work to develop and update action plans based on the framework represented by the revised set of recommendations in this report and the associated scientific evidence that has been showcased by our report.

Enlicitide (früher MK-0616) ist ein neuartiger, oraler PCSK9-Hemmer zur Senkung des LDL-Cholesterins, der sich 2026 in fortgeschrittenen Phase-III-Studien befindet. Als makrozyklisches Peptid ermöglicht es erstmals eine tägliche Tabletteneinnahme statt Injektionen. Studien zeigten eine signifikante LDL-Senkung um ca. 57-60%

Wichtige Fakten zu Enlicitide:

•**Wirkmechanismus:** Es hemmt das Protein PCSK9, was die Anzahl der LDL-Rezeptoren auf Zellen erhöht und somit mehr LDL-Cholesterin aus dem Blut entfernt.

•**Wirksamkeit:** In der CORALreef-Lipids-Studie (Phase 3) sank der LDL-Wert nach 24 Wochen um durchschnittlich 57% im Vergleich zu 3% bei Placebo.

•**Anwendung:** Es ist als einmal tägliche Tablette konzipiert.

•**Studienlage:** Mehrere Studien (CORALreef-Lipids, -HFH, -Add-on) untersuchen den Einsatz bei Patienten mit hohem kardiovaskulärem Risiko.

•**Status:** Bisher nicht offiziell zugelassen, aber als vielversprechende orale Alternative zu injizierbaren PCSK9-Antikörpern (Evolocumab) eingestuft.

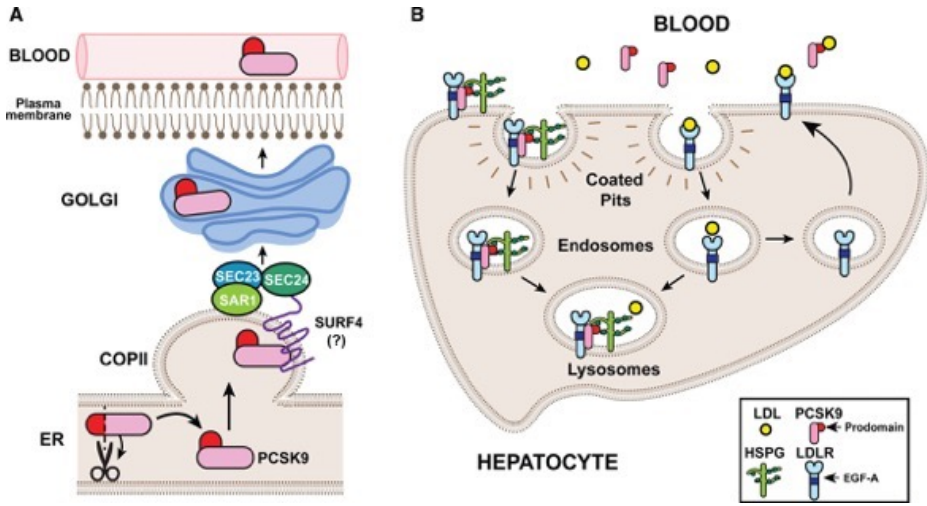

HSPGs (Heparansulfat-Proteoglykane) auf Leberzellen fungieren als Co-Rezeptoren, die PCSK9 binden und an der Oberfläche konzentrieren, was den Abbau des LDL-Rezeptors (LDLR) durch PCSK9 fördert. Die Bindung an HSPG ist entscheidend für die Aktivität von PCSK9; eine Störung dieser Interaktion könnte theoretisch den LDLR schützen-

Building an oral peptide drug

Biologics are nature-inspired pharmaceutical compounds for treating diseases such as cancer, chronic autoimmune disorders, and high-cholesterol conditions. They are often based on proteins in which amino acids are linked by amide bonds that undergo rapid degradation by digestive enzymes if taken orally. Biologics are therefore primarily administered through intravenous injection. Orally available alternatives can improve patients' quality of life and adherence to health management. Peptide-based drugs can be chemically modified to withstand degradation and are simpler alternatives to biologics. However, their synthesis often involves many steps and is inefficient. Klapars *et al*. report a kilogram-scale synthesis of enlicitide, a peptide drug for lowering low-density cholesterol that is in a Phase 3 clinical trial for atherosclerotic cardiovascular disease. This new synthesis route leverages engineered enzymes and crystallization of key intermediates, substantially cutting down the number of reaction steps while improving yield.

Biocatalytic retrosynthesis of an oral peptide drug

Enlicitide, a peptide-based drug for reducing low-density cholesterol, has a complex interlocked ring structure.

Biocatalytic retrosynthesis avoids complicated protecting group manipulations and inefficient chromatographic purification of reaction intermediates.

This enables production of kilogram-scale enlicitide with >99% purity in three cascade reactions, which is a substantial improvement from the conventional synthesis route that requires 64 steps in dilute conditions.

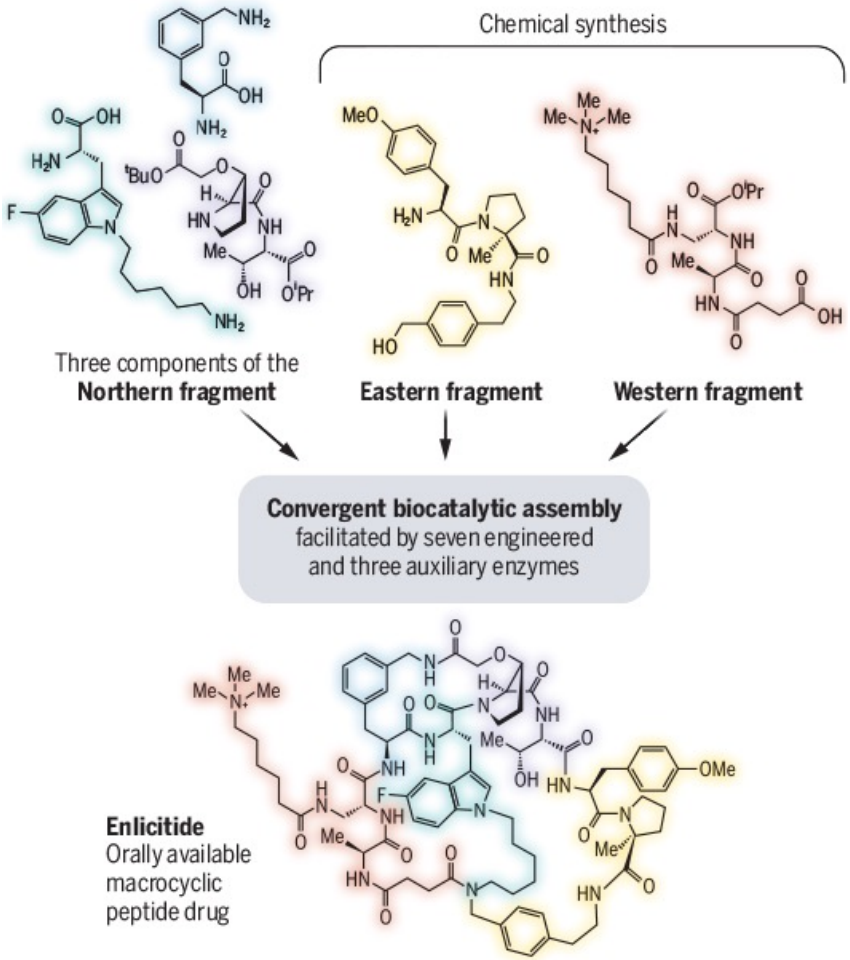

US medical journal rejects call from RFK Jr to retract vaccine study

Kennedy described the research as "a deceitful propaganda stunt by the pharmaceutical industry", and said the scientists who authored it had "meticulously designed it not to find harm" in a detailed 1 August opinion piece on TrialSite News, an independent website focused on clinical research. He called on the journal to "immediately retract" the study.

Kennedy had a number of criticisms, including the lack of a control group, that the study deliberately excluded different groups of children to avoid showing a link between aluminum and childhood health conditions - including those with the highest levels of exposure - and that it did not include the raw data.

Hviid responded to the criticisms on TrialSite. He said some of the points were related to study design choices that were reasonable to discuss but refuted others, including that the study was designed not to find a link. In fact, he said, its design was based on a study led by Matthew Daley, a pediatrician at Kaiser Permanente Colorado, which did show a link, and which Kennedy cited in his article.

There was no control group because in Denmark only 2% of children were unvaccinated, which was too small for meaningful comparison, Hviid added. The data was available for researchers to analyze, but individual-level data was not released under Danish law, he said.